European Science Meeting (ESM), February 23rd, 2026

VNS magnetic cage: innovations and challenges

L. Giannini, C. Luongo and DCT

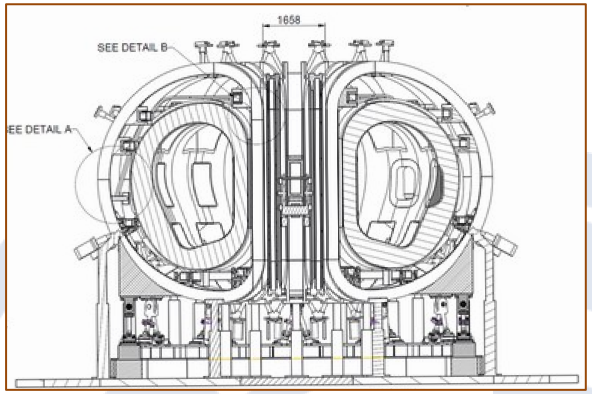

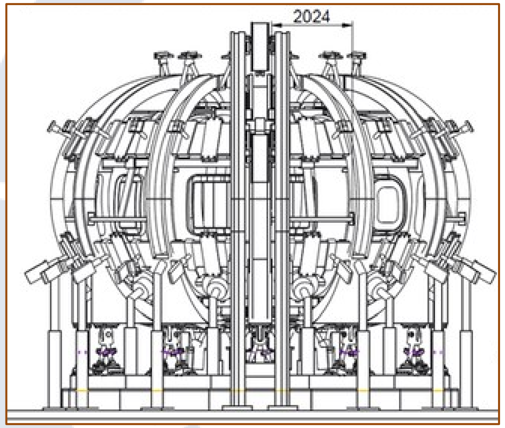

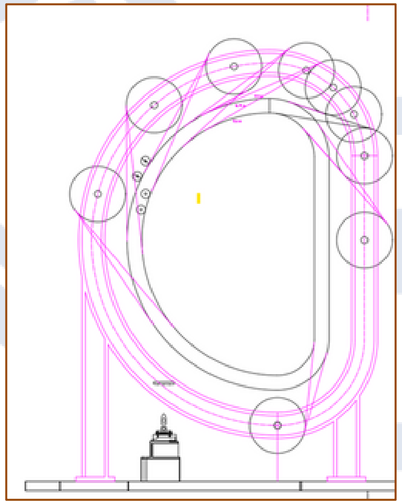

This work has been carried out within the framework of the EUROfusion Consortium, funded by the European Union via the Euratom Research and Training Programme (Grant Agreement No 101052200 — EUROfusion). Views and opinions expressed are however those of the author(s) only and do not necessarily reflect those of the European Union or the European Commission. Neither the European Union nor the European Commission can be held responsible for them.

Overview

I. Magnet System
   → PF-out-TF, LTS reference
   → PF-in-TF, HTS alternative

II. Thermal Shielding

III. Feeders

IV. Maintenance Hatches

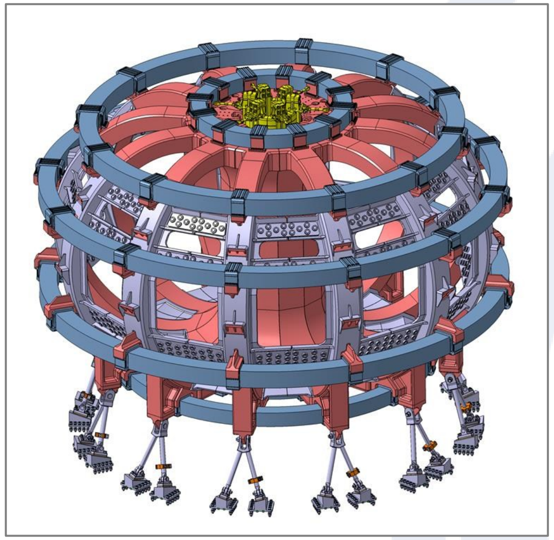

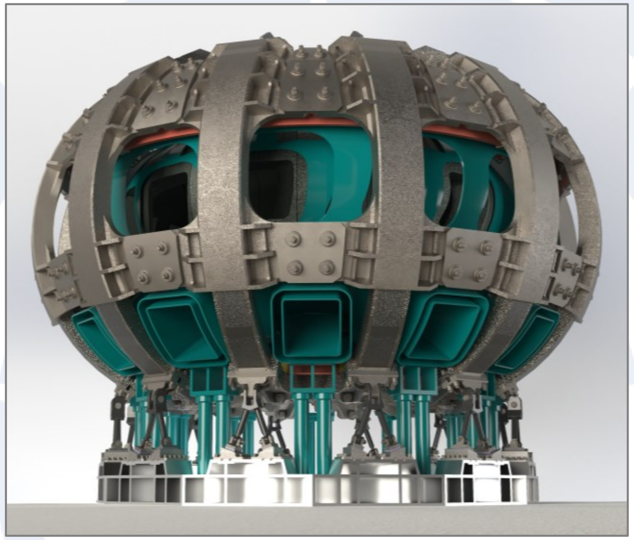

Options considered for the magnetic cage

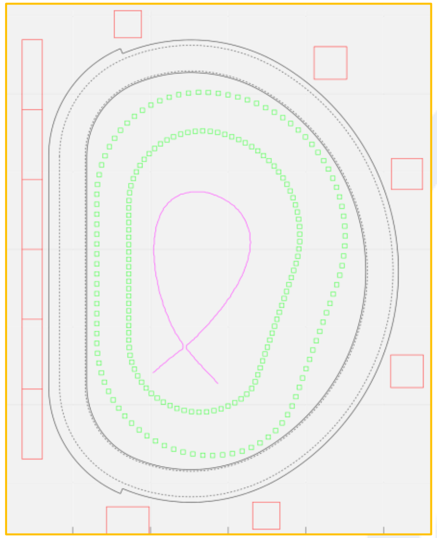

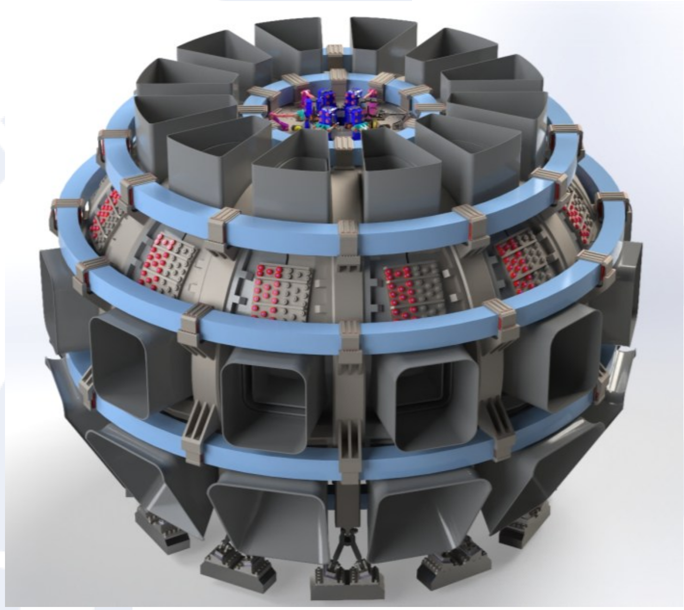

Option 1: PF coils Outside TF coils

- Plasma more difficult to control, however machine assembly is standard (same as ITER/JT60sa) and all coils can be manufactured in factory LTS
- No specific qualification needed

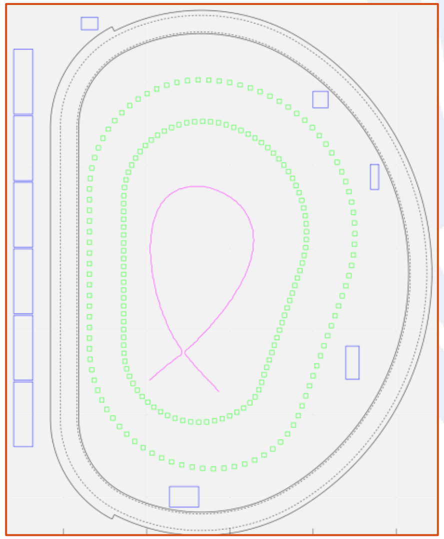

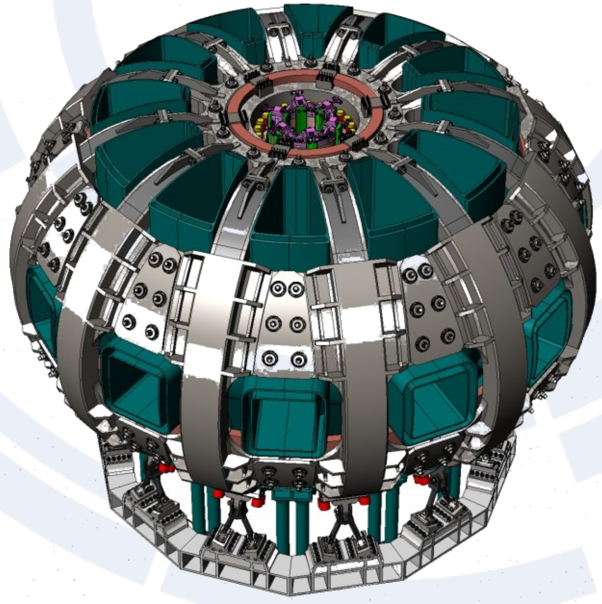

Option 2: PF coils Inside TF coils

- Better plasma control, but coil winding must be done in-situ and HTS are needed to avoid heat treatment in-situ
- Magnet technology development and qualification program prior to project start

See L. Giannini et al., 10.1109/TASC.2024.3365097

Magnet system description – PF-out-TF configuration

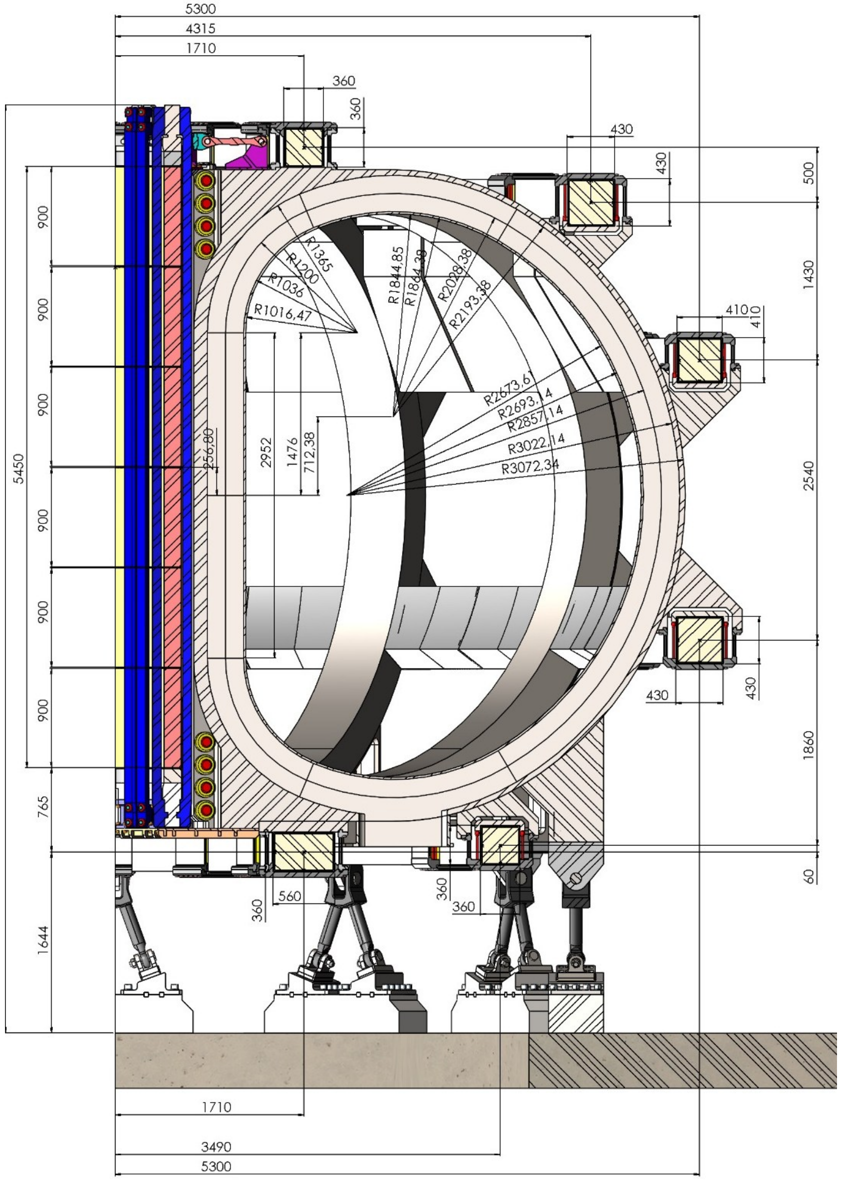

Number of TF coils	12
Total current per coil [MAt]	6.23
J_{eng} [MA/m2]	65
Stored Energy (total) [GJ]	~4 (1 tons of TNT)
Nominal peak field on TF coil [T]	13.2
Centering force [MN]	144
Hoop force innerleg [MN]	32
Length of the TF coil centerline [m]	15
Discharge time during quench τ [s]	4
TFC terminal voltage [kV]	2.5
Conductor concept	CICC
Superconductor/Stabilizer	Nb3Sn/Cu
Winding scheme	2 pancake 1 internal joint
weight per coil (WP, case and OIS)	~40 tons

There is a trade-off between nuclear shielding thickness and the distance between the plasma and TF coil inner leg.

- More compact brings the inner leg closer to the plasma --> Lower B peak
- Innerleg location and shielding thickness optimized using 50 MGy magnet insulation limit (see EFDA_D_2S3VZM; EFDA_D_2SYE5)

Trade-off between TF peak field and nuclear shielding thickness

The logarithmic lines represent three cases, parametric on the shielding material attenuation factor. By intersecting these curves with the blue curve representing the maximum lifetime dose for the magnet insulation in 10 FPY, it is possible to obtain the peak field on the magnet for each case study (ascending curve is the peak field on the TF as a function of inner leg distance to plasma)

See L. Giannini et al., 10.1109/TASC.2024.3365097

50 MGy limit on magnet insulation (EFDA_D_2S3VZM)

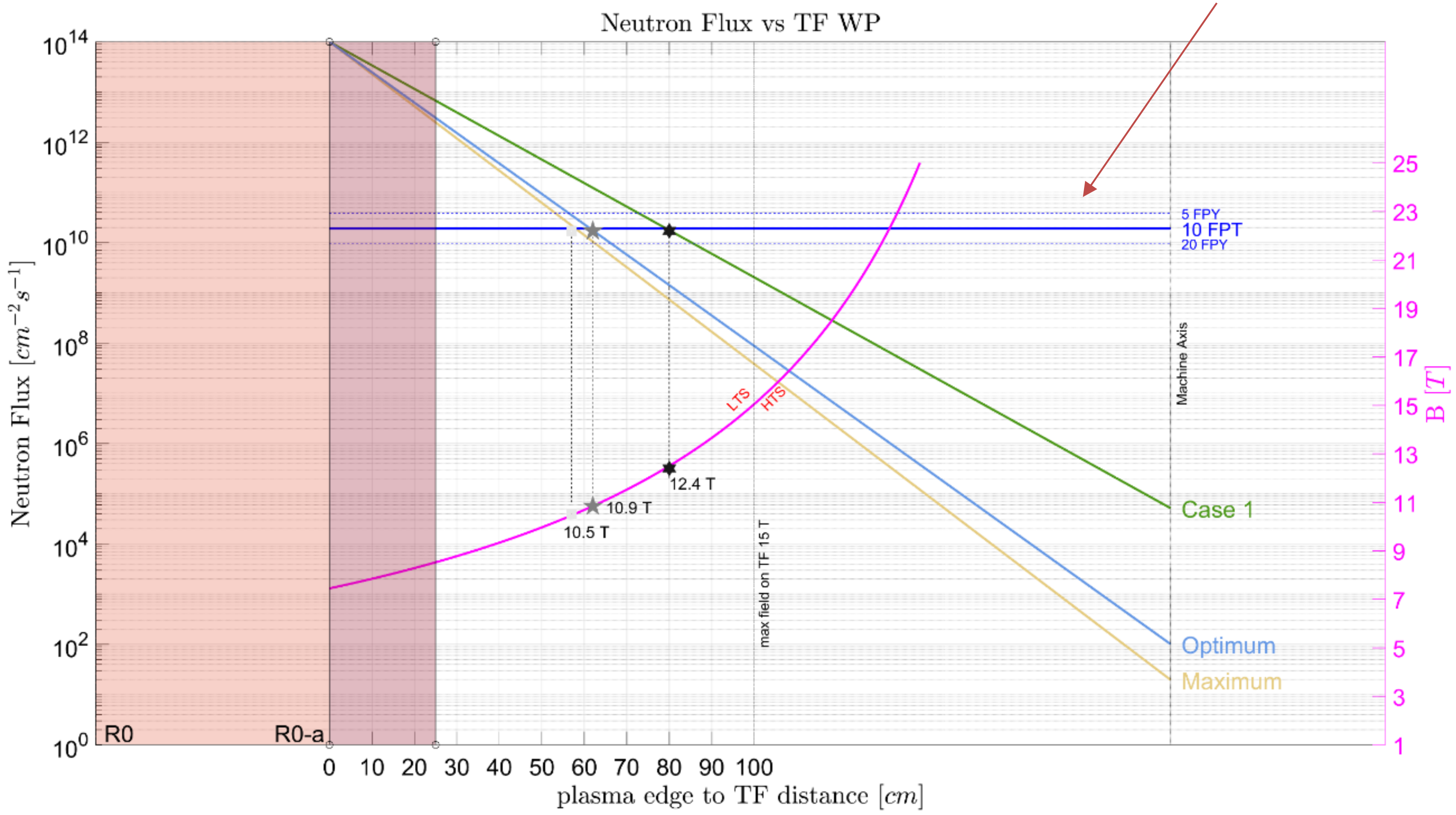

1) **Case 1**:
   - SB: W2B5*(87%)*+Water*(8%)*+SS316L*(5%)*
   - VV body: B4C*(92%)*+Water*(8%)*

2) **Maximum (best shielding efficiency)**:
   - SB: WC*(87%)*+Water*(8%)*+SS316L*(5%)*
   - VV body: W2B5*(87%)*+Water*(8%)*+SS316L*(5%)*

3) **Optimum (an intermediate shielding option)**:
   - SB: WC*(87%)*+Water*(8%)*+SS316L*(5%)*
   - VV body: 1st layer: WC *(87%)* + Water *(8%)* + SS316L *(5%),* 2nd layer: W2B5 *(87%)* + Water *(8%)* + SS316L*(5%)*

TFC – D shape bending free

B~1/R → B(r,z)

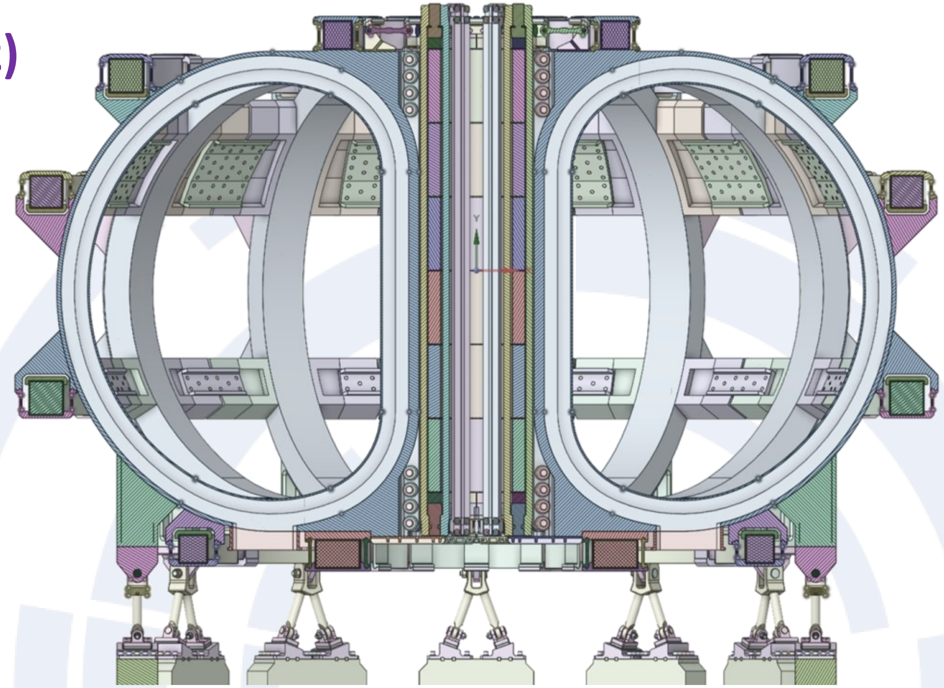

- The TF coil shape is based on an initial *bending-free theoretical shape*.
- From this, we derived an *improved shape* by considering the magnetic field generated by **N coils**, rather than the ideal toroidal field.
- We then used a *set of three tangent arcs* to best approximate this theoretical shape.
  - The result is a *lower coil profile*, which minimizes the distance between the plasma and the control coils.
  - As a consequence, the required currents in the poloidal coils can be reduced, improving the *overall machine performance*.

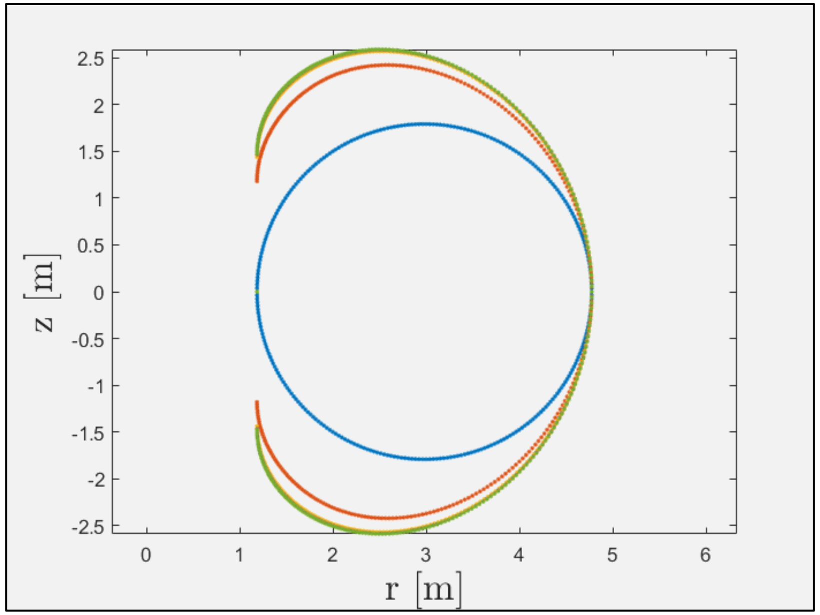

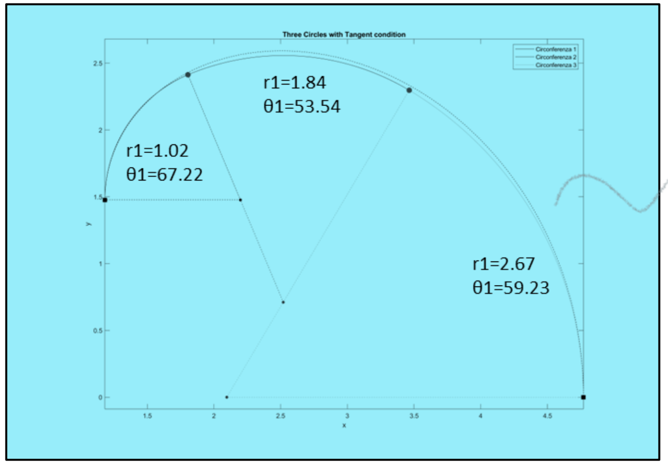

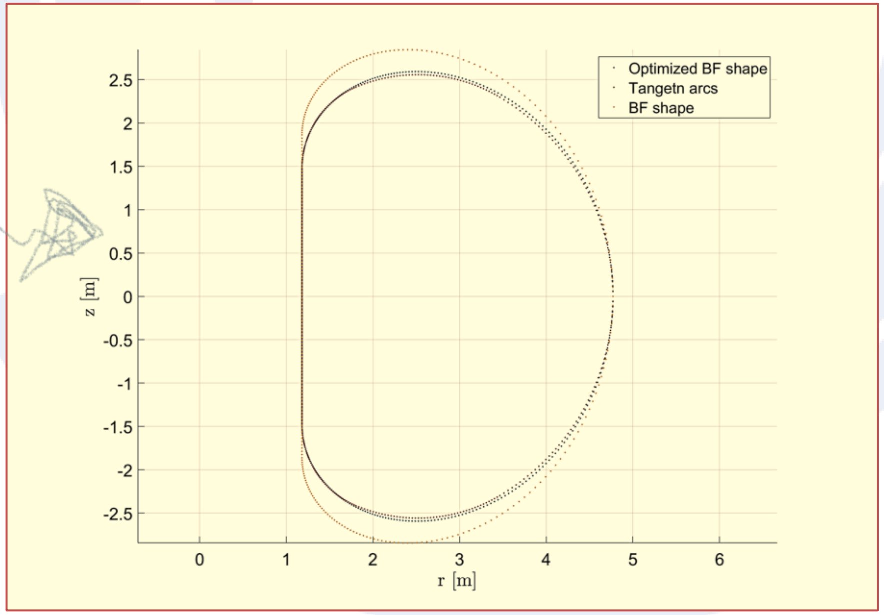

TFC – LTS WP

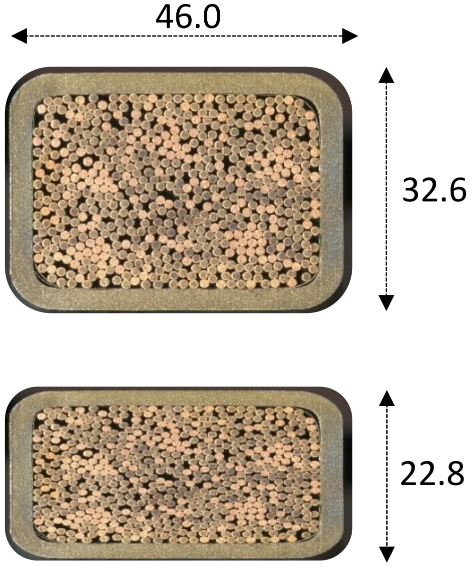

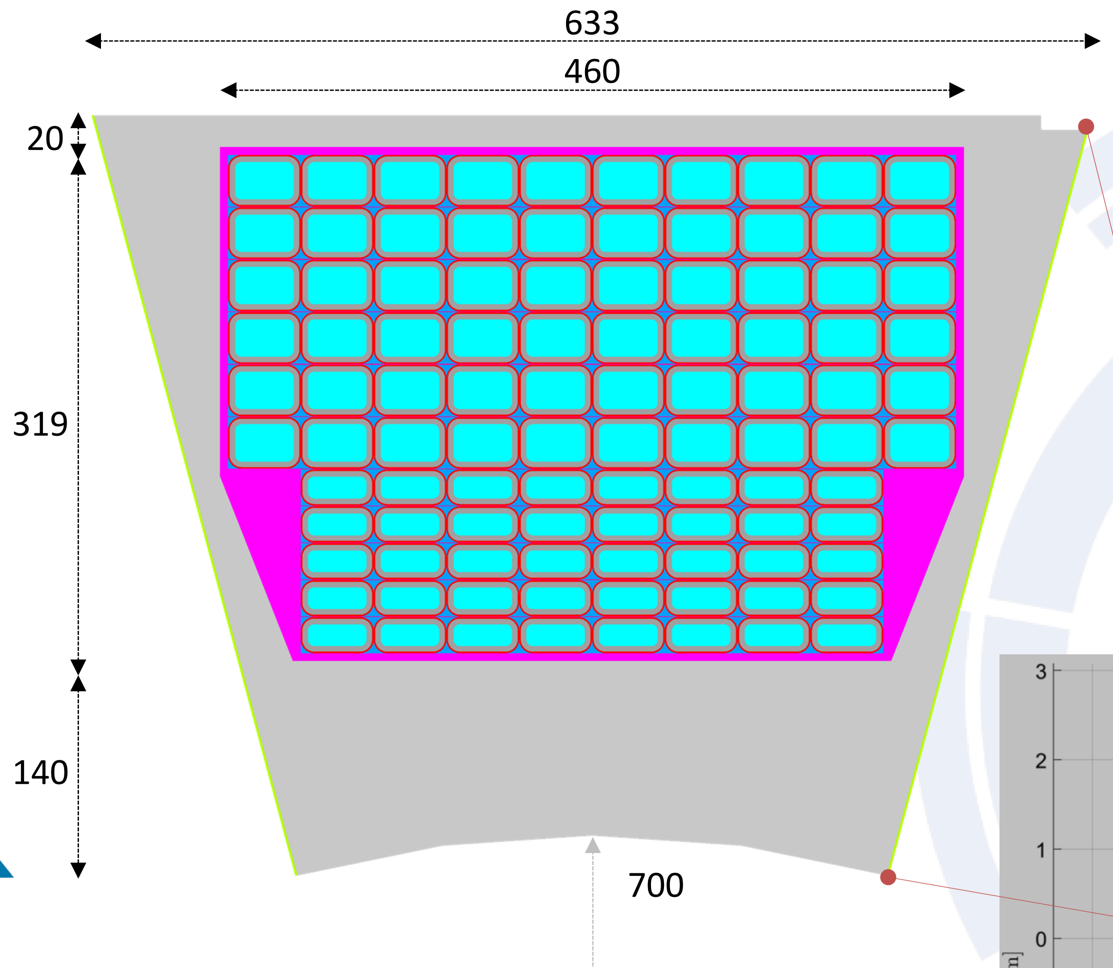

Two grades of conductor used (HF and LF) to reduce cost and compactness

Conductor	HF	LF
N layers	6	5
N turns	10	8
Width [mm]	46	46
Height [mm]	32.6	22.8
Jacket 316LN [mm]	3.5	3.5
Turn insulation [mm]	1	1
Ground insulation [mm]	5	5
Layer insulation [mm]	0.5	0.5
jacket material	316LN	316LN

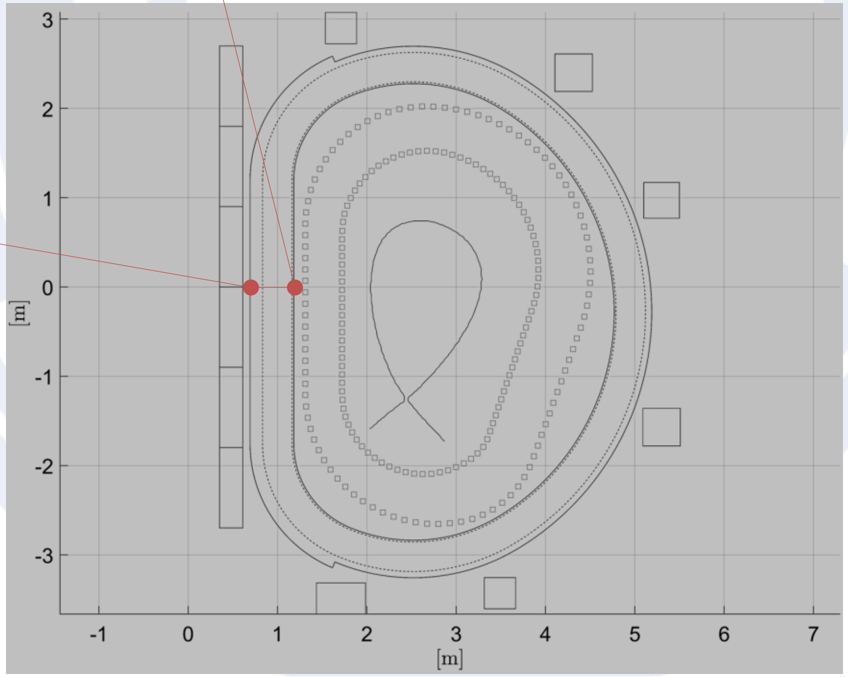

Already qualified strand

Ic Nb3Sn DTT TF KAT	
Strand diameter [mm]	0.82
Deviatoric strain	36.04
Deviatoric strain	0
Hydrostatic strain	0.0022
Thermal pre-strain	0
Maximum upper critical feld [T]	27.6
Maximum critical temperature[K]	16
Pre-constant [AT]	25304
p	0.5
q	1.75
Cu : non : Cu	1

ENEA

T [K]	5.7	5.7
Intrinsic strain (W&R)	-0.0055	-0.0055
Ic [A]	98.5	806
Iop [kA]	**62.3**	**62.3**
B max [T]	13.5	5.3
Strand Nb3Sn	635	78
Non segregated Cu strand	0	376
T hotspot [K]	250	250
Cooling channel diameter [mm]	5	5

3D electromagnetic loads

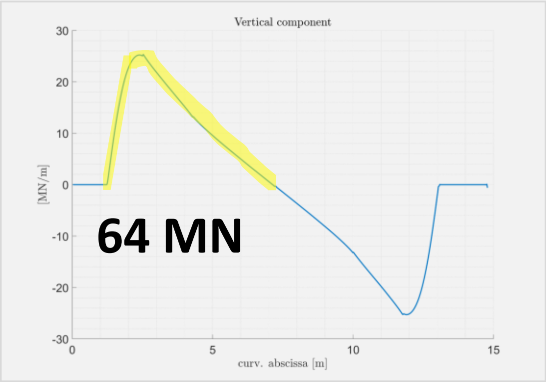

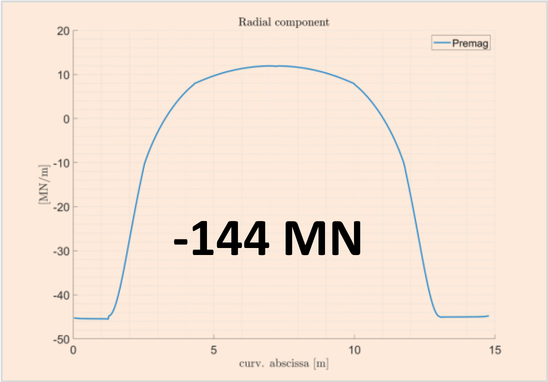

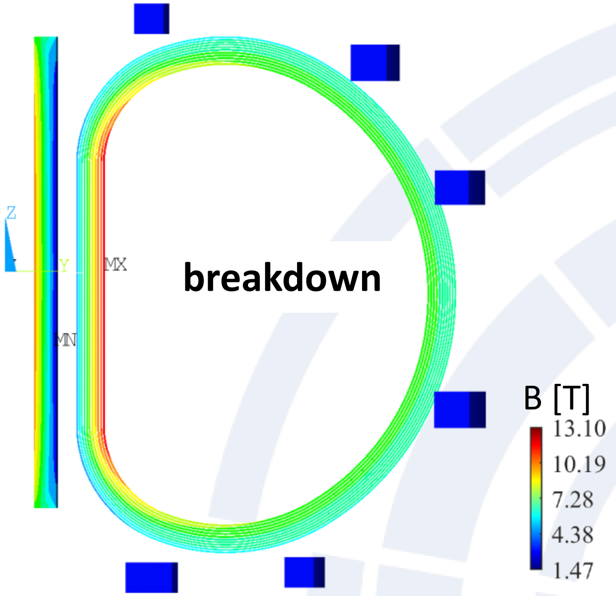

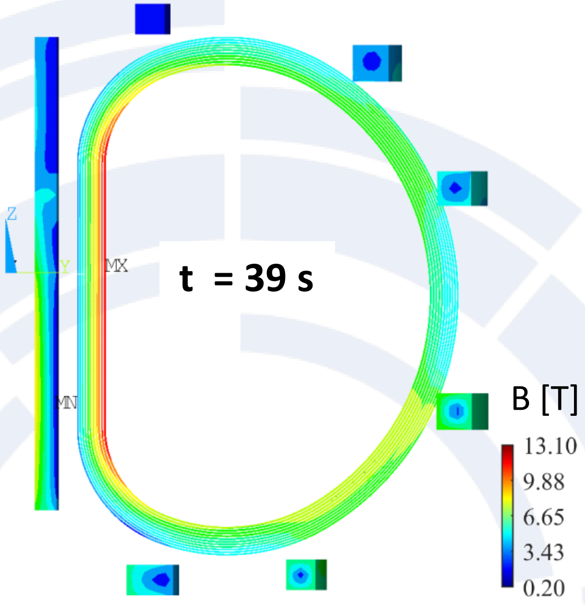

Current Scenario

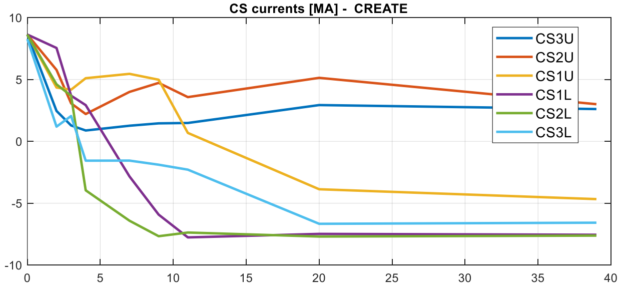

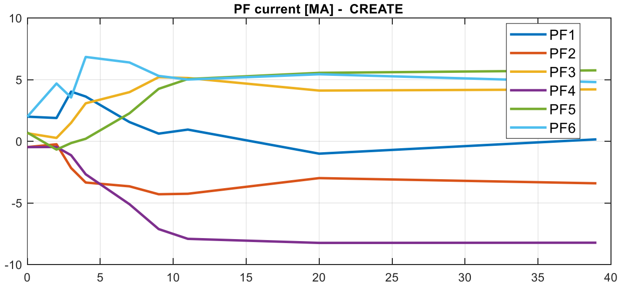

Out of plane loads comparison

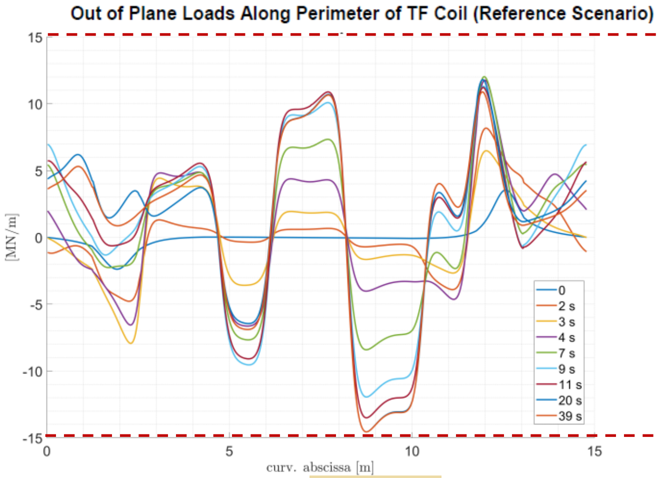

VNS

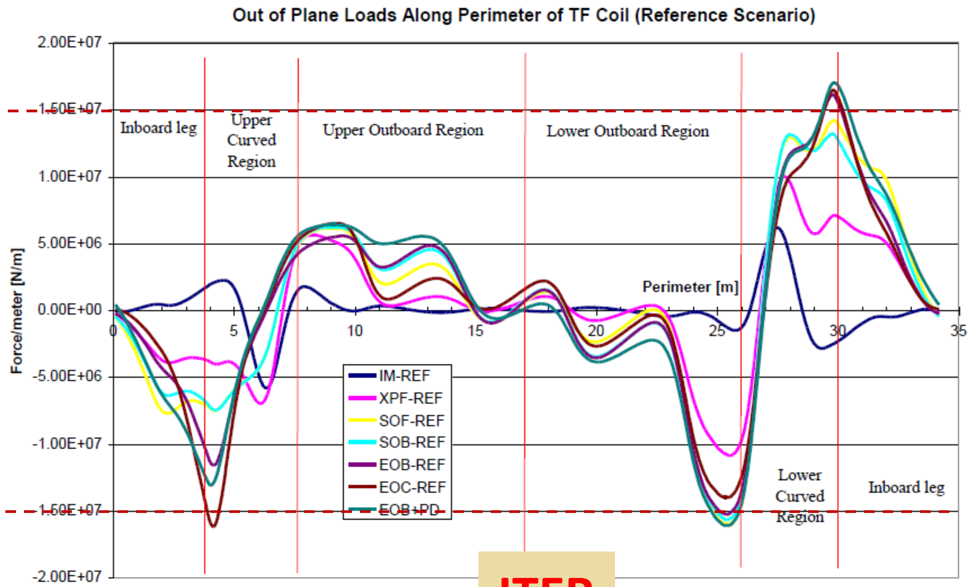

ITER

TFC – 3D structural assessment

- The aim of this initial runs is to assess the stress levels on the casing considering in-plane (IP) and out-of-plane (OOP) loads
- Several interfaces are managed by means of mechanical contact elements to capture the real stiffness of the magnetic cage
- The thicknesses of the casing, mostly on the outerleg, have been modified to reduce the stress levels
- **The upper OIS will be massively reduced in the next iteration**

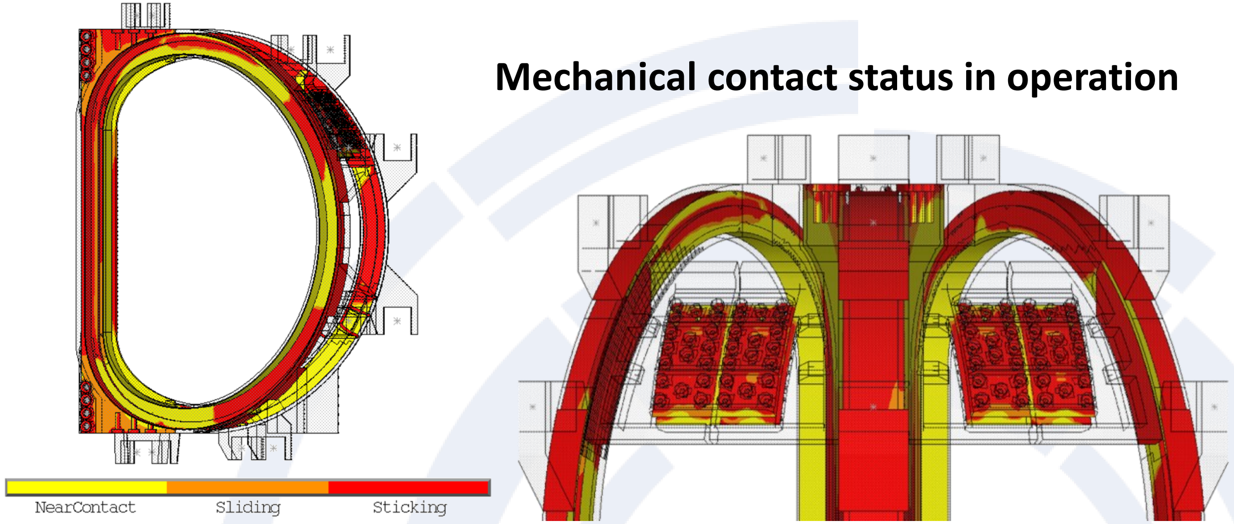

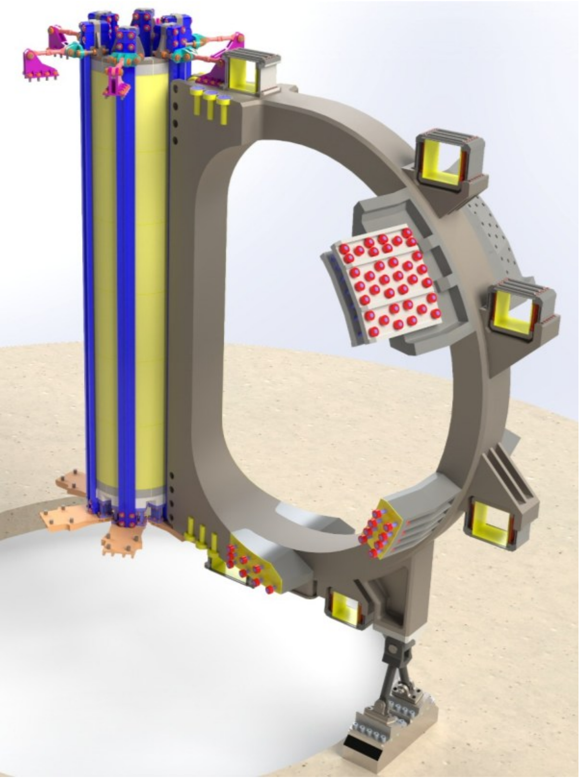

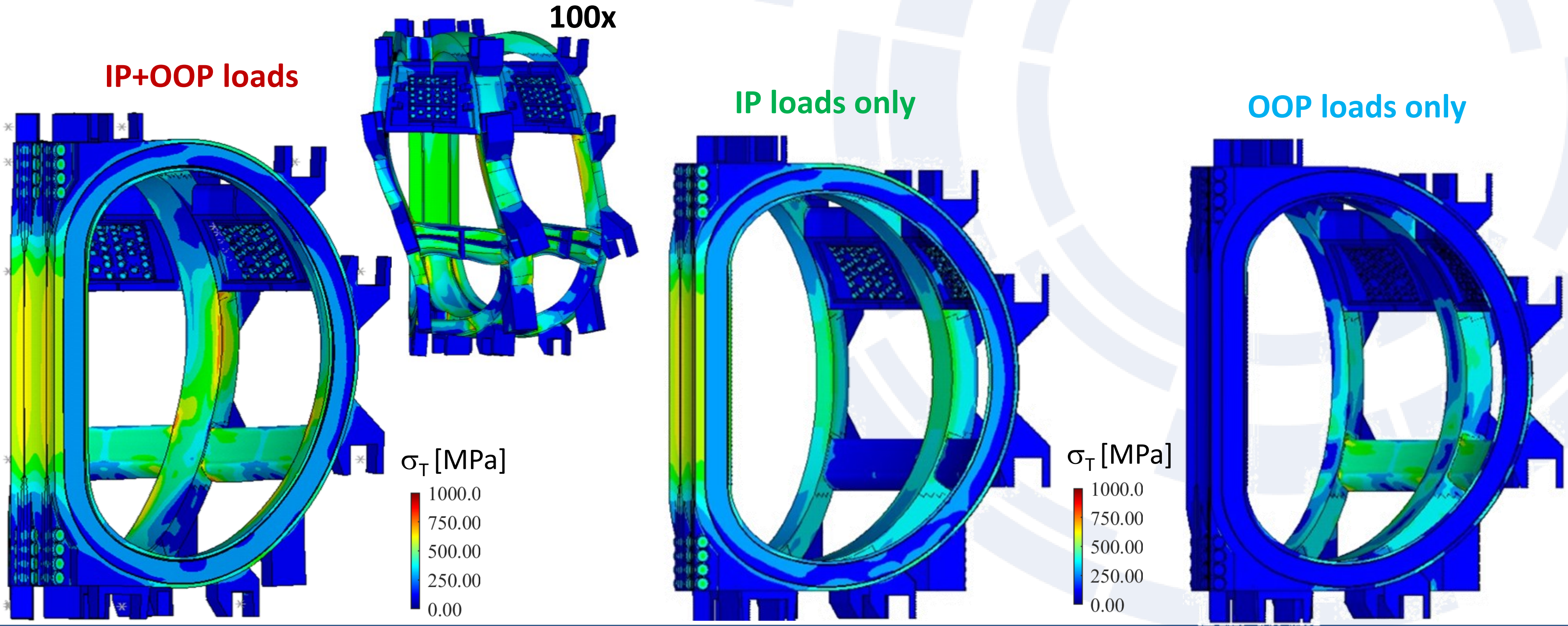

TFC – 3D thermal-hydraulic assessment

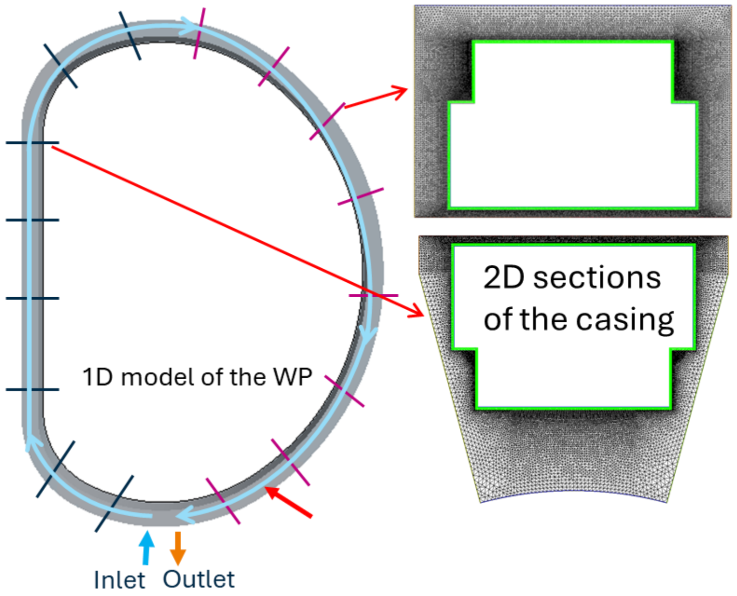

Magnetic field and cooling path

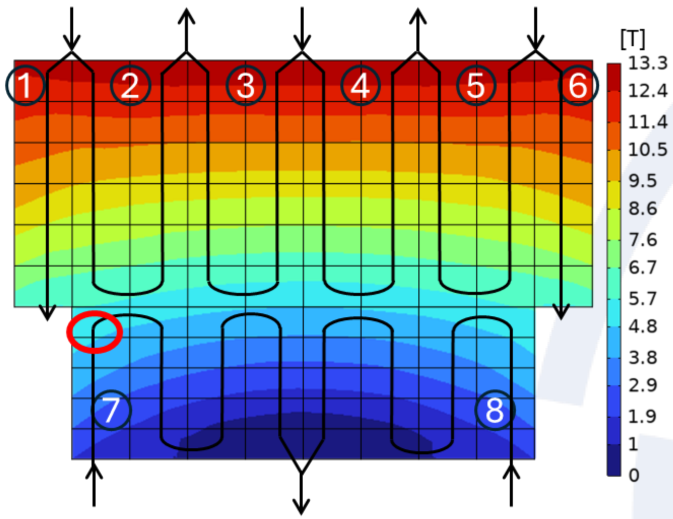

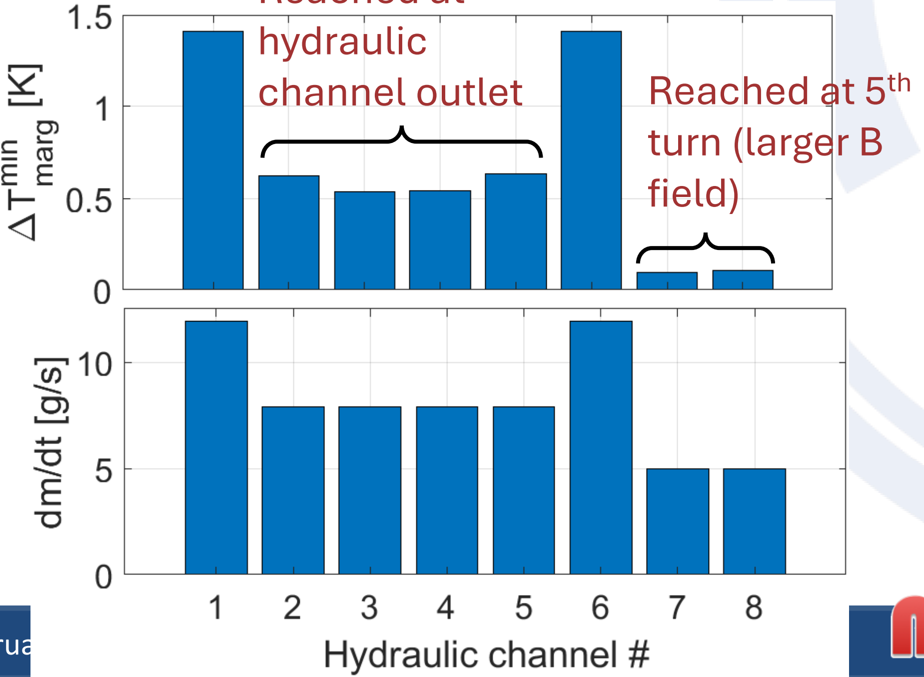

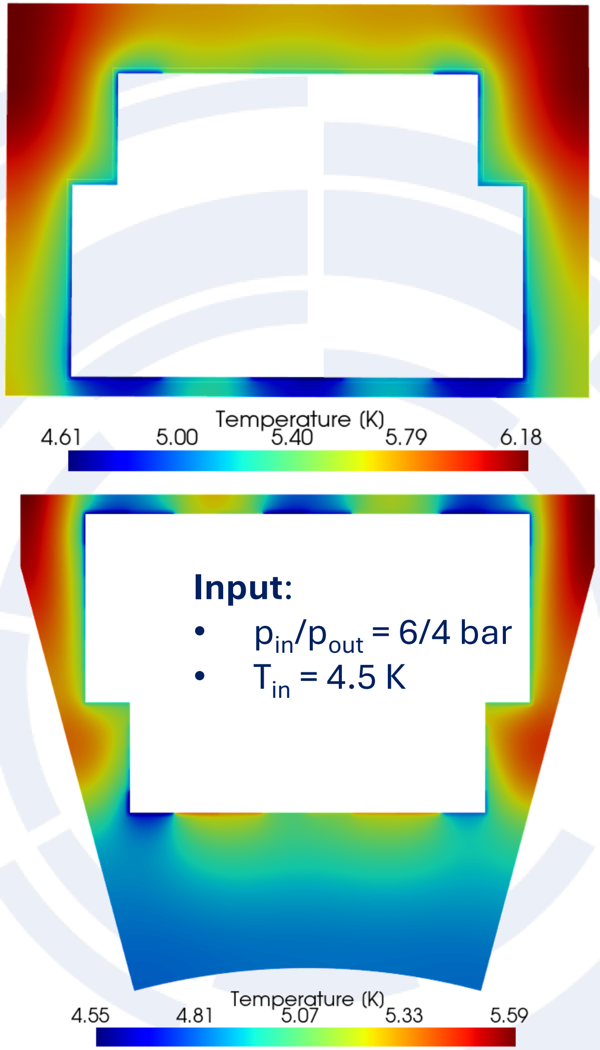

The models solves:

- 1D flow of He (v, p, T) along the cooling channels
- 2D heat conduction (T) in each section

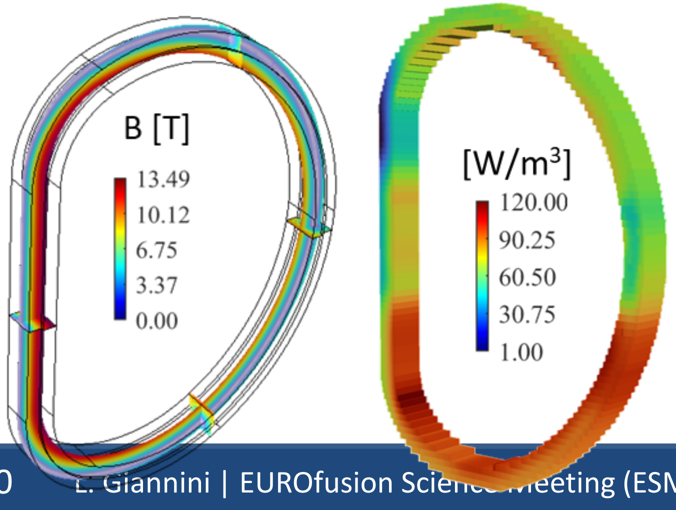

Preliminary results

1. **Nuc load on casing could be handled by the He in the WP**
2. **This task is ongoing**

CS – Winding Pack

- CS coil is not a challenging magnet in VNS

Conductor	
Width [mm]	22
Height [mm]	22
Jacket 316LN [mm]	3.3
Turn insulation [mm]	1
Ground insulation [mm]	4
Layer insulation [mm]	1
Jacket material	316LN

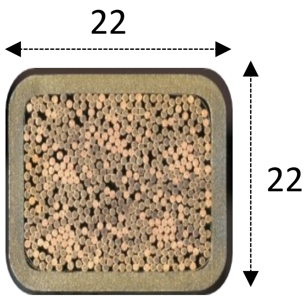

Nb3Sn conductor

DTT CS strand parametrization	
strand diameter [mm]	0.82
Deviatoric strain	44.48
Deviatoric strain	0
Hydrostatic strain	0.00256
Thermal pre-strain	-0.00049
Maximum upper critical feld [T]	32.97
Maximum critical temperature[K]	16.06
Pre-constant [AT] / A strand	20918.1
p	0.63
q	2.1
CunonCu	1
T [K]	5.7
intrinsic strain	-0.0055
Ic [A]	125
Iop [A]	**27500**
N strand	220
N Cu	0
Thotspot [K]	250

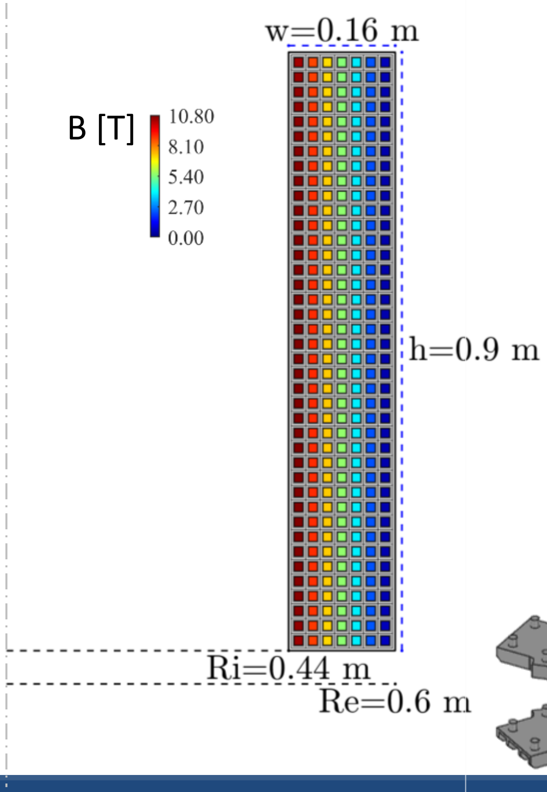

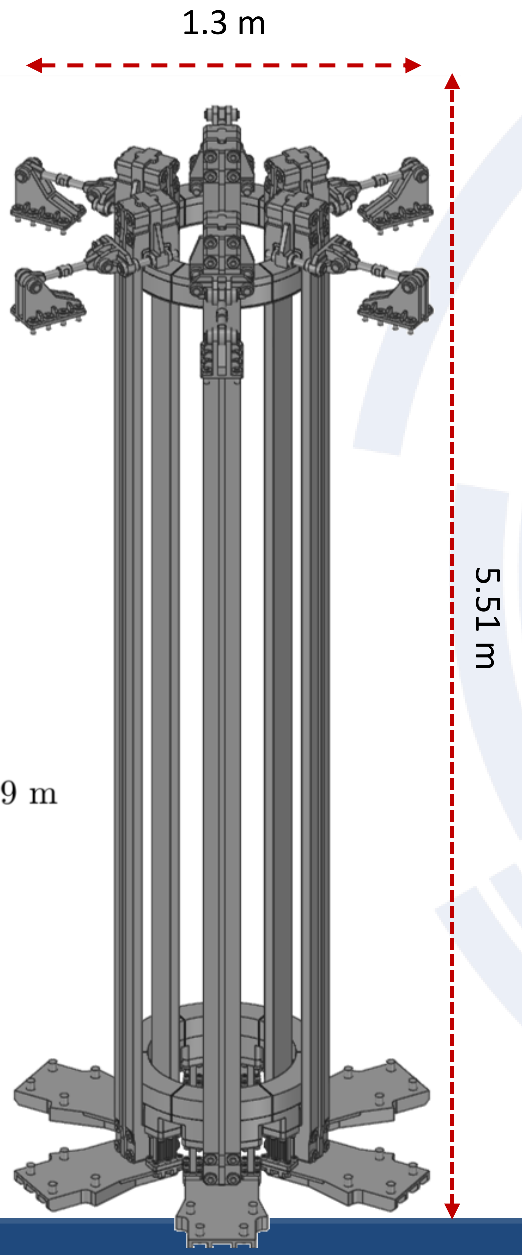

- VNS: 8 Wb in 1.2 m bore
- DTT: 17 Wb in 1.5 m bore
- The CS is used along with the PF system for plasma shaping

Width [mm]	160
Height [mm]	900
N module	6
Voltage term-to-term [kV]	2.5
Discharge constant [s]	1
Delay constant [s]	3
Jeng [MA/m2]	58
E CS stack [MJ]	108
Flux [Wb]	9.2
Stack weight	35 tons

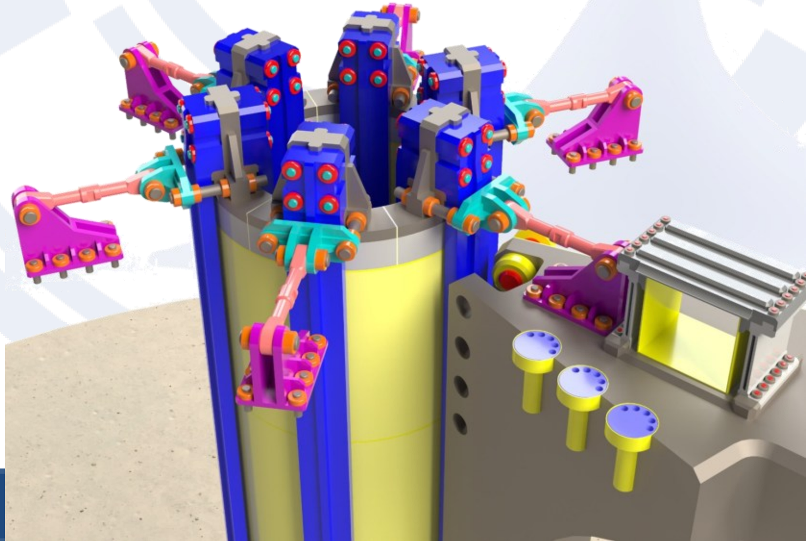

PFC – Winding Packs

	PF1	PF2	PF3	PF4	PF5	PF6
B [T]	6.2	5.7	5.4	6.0	6.0	7.9
Jeng [MA/m^2]	52	48	38	27	38	48
I_{op} [kA]	19.5	31	31	34.5	27.5	33
MAt (max)	4.1	4.3	5.2	8.3	5.8	6.8
N layers	21	14	12	15	15	26
N turns	10	10	14	16	14	8
SC mat	NbTi	NbTi	NbTi	NbTi	NbTi	Nb3Sn
Cond w [mm]	17	22	26	34	24	23
Cond h [mm]	22	29	32	37	30	30
Jacket 316LN [mm]	1.9	3.0	3.9	5.4	3.7	3.5
E [MJ]	48	181	319	719	225	118
Weight [t]	9	34	38	43	19	15

The PF supports were sized based on the ITER concept and can withstand the forces.

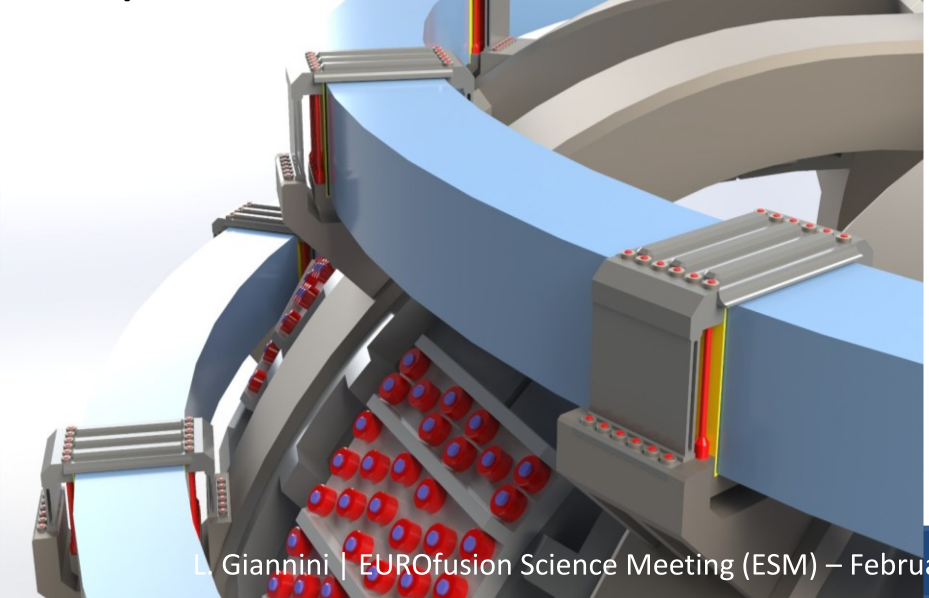

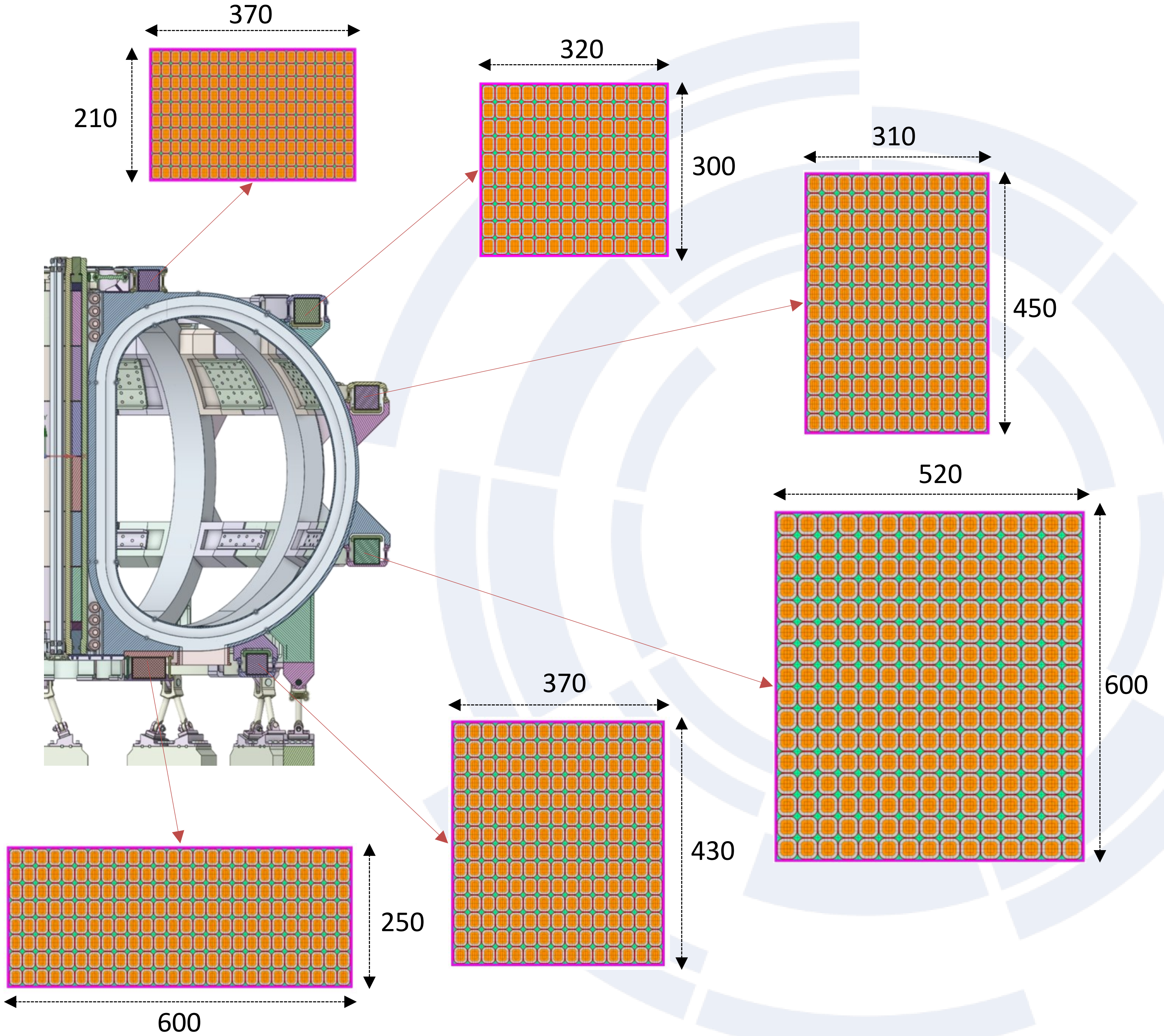

Magnet system description – PF-in-TF configuration

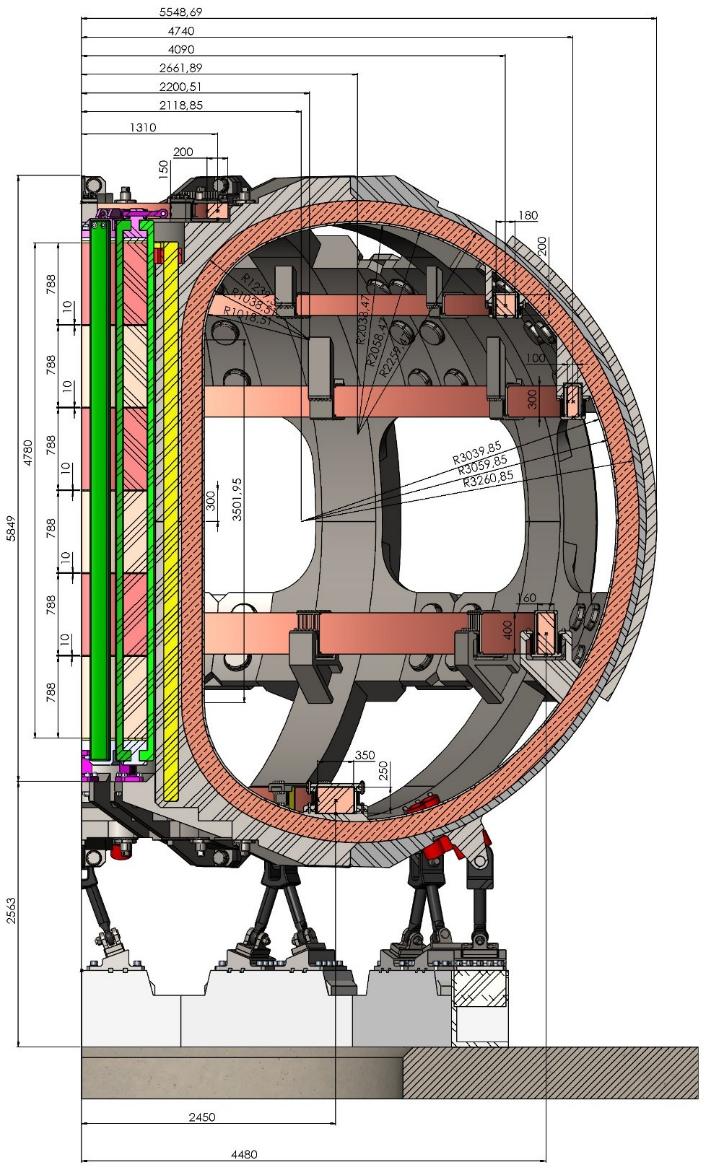

- The aim is to significantly simplify the PF coil system in a machine where the shielding is thick, and the coils are relatively far from the plasma.

- Develop and demonstrate an innovative tokamak assembly and manufacturing sequence that reduces complexity, risk, and cost.

Number of TF coils	12
Total current per coil [MAt]	6.23
J_{eng} [MA/m2]	65
Stored Energy (total) [GJ]	~4
Nominal peak field on TF coil [T]	13.2
Centering force [MN]	144
Hoop force innerleg [MN]	32
Length of the TF coil centerline [m]	17
Discharge time during quench τ [s]	4
TFC terminal voltage [kV]	2.5
TFC conductor concept	HTS dry conductor
TFC Winding scheme	6 pancake 3 internal joint

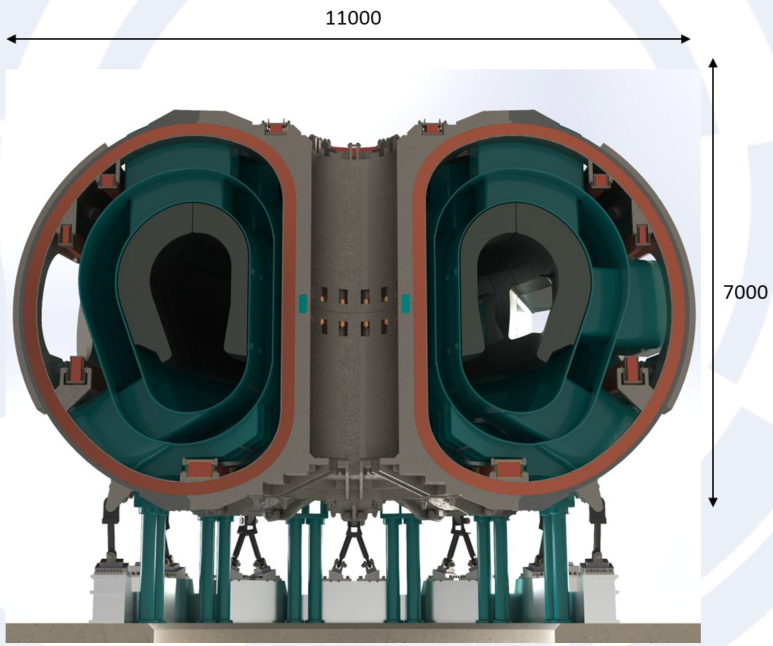

TFC Winding

Design based on ReBCO tapes in **LASSO** conductor (LAminated Stacked-tape Soldered) with co-wound strip for insulation and quench detection probes

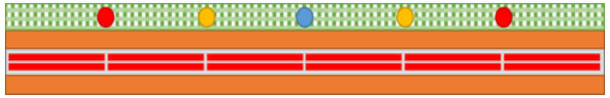

Iop 54.64 kA, 20 K operation + 5 K margin

Conduction cooling through in-parallel He lines around and inside (between pancakes) the WP

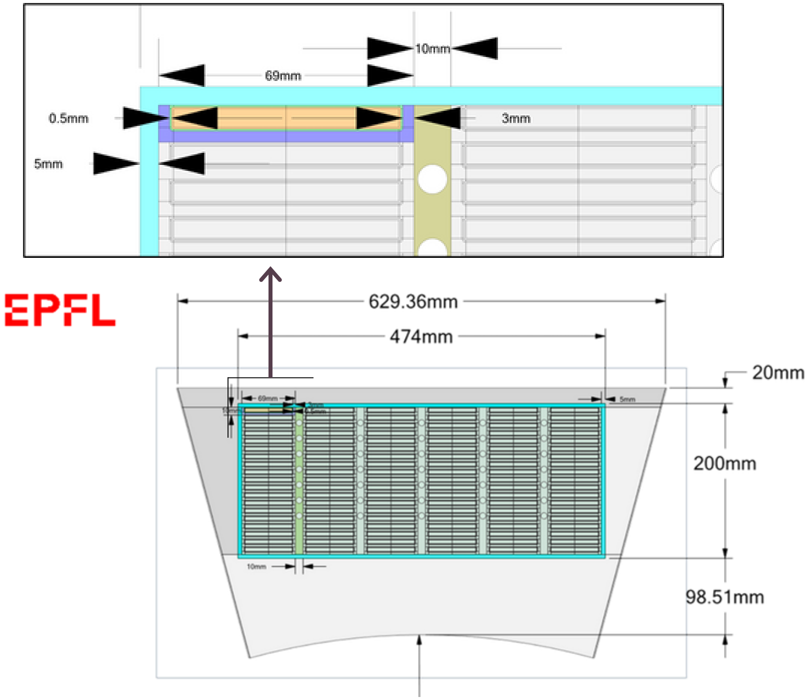

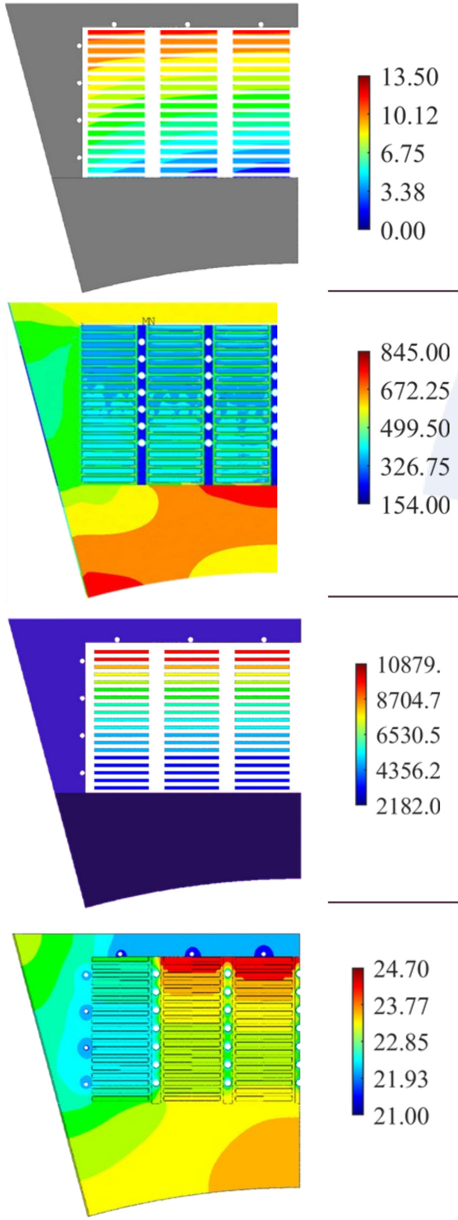

1 Electromagnetic Analysis

2 Structural Analysis

3 Neutronic calculation → nuclear heating distribution

4 Thermal-Hydraulic calculations

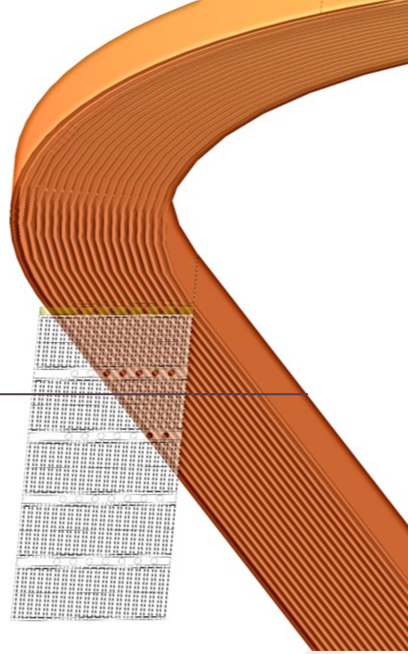

- **AC losses analysis ongoing**

TFC - Thermal-hydraulic assessment

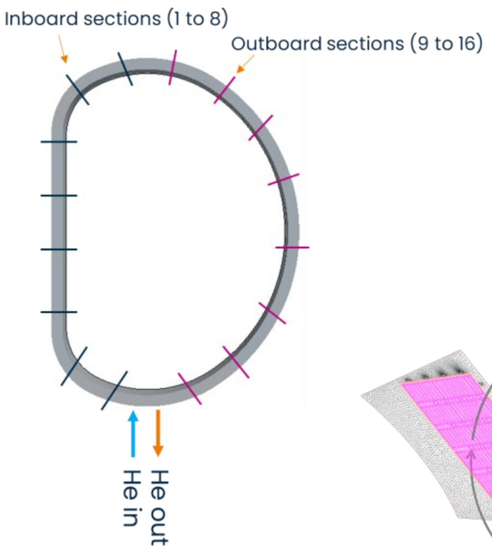

The models solves:
- 1D flow of He (v, p, T) along the cooling channels
- 2D heat conduction (T) in each section

The 1D He flow and 2D sections are thermally coupled (exchanging temperature and heat flux)

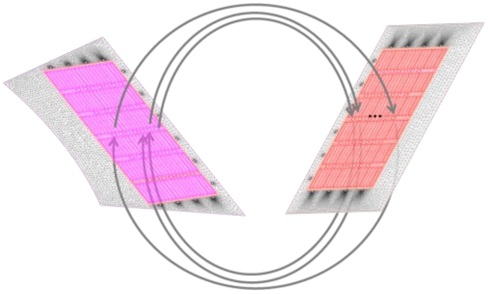

- Mass flow rate in each channel = 2 g/s
- p_{in}/p_{out} = 15/14.8 bar
- T_{in} = 20 K
- Ic(12 T, 20 K) = 130 A
- Nuclear heating deposited in the TF sections

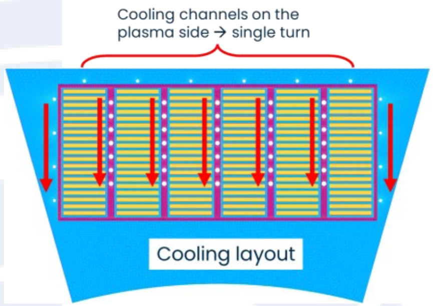

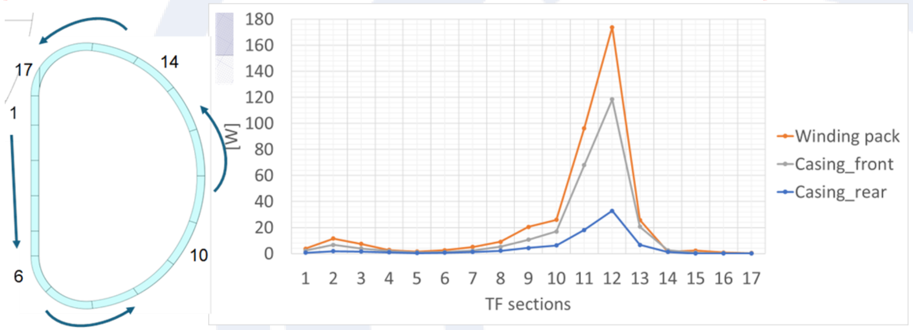

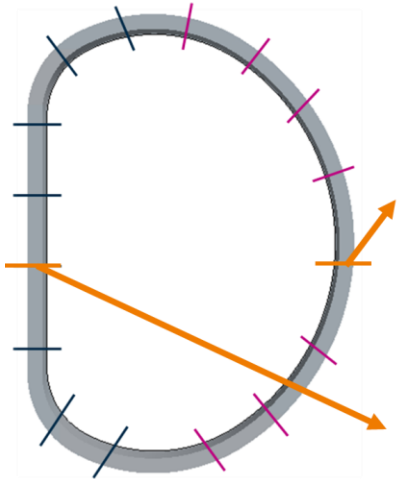

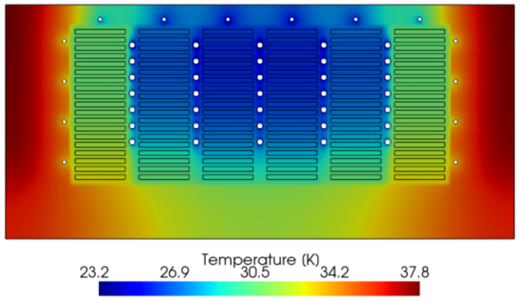

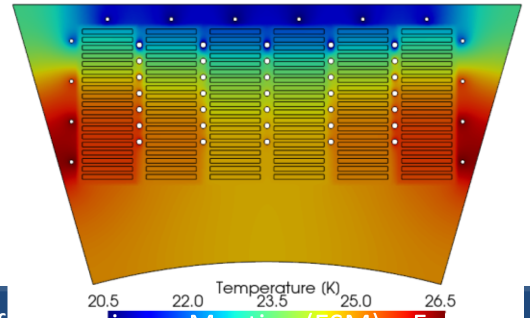

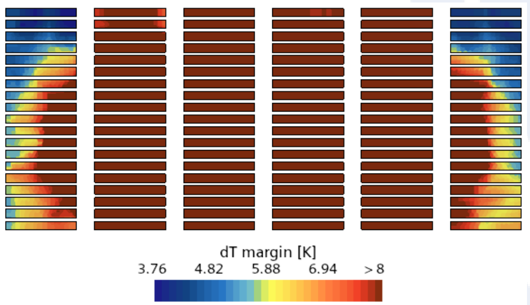

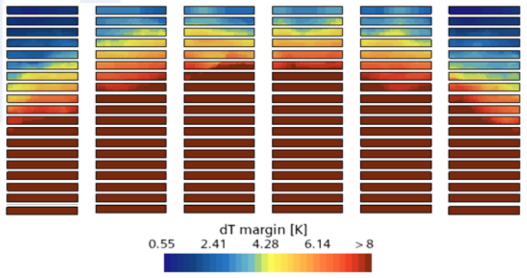

- Strong heating on the outboard section is handled with this cooling layout
- Minimum margin on the inboard section in the side pancakes (due to heat coming from the case)

WP & conductor design - Quench Detection

Conductor path

4 double pancakes

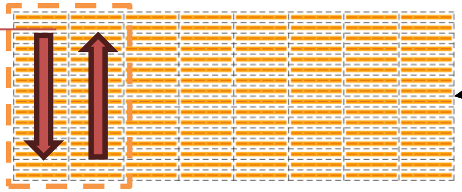

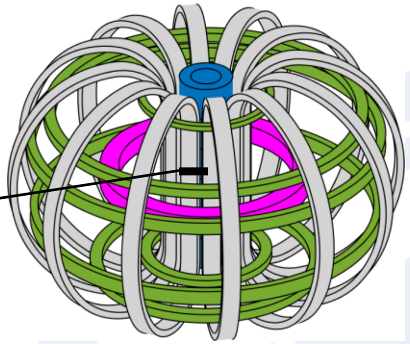

→ Conductor requirements:

- Operating current ~50 kA at 12 T peak field
- Stored on a winding spool of OD ~1.2 m

CICC not applicable, instead we consider thin and wide conductor cooled indirectly:

1. ReBCO tapes in laminated stacked-tape soldered (LASSO) conductor:

2. Nb_3Sn wires in two-stage *or* two-ply single stage Rutherford conductor:

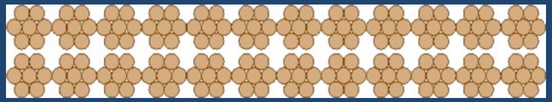

Both concepts being developed at SPC, short conductor pieces already manufactured

Three Quench Detection methods (developed at SPC) having in common:

- Temperature-based response
- Immune to EM noise and mechanical strain
- Potentially, non-invasive instrumentation
- So far, none of them tested on large magnet

1. SQD twisted-pair

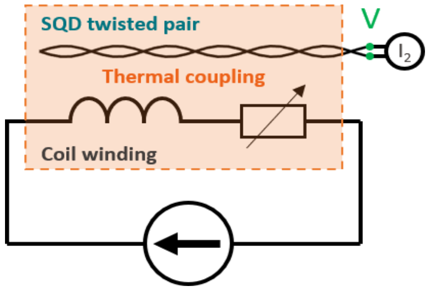

→ measuring resistance of SC quench detection (SQD) wire

Pros: distributed spatial sensing, sensitivity controlled by I_2

Cons: limited choice for Tc(B) threshold

2. Thermocouple chain

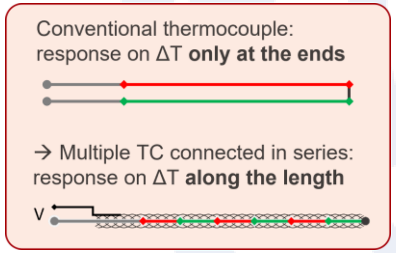

→ measuring voltage over series connected thermocouple wires

Pros: continuous response on temperature gradient among joints

Cons: discrete sensing

3. FBG optical fibers

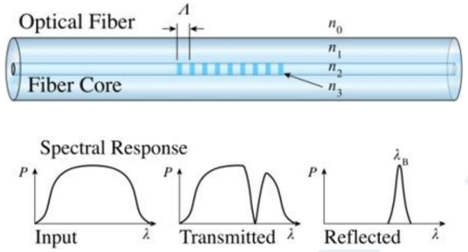

→ measuring spectral shift of light reflected by each FBG

Pros: continuous temperature monitoring at each FBG location

Cons: brittle, high resolution over long length is cumbersome

HTS model coil – Phase

- In collaboration with CERN and F4E developing a European program to demonstrate **the feasibility of quench protection** in High Temperature Superconducting (**HTS**) coils at a scale relevant for VNS or the Muon Collider
- A phased approach:
  - I. Show feasibility of quench detection methods **(< 1 MJ) - completed**
  - II. Show feasibility of integrated quench protection in sub-scale coil **(~ 10 MJ)**
  - III. Show feasibility of quench protection at full-scale for VNS **(300 MJ test coil)**
- Phases I and II carried out in JORDI facility at EPFL-SPC, Phase III requires a new dedicated test facility
- Program completed within ~ 5 years
- 300 MJ model coil itself can then become a permanent high-field test facility (20 T) for the development of HTS components

PHASE I

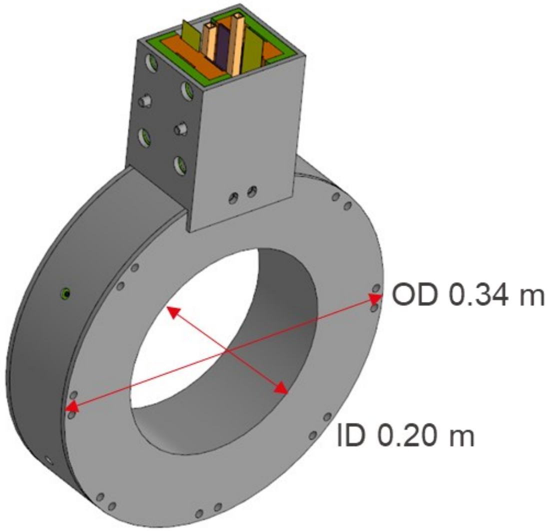

Double pancake HTS coil:

- ~70 m long LASSO cable using varying number of tapes along the length (18 to 14)
- Pancake transition by a splice made of copper strip soldered to cable terminals
- Cooling pipe placed between the pancakes
- Diagnostics by voltage taps, temperature sensors, strain gauges, hall probes and heaters
- Quench detection by a co-wound instrumentation strip containing SQD wires, thermocouple arrays and optical fibers

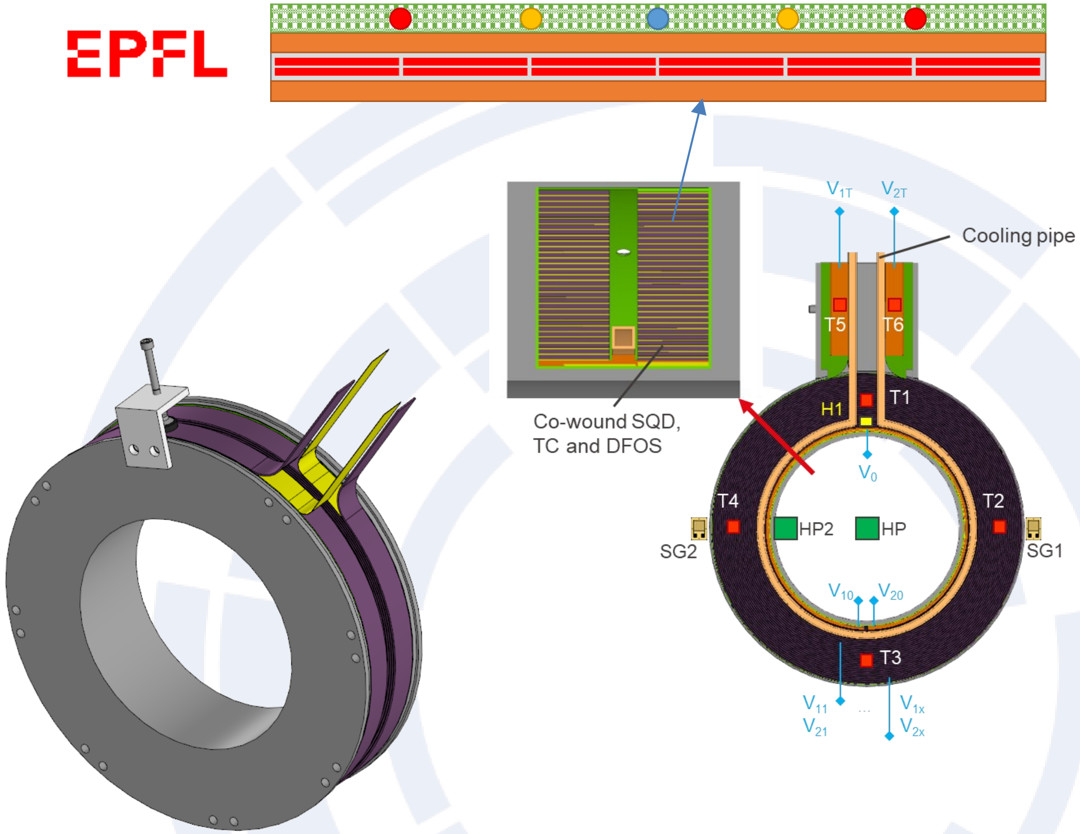

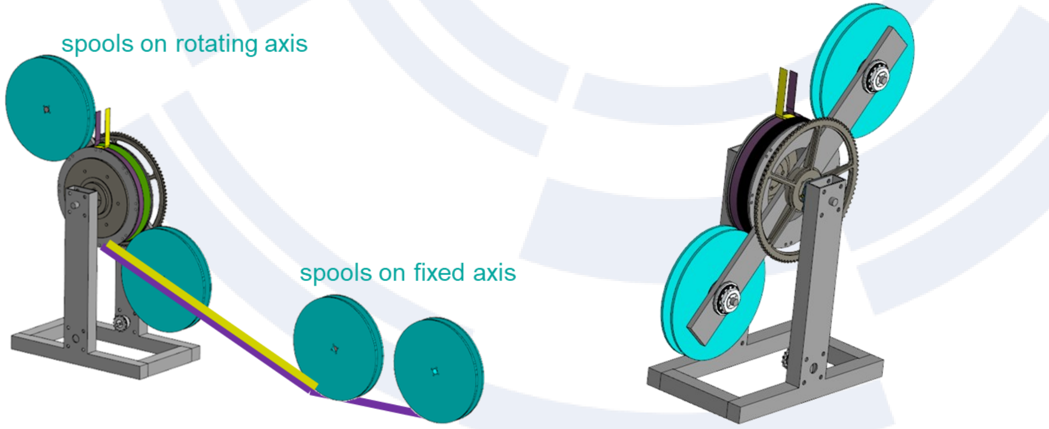

Assembly sequence – In-situ winding

See L. Giannini et al.,
https://doi.org/10.1016/j.fusengdes.2024.114530

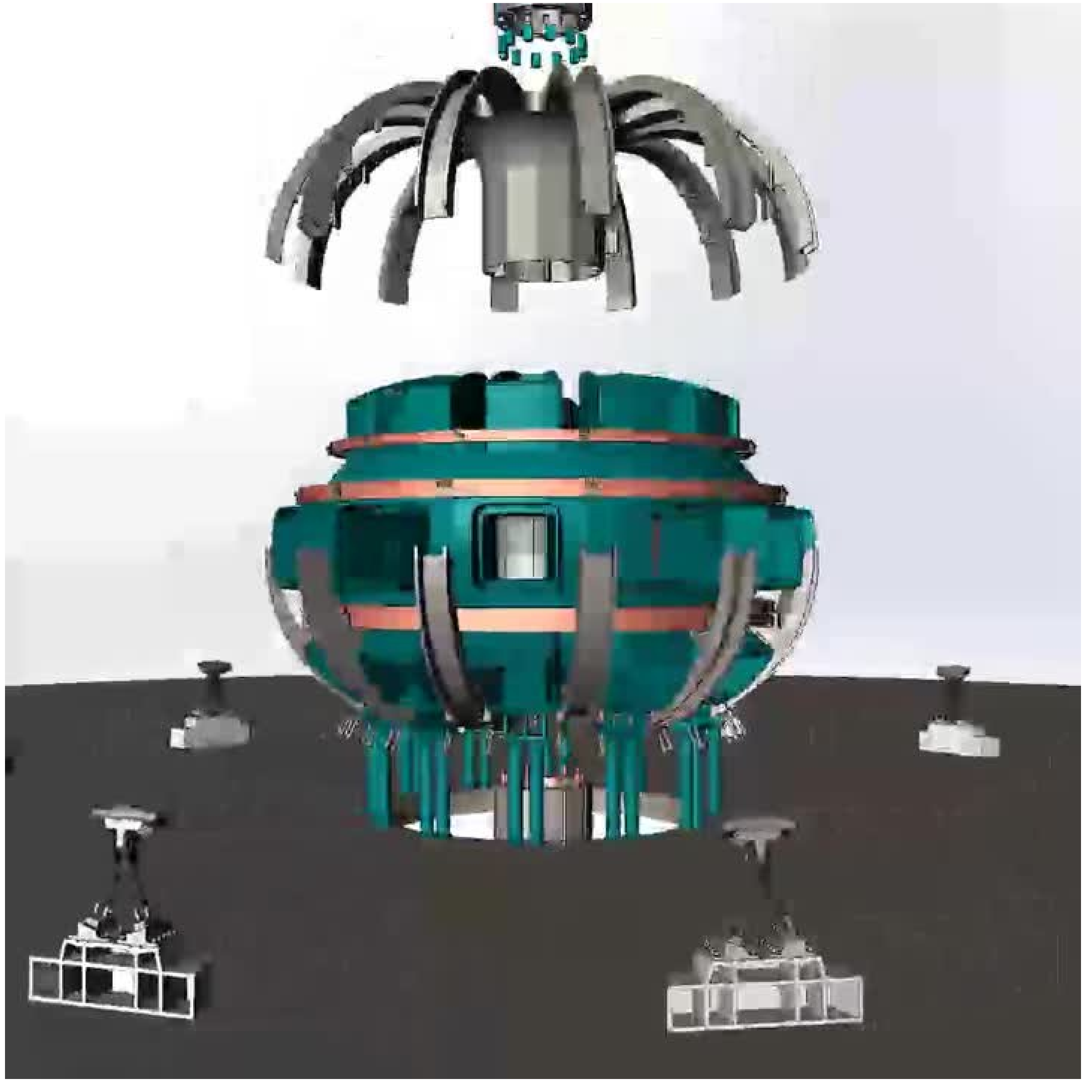

Point 01

Vessel as a single piece.

The process begins by inserting the vessel with its supports into the lower sector, which is formed by half of the inner casing shell.

This single component is prefabricated and tested by welding together 12 individual segments.

Point 02

After positioning the lower PF coils, the vacuum vessel is inserted and connected by its supports.

The upper PF coils, located within the TF coil envelop, are then installed.

Finally, the inner casing is closed by adding the second half of the casing shells, which has also been pre-fabricated and tested beforehand.

Point 03

To avoid several in-situ weldings, the casing is reconstructed from three components:

1. a central bucking cylinder made of two halves joined at the midplane,
2. and an outer closing plate, which is joined to the central cylinder at the top and bottom.

Point 04

To ensure mechanical strength and to compress the outer closing plate, an additional external reinforcement is added.

This structure integrates with the outer intercoil structures, which are then secured using flange joints.

Assembly sequence – In-situ winding

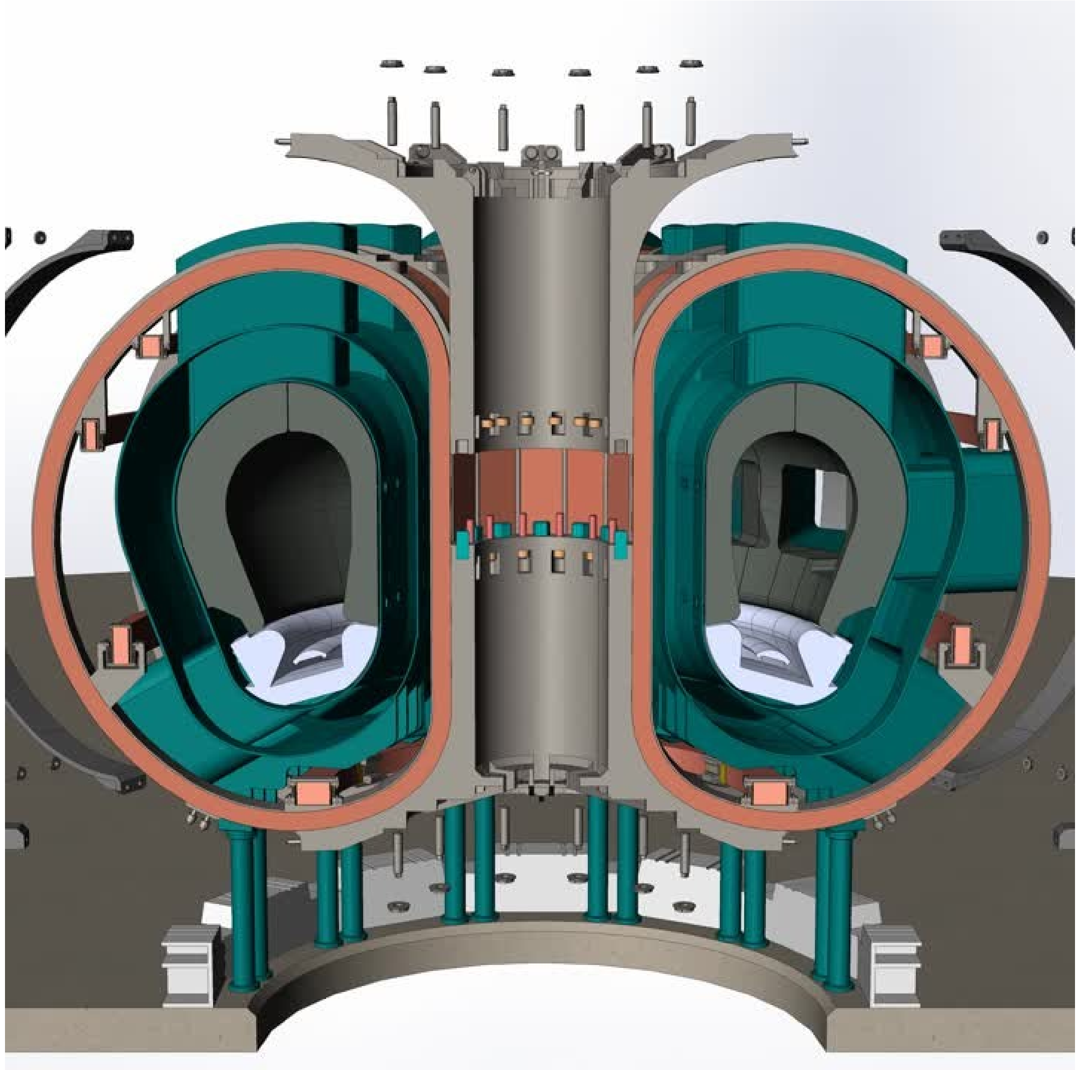

Point 05

The two halves of the central compression cylinder are inserted into the bore.

The cylinder is shaped to accommodate the windings in a JET-like configuration.

Point 07

A second set of bolt assemblies secures the cylinder to the inner casing shells.

We are currently evaluating whether to include dowel pins (spines) as part of this joint strategy.

Point 06

A set of bolted joints along the equatorial plane is under evaluation.

Their exact positioning will be defined based on structural analyses, to ensure they are not located in critical areas where the structure may not sustain the loads effectively.

Point 08

The top and bottom interfaces between the outer closing plate and the central cylinder are based on an inclined plane.

By tightening the horizontal bolts, pre-compression is applied to the winding pack.

Assembly sequence – In-situ winding

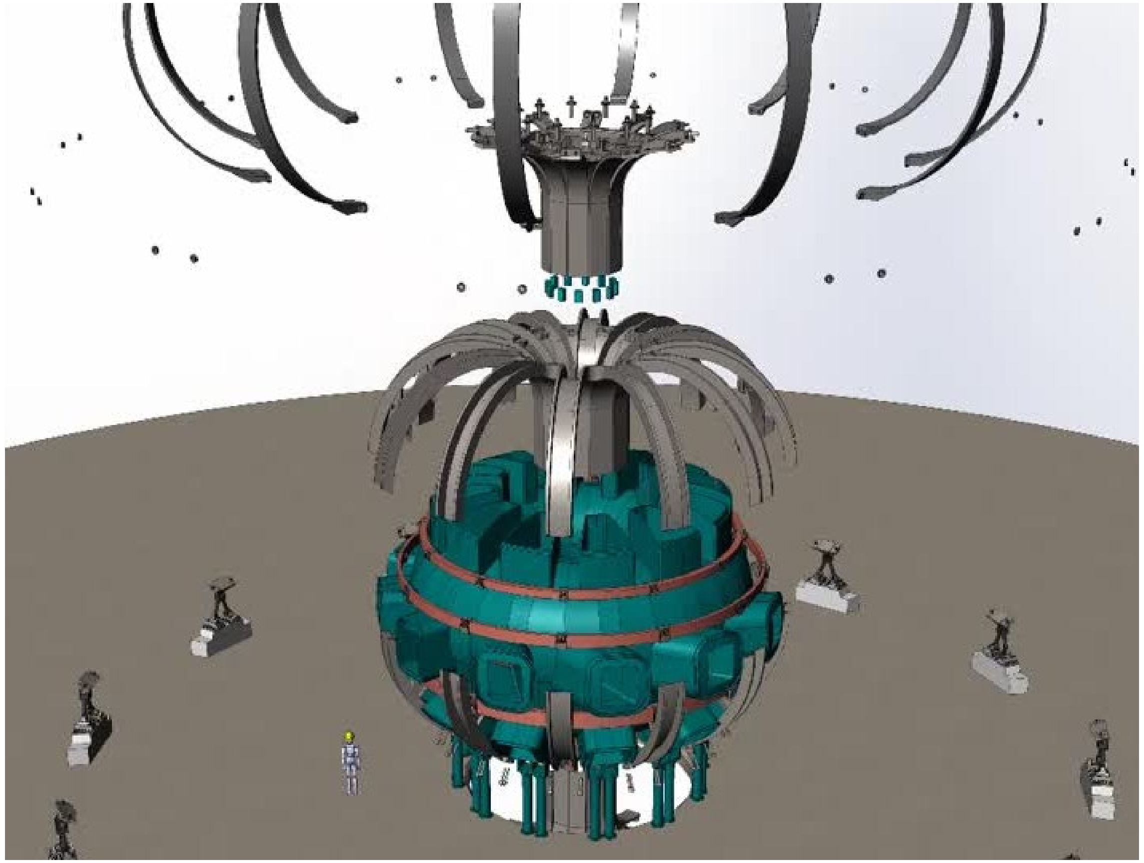

Point 09

The external reinforcement is inserted laterally to avoid welding the closing plate.

This component adds stiffness to the structure, which is already pre-tensioned by design.

Point 10

By connecting the external reinforcements with flange joints, a toroidally continuous cage is formed, capable of withstanding out-of-plane loads resulting from interactions between the magnetic systems.

Winding machine

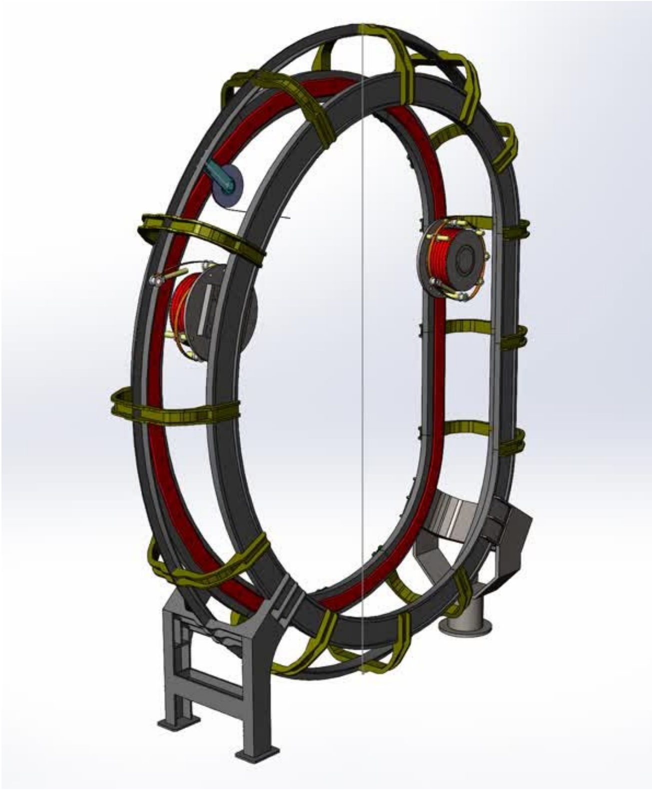

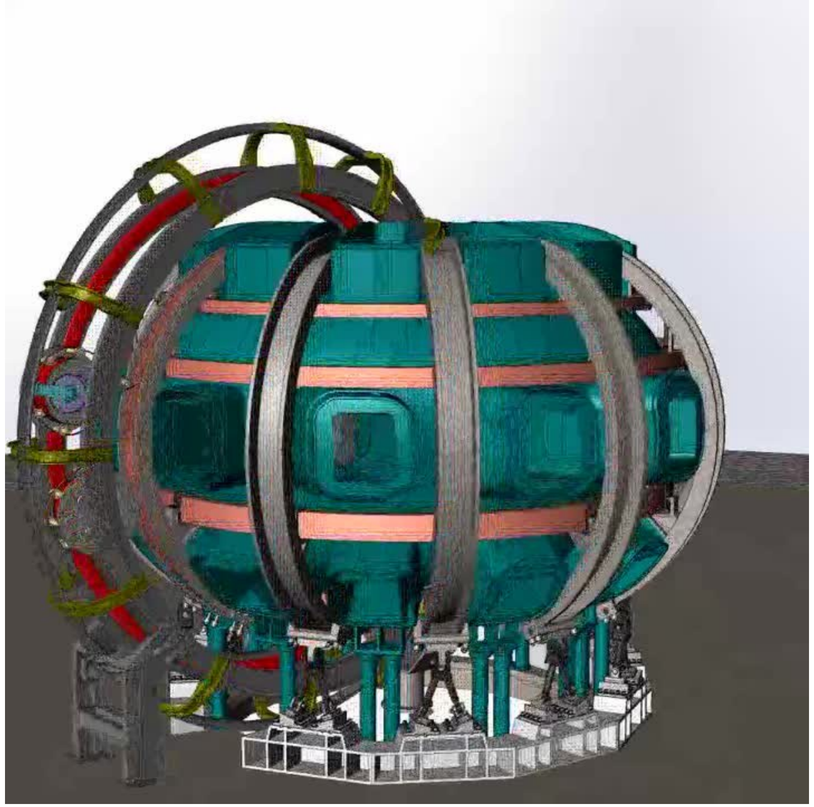

Point A

The winding system is based on double pancakes. Thanks to the high flexibility of the cable, the required lengths can be pre-wound on two spools and unwound in situ without damaging the tapes.

Point B

The system winds from the inside outward, completing one pancake at a time. Between the pancakes, parallel helium pipes are inserted to enable conduction-based cooling.

Point C

Currently, the TF coils are wound in series, one at a time. The structure can rotate internally to move from one TF coil to the next.

Point D

At the end of the winding process, the coils are impregnated. Temporary vacuum-tight closing plates are installed, along with heaters to cure the resin.

Results of ASG study so far: in-situ winding feasibility

- The main issue is the lack of space that prevent the installation of a calender in-line
- **The minimum radius of the conductor spool is determined by the max bending strain the HTS conductor can tolerate and by the length of a winding layer**
- The conductor shall be already insulated owing to the lack of space to fit a taping machine in-line

- A study is ongoing at ASG to assess which is the best combination of tension and bending roller(s) pressure on the insulated conductor to allow its correct shaping around the D shaped casing, limiting the spring back to avoid conductor detachment from the profile

- Elastoplastic analysis is ongoing on a bulk copper conductor and on a s. steel jacket having the same outer dimensions

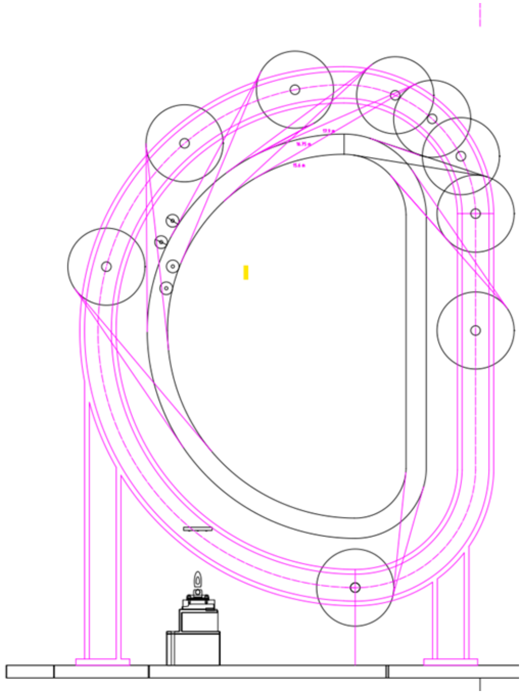

ASG SUPERCONDUCTORS magnets & systems unit

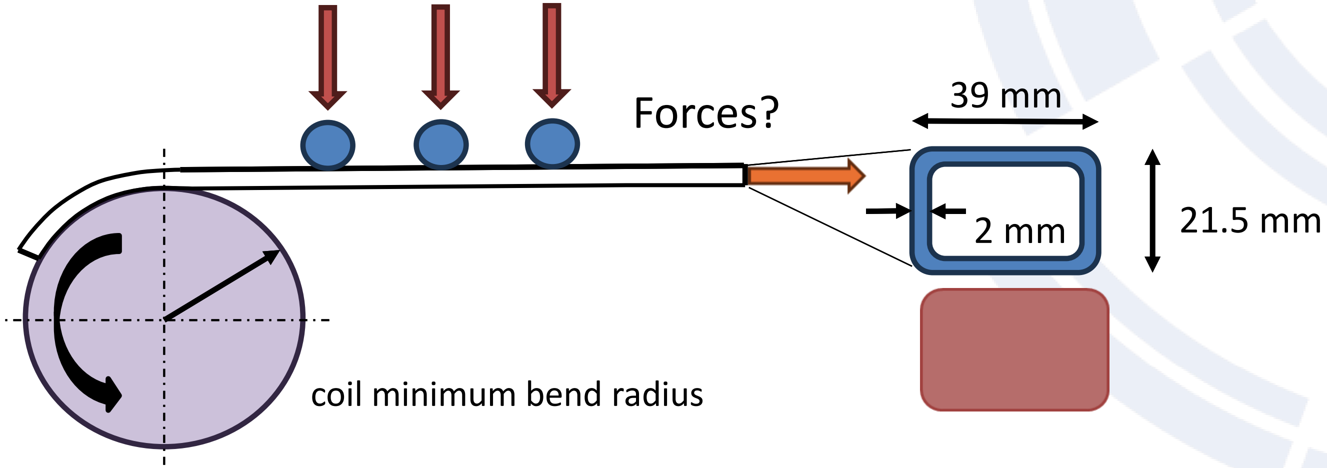

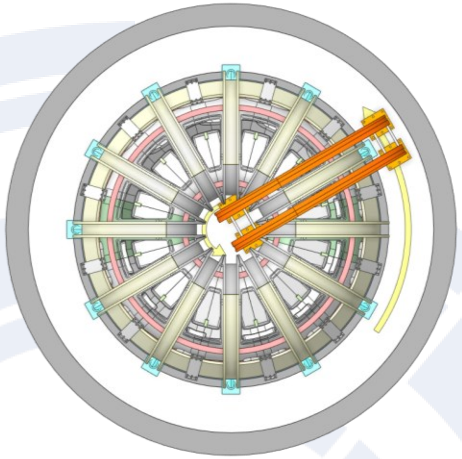

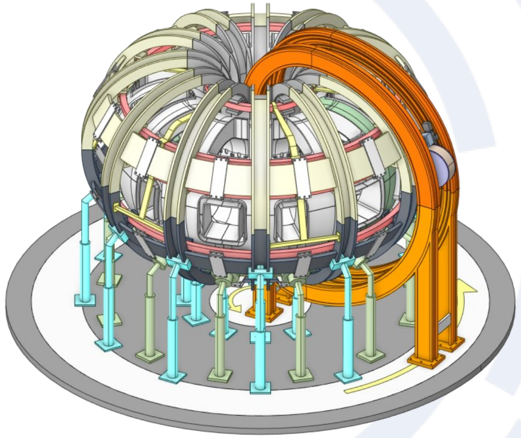

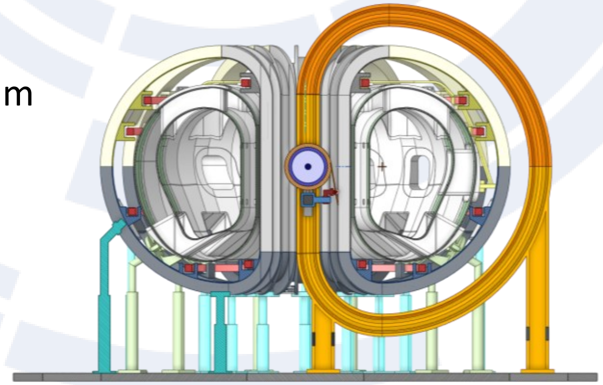

Portal winding machine - conceptual study

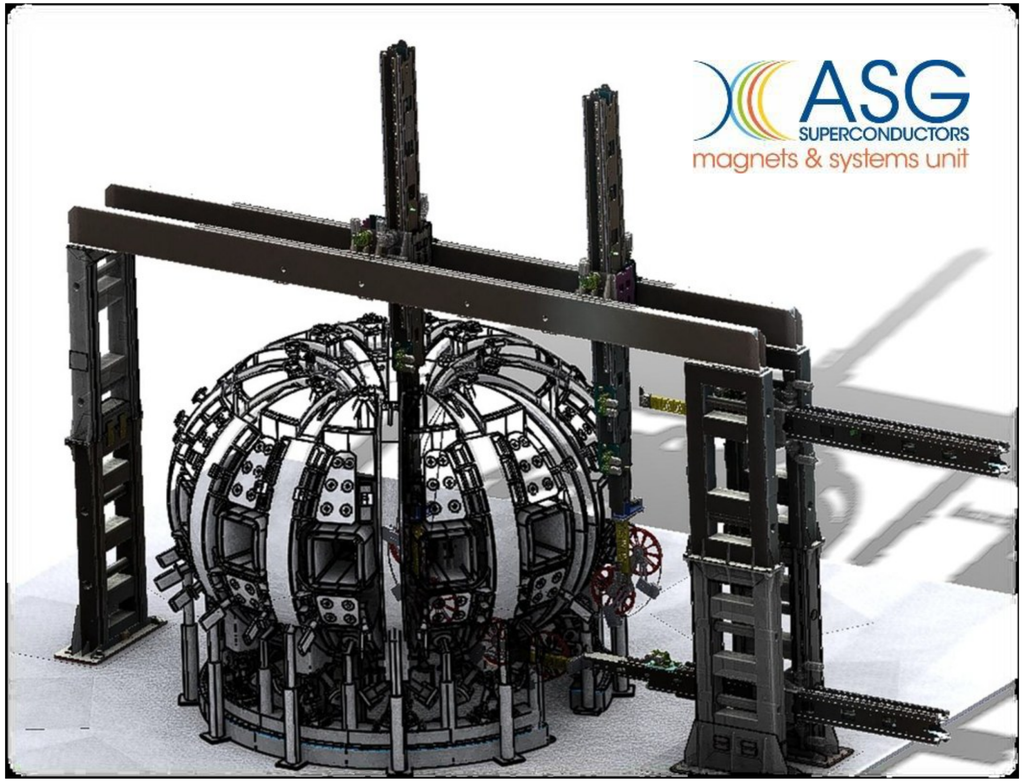

Supports of the TF case and VV **critical** (they should avoid local deformation of the nozzles and shells), the unitary bearing load is quite high, about 80 tons, and they should be retractable.

A different scheme of winding machine is being considered to assess pro and cons:

- The carriage with two spools (conductor and jacket) is moved in poloidal (azimuthal) direction by **four telescopic arms** (two horizontal and two vertical), one at a time. The carriage has a tilting movement around its horizontal axis (parallel to ground)
- The carriage has a cubical interface block, its bottom face is always kept level (parallel to ground) so the horiz/vert arms can get connected/released at the corners of a planar, rectangular path in space.
- **Quick electrical connections** could ensure a reliable feeding of the carriage, avoiding sliding contacts.
- In a more sophisticated version one horizontal arm moves in both horiz and vert direction guiding the carriage in a curved D path (outboard) then the vertical arm comes in guiding the carriage in vertical direction inside the vault.

Portal winding machine - conceptual study

- Each single group travels around the coil casing perimeter, the leading unit is the payoff group, followed by the straightening-bending unit and last the compaction unit.

- Each unit is passed in turn from one arm to the next by a quick connection joint that provides electric power and control signal to the group.

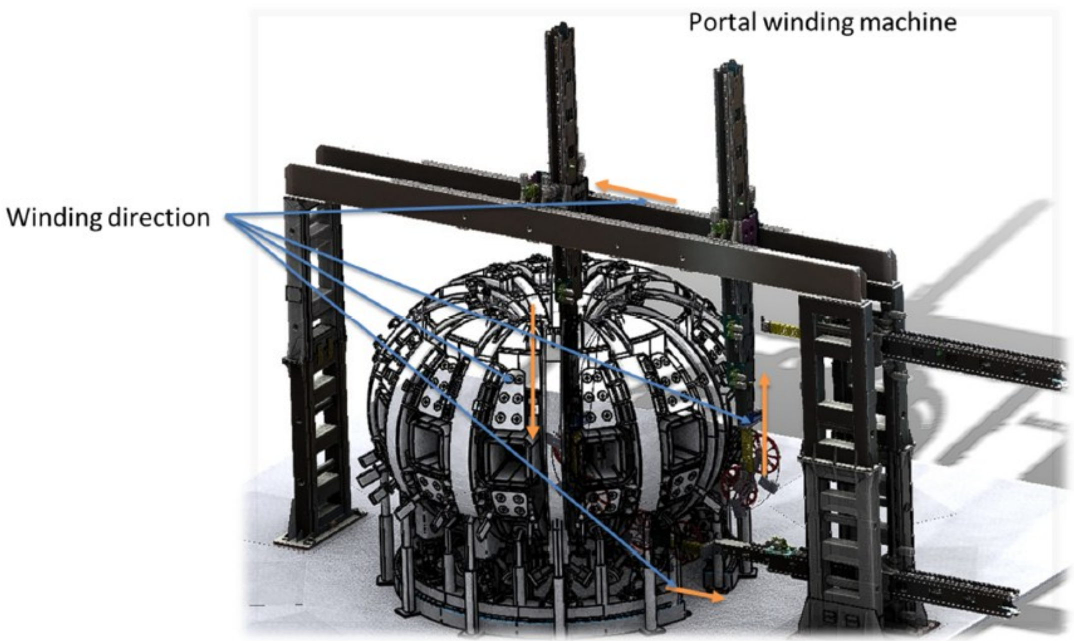

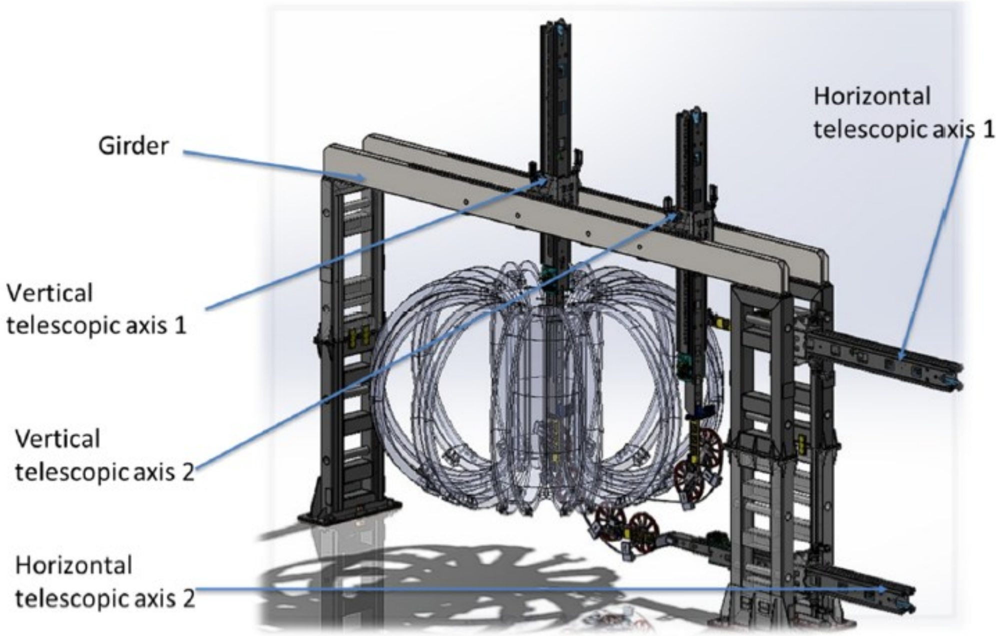

Portal winding machine - conceptual study

- The winding machine is moved from one TF to the next by releasing the pillar baseplates, lifting and rotating it using the overhead crane.

- The pay-off group is made of a pivoted arm with a spool at either end, mounted on a power drive hub.
- The first spool deploys the C jacket and the other one the pre-insulated cable.
- The two components are coupled at the entrance of the second calendering unit.
- The two pre-calendering units enlarge the curvature radius of the cable and jacket after unspooling.

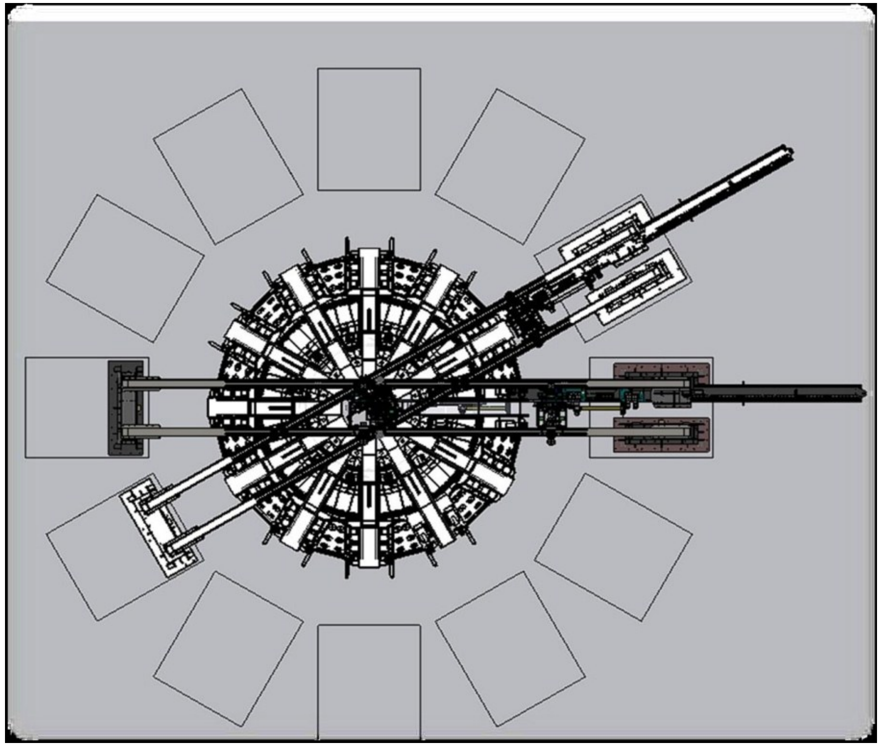

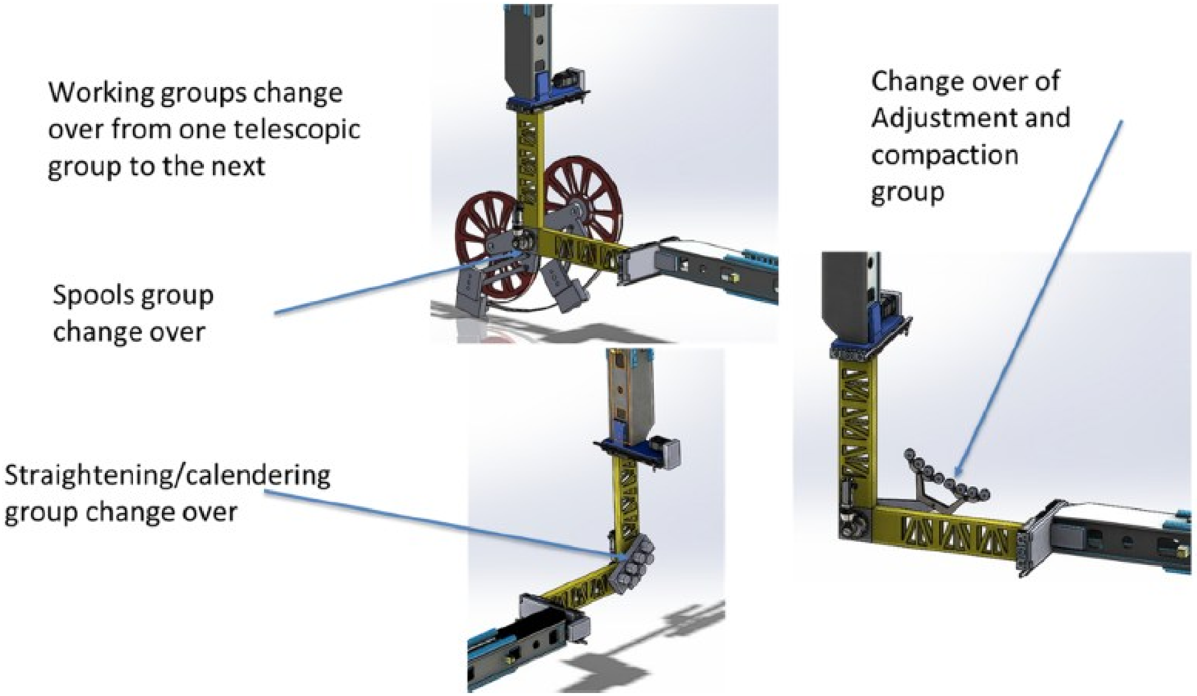

Portal winding machine - conceptual study

- Each arm features a sled glide that allows to move the working group sideways respect to the arm axis, in a periodic oscillation motion.
- That movement allows a smooth laying down of the conductor along the casing former width, from one side to the other.

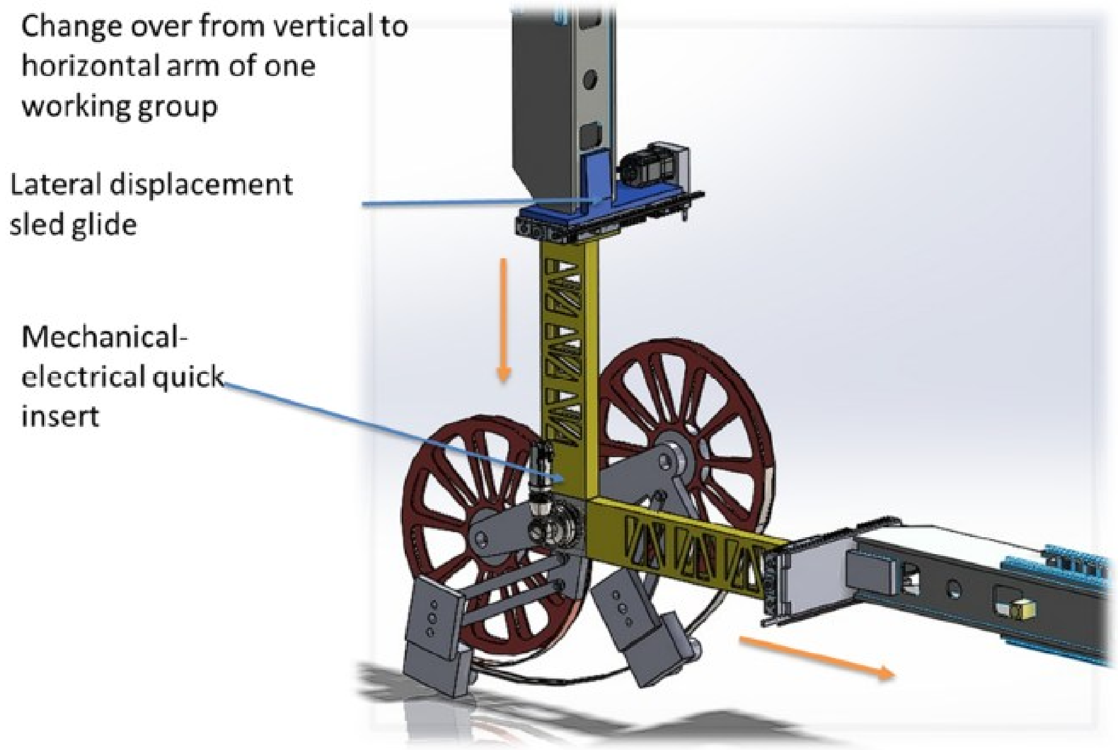

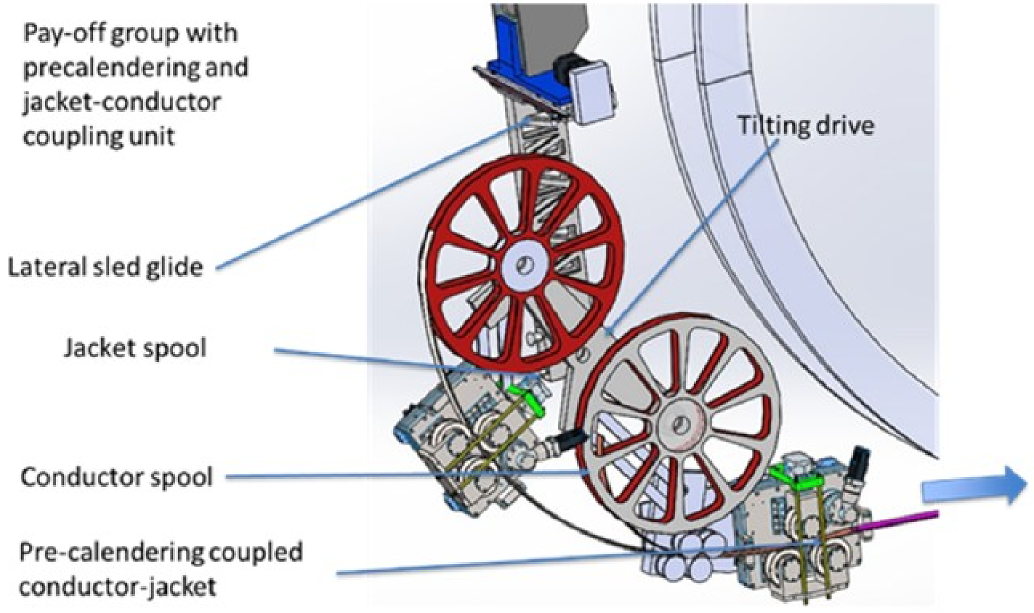

Portal winding machine - conceptual study

- The cable and jacket spools support beam is hinged at midlength.
- The hinge is driven by a power drive that gives the required rotation angle to the group, keeping the outcoming conductor correctly aligned respect to the winding surface.

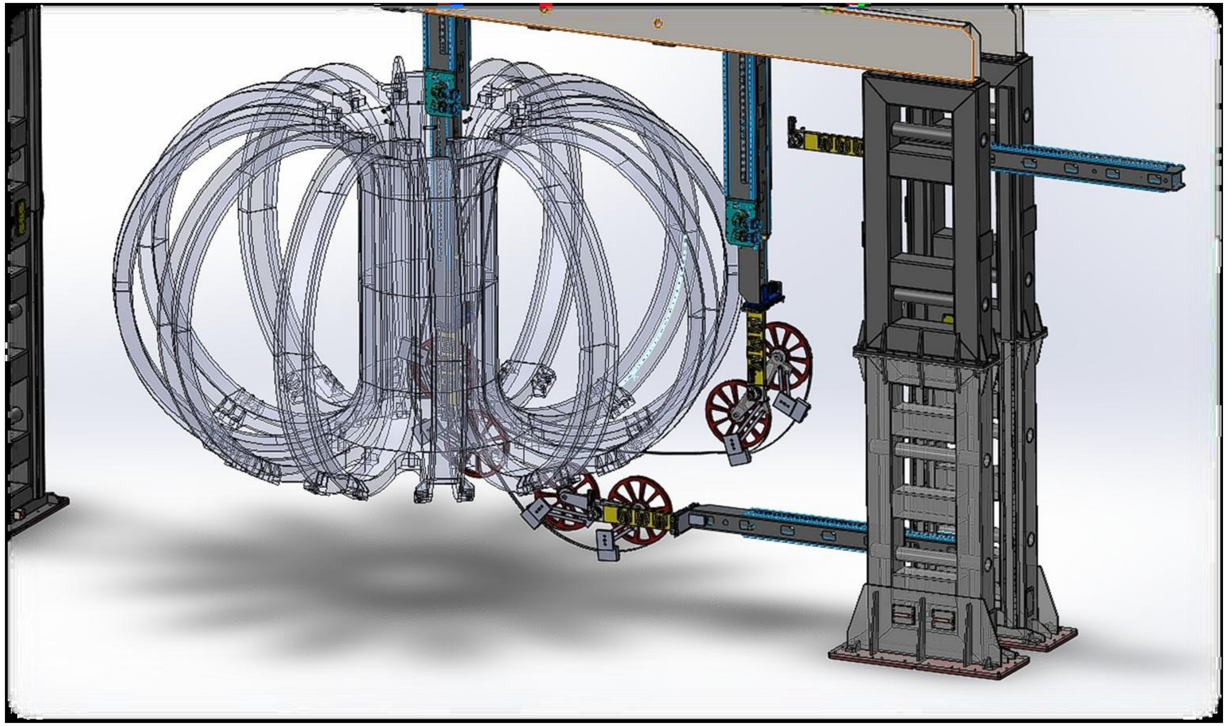

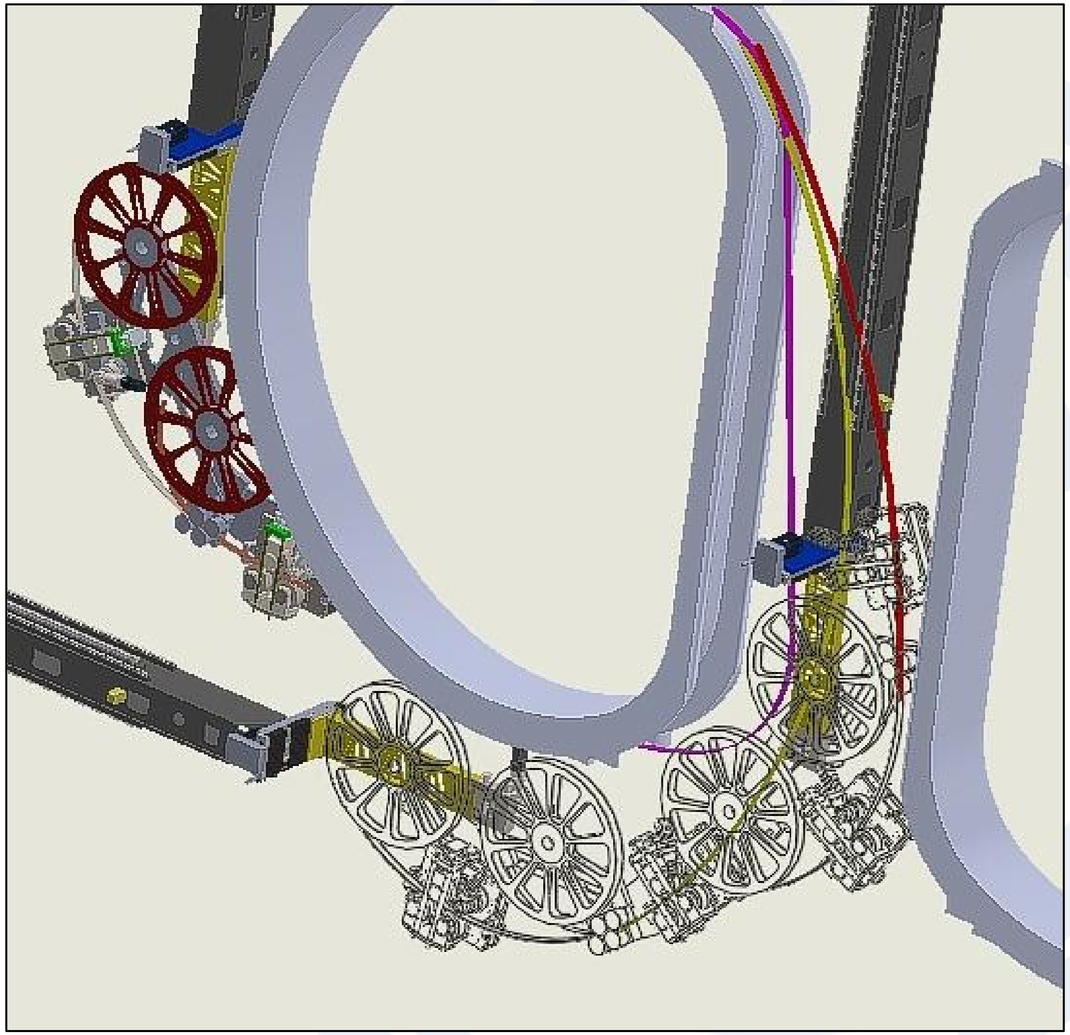

Portal winding machine - conceptual study

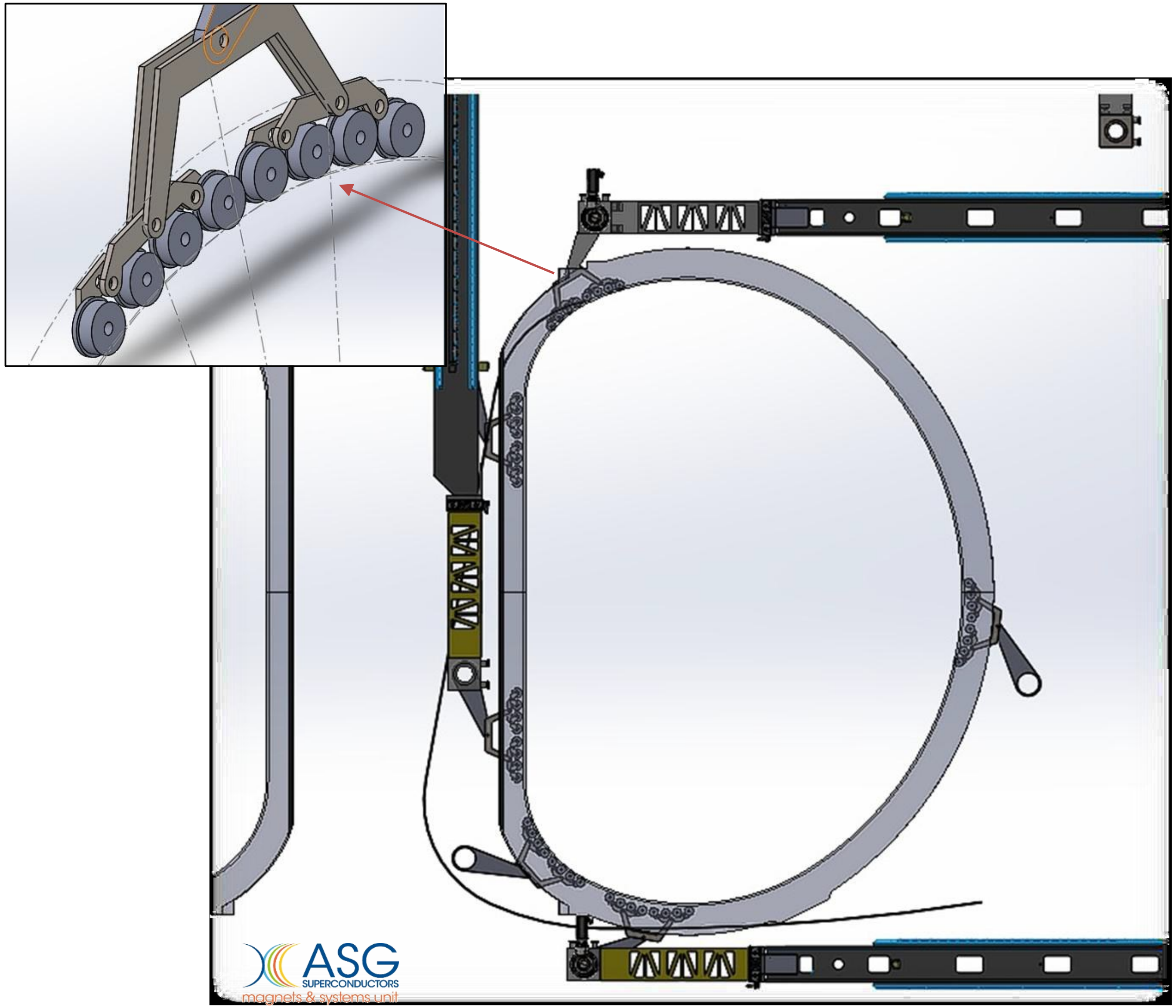

- The compaction unit consists of a set of rollers mounted on pivoted arms, allowing them to self-adjust and follow the winding profile.

- The rollers include a shoulder that presses the conductor side into position on each layer.

- On the final pancake, there may be insufficient space for the roller shoulder, so an additional compaction method may be needed to ensure good alignment.

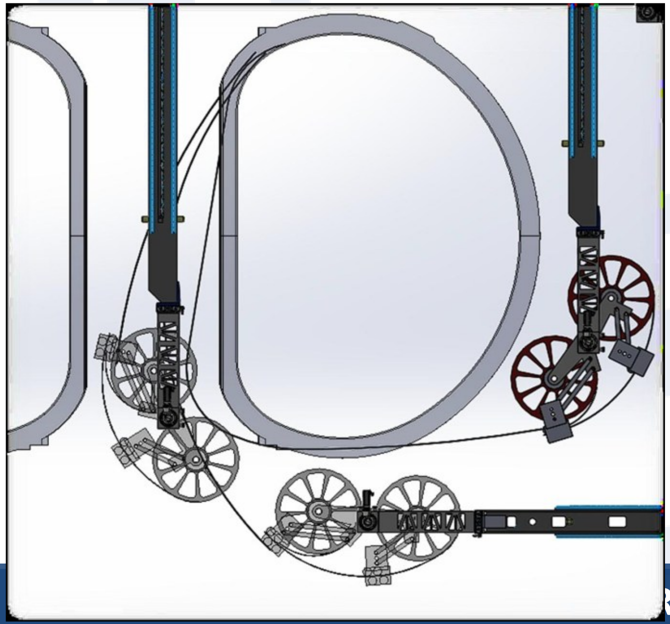

Results of RINA study so far: in-situ winding feasibility

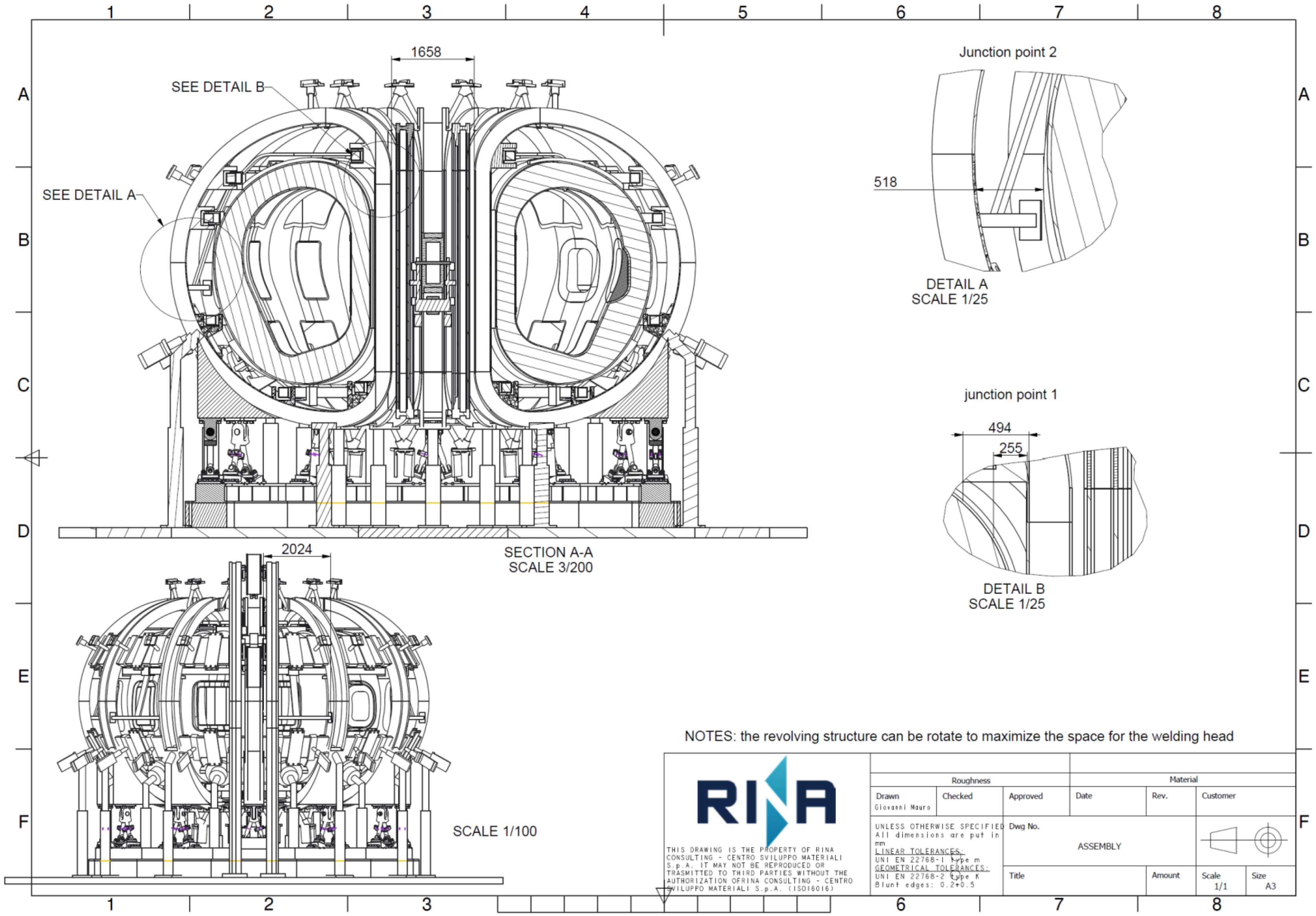

Analysis to identify critical areas affecting accessibility for welding torque application

Inner bore accessibility

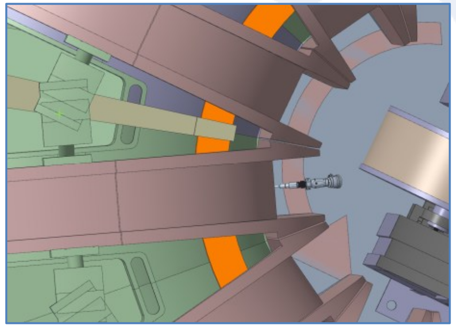

Clearance between the VV and the TF coils

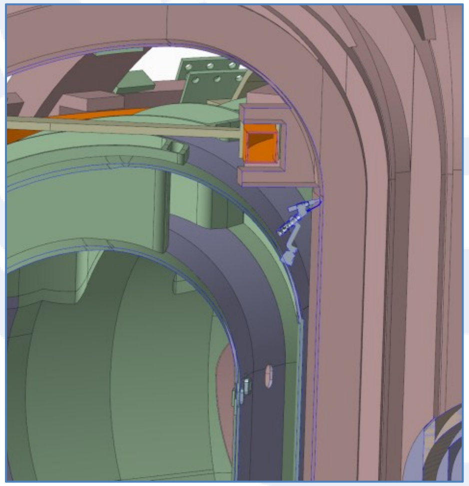

Results of RINA study so far: in-situ winding feasibility

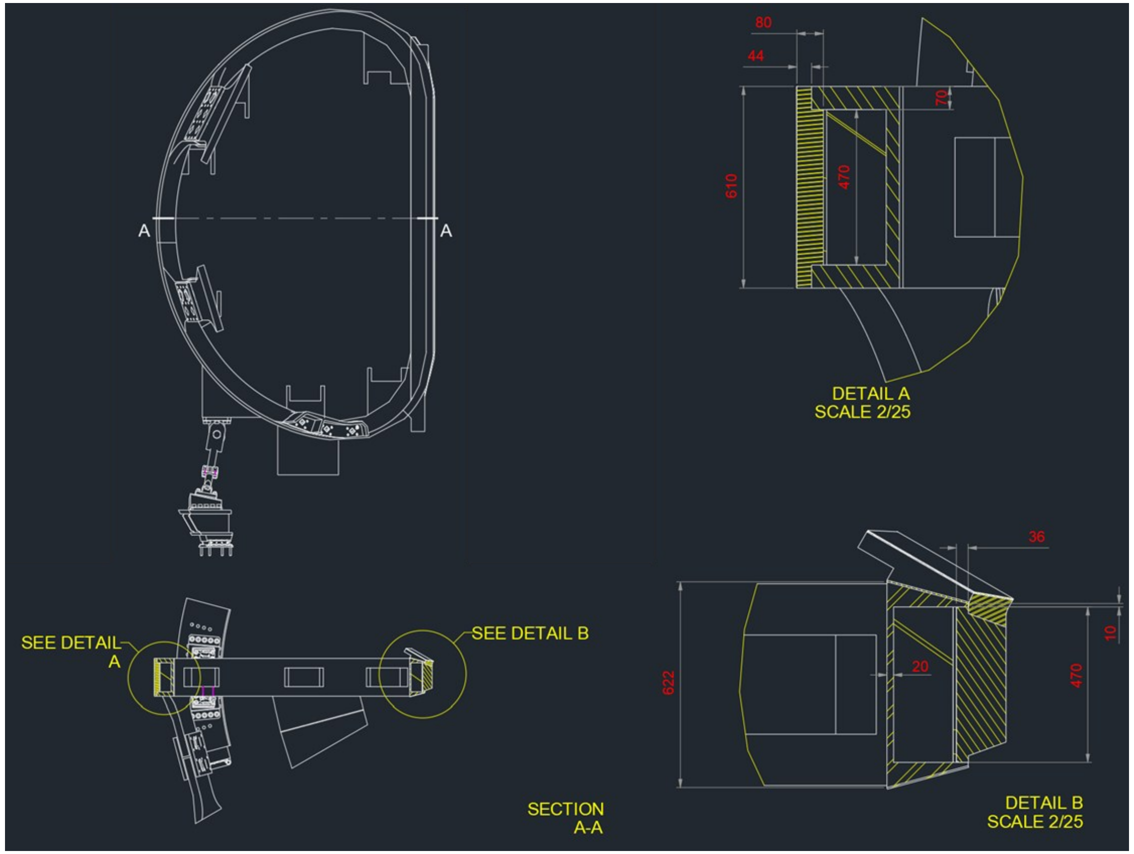

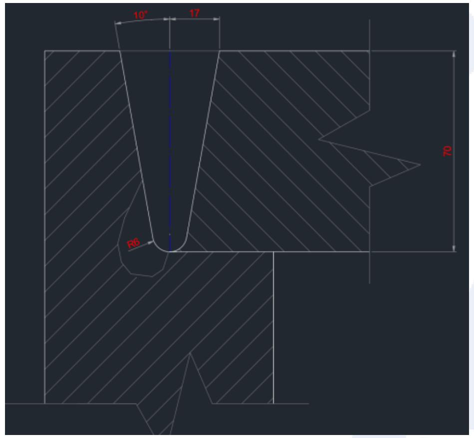

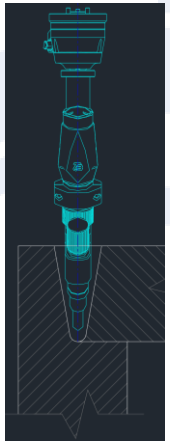

Considering the U-bevel, an access simulation of the TIG welding head was performed to assess potential interferences. No issues were identified in this region. However, welding in the area within the marked square is not feasible due to geometric constraints.

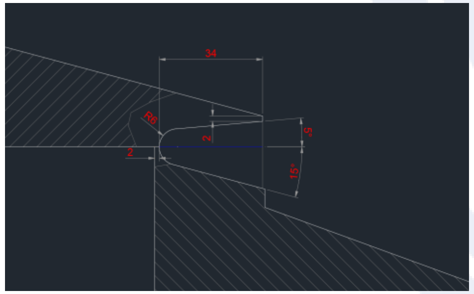

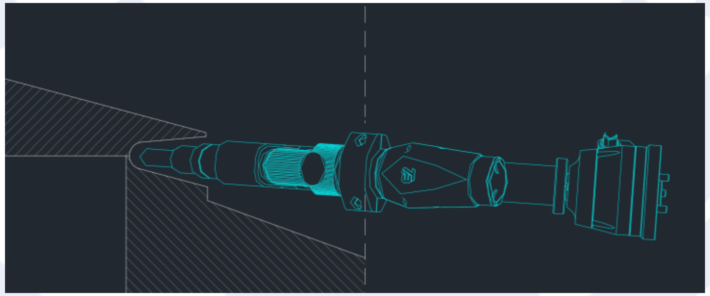

Considering the U-bevel, an access simulation of the TIG welding head was carried out to evaluate potential interferences. The figure shows that the size of the sealing head poses no issues.

Manufacturing of mock-ups is proposed to validate the assembly and welding procedures.

Identification of potential show-stoppers based

•**Key 2024 finding:** Welding feasibility was identified as *critical* because the VNS operates in a high-stress environment, requiring:

- •very high-quality welded joints, and
- •tight dimensional tolerances.

•**Design change after 2024:** The VNS structure was redesigned to eliminate most **in-situ** welds.

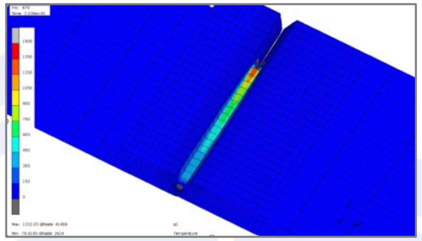

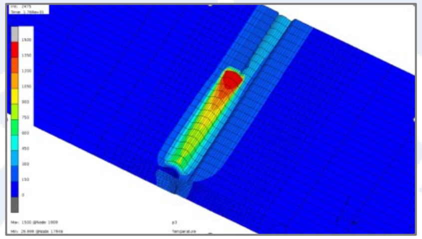

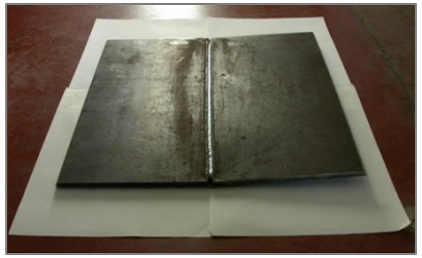

•**Remaining unavoidable weld:** The only weld that could not be removed is the **butt weld between the upper and lower parts of the TF structure**.

•**New assembly approach (2025 redesign):**

- •The **lower TF part** is now fully assembled in the workshop (same as the upper TF part).
- •The **upper and lower TF parts** are then brought on site and **welded together**.

•**2025 analysis focus:** Detailed analysis of the **butt welding** between the upper and lower TF structure parts.

•**Two scenarios analyzed in 2025:**

1. Butt welding of a **single TF segment**, as in the 2024 VNS design
2. Butt welding between the **entire upper TF part** and the **lower TF part**

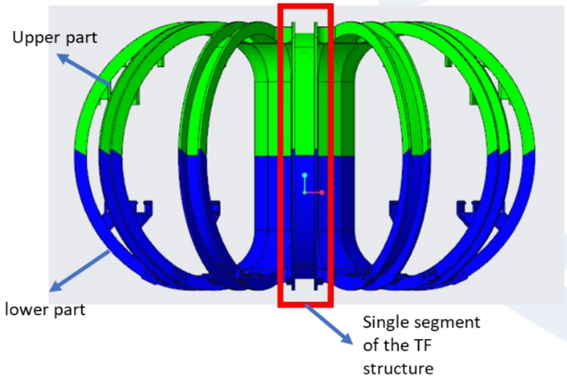

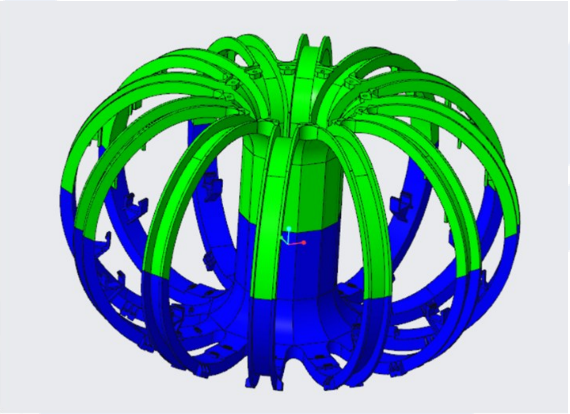

In-situ winding: welding on a single TF segment

- A mechanical FEM model of the TF structure was set up to evaluate the distortion due to the butt welding of the two joints (joint 1 and joint 2)

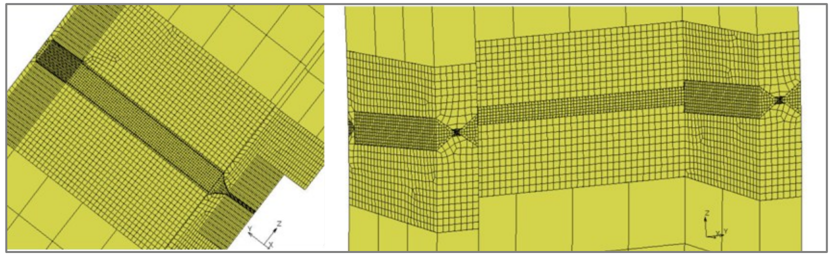

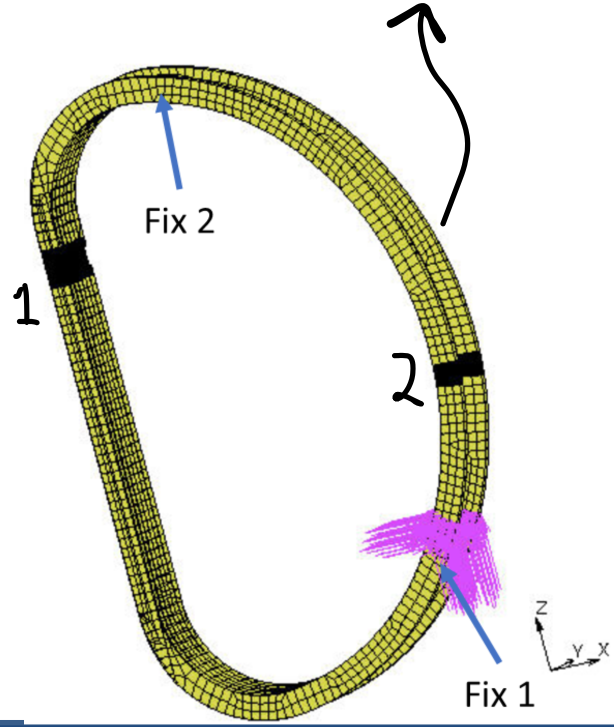

a) The single segment of the structure was assumed constrained in two zones (Fix 1 and Fix 2)
b) Once both joints are welded, Fix 2 is removed to evaluate the free deformations of the structure.
c) Joint 1 and joint 2 are welded at the same time
d) The welding of the inner and outer parts of the butt weld occurs in two successive phases (first outer part)

First phase	Second phase	Third phase	fourth phase
Joint 2: 1st and 2nd outer passes **joint 1:** 1st and 2nd passes	**Joint 2:** 3rd outer pass **joint 1:** 3rd pass	**Joint 2**: 1st and 2nd inner passes **joint 1:** \	**Joint 2:** 3rd inner pass **joint 1:** \
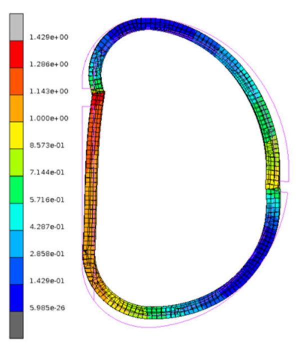	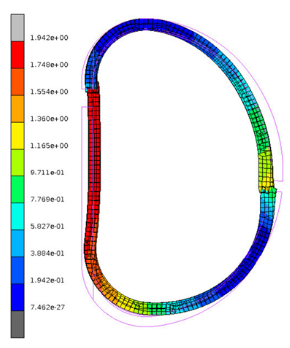	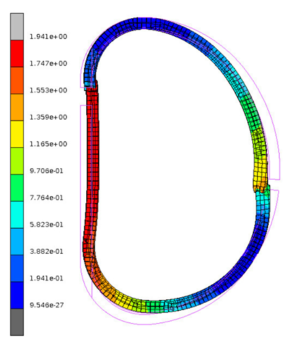	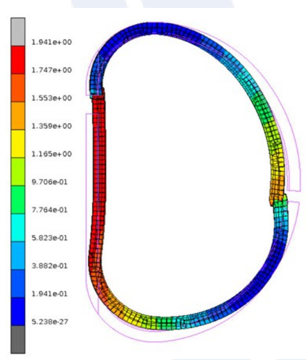

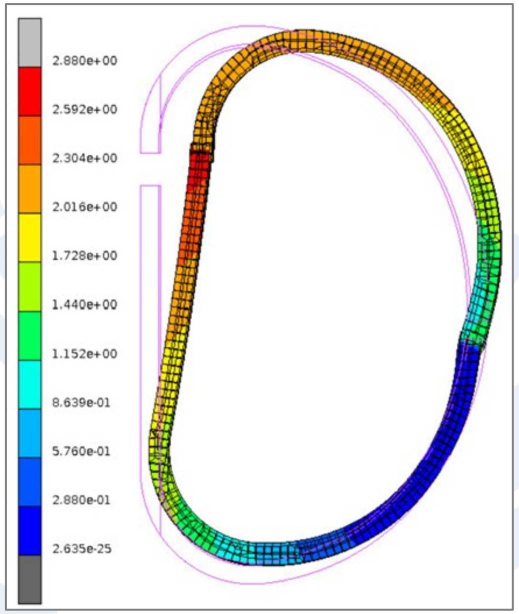

Phase [#]	1	2	3	4	Fix removed
Deformation [mm]	1.43	1.9	1.9	1.9	2.9

Butt welding between the entire upper part and lower part of the TF

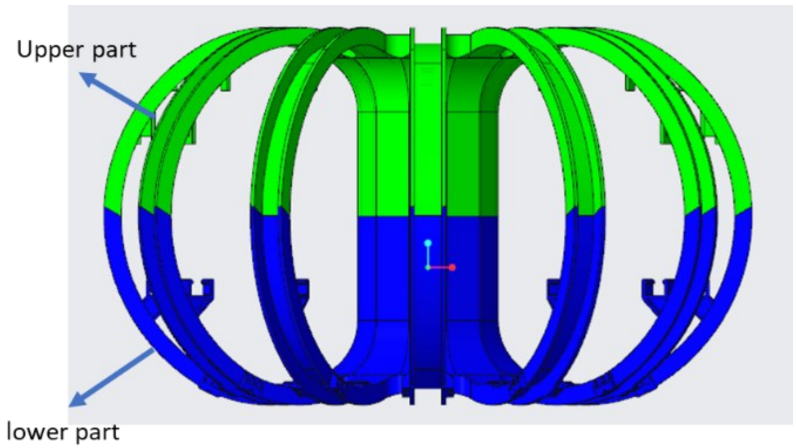

a) Only 1/4 of the structure was modeled by exploiting the symmetry of the system.

b) The butt welds of joint 1 and joint 2 have been modelled according to the following steps:

- STEP 1: initial condition with all the components of the weld seam at 1500°C
- STEP 2: the part of the seam that is welded undergoes a temperature reduction to simulate the welding shrinkage that subsequently induces the deformations

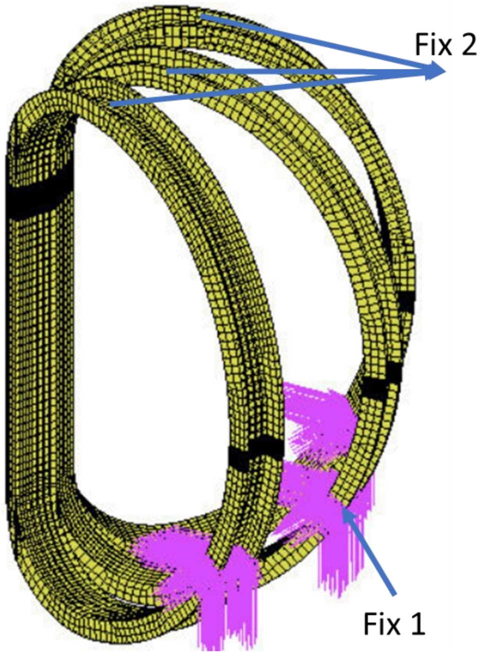

MODEL 1:

- **joint 1 and joint 2 are welded at the same time.**
- **The welding of the inner and outer parts of the butt weld also occurs at the same time.**
- **Fix displacements are imposed in two zones of the.**
- **After the completion of the welding, the fix 2 is removed to evaluate the free displacement of the structure due to the butt welding.**

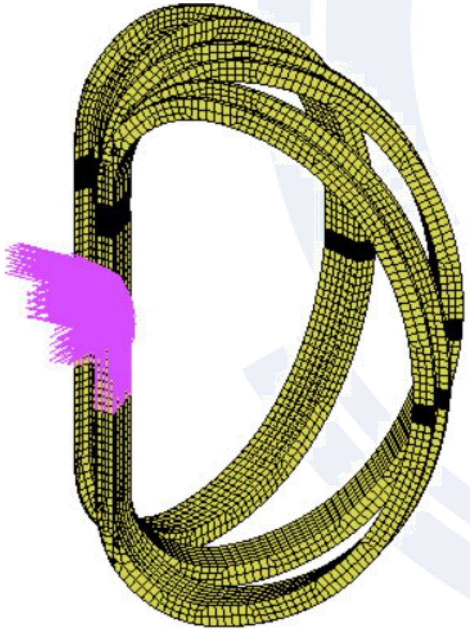

MODEL 2:

- **joint 1 and joint 2 are welded at the same time.**
- **The welding of the inner and outer parts of the butt weld also occurs at the same time (same the MODEL 1).**
- **Fix displacements are applied only to the central zone of the structure**

Results of MODEL 1 (entire TF Structure)

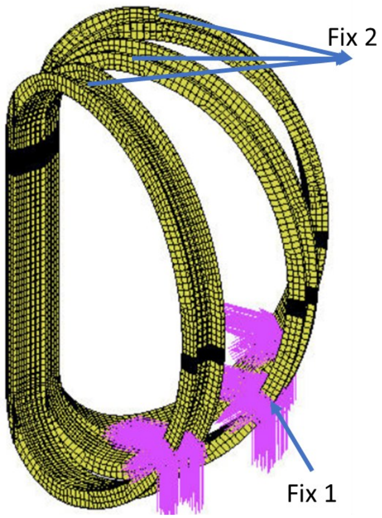

First phase	Second phase	Third phase
Joint 2: 1st inner pass and outer pass **joint 1:** 1st pass	**Joint 2:** 2nd inner pass and outer pass **joint 1:** 2nd pass	**Joint 2**: 3rd inner pass and outer pass **joint 1**: 3rd pass
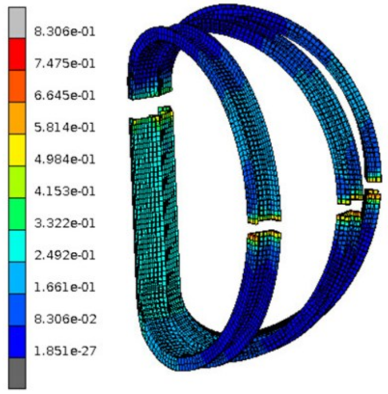	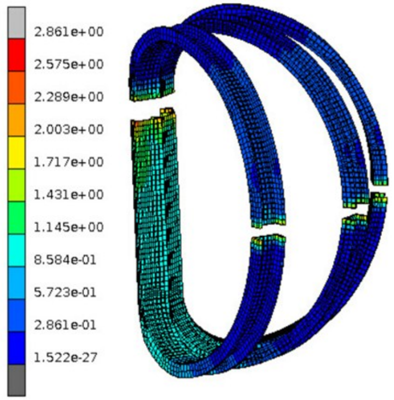	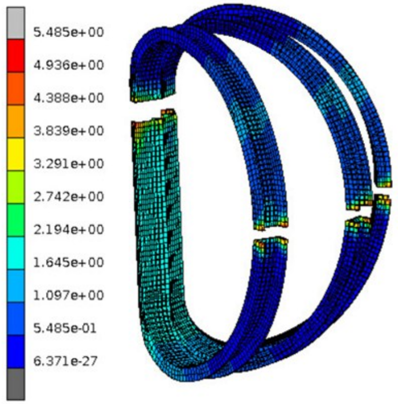

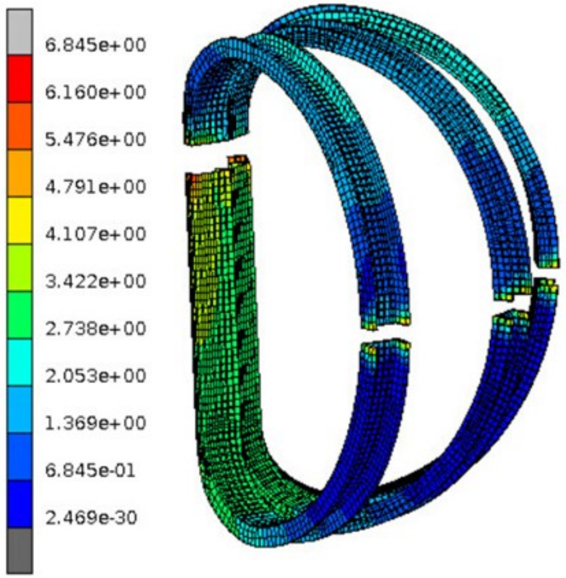

Phase [#]	1	2	3	Fix removed
Deformation [mm]	0.8	2.9	5.5	6.8

- At the end of the welding the displacement of the entire segment of the TF structure is almost 5.5 mm.
- When the fix 2 is removed the displacement becomes almost 7 mm.

Results of MODEL 2 (entire TF Structure)

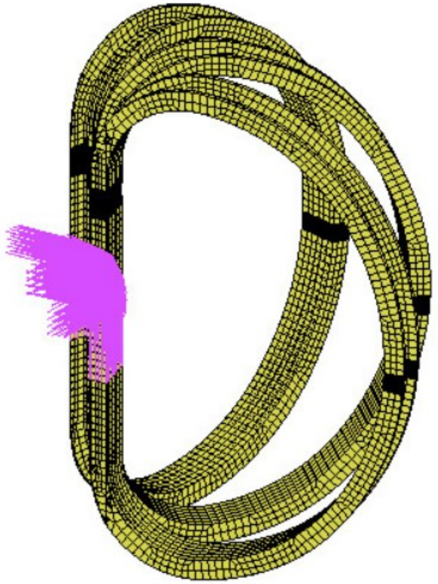

First phase **Joint 2:** 1st inner pass and outer pass **joint 1:** 1st pass	Second phase **Joint 2:** 2nd inner pass and outer pass **joint 1:** 2nd pass	Third phase **Joint 2**: 3rd inner pass and outer pass **joint 1**: 3rd pass
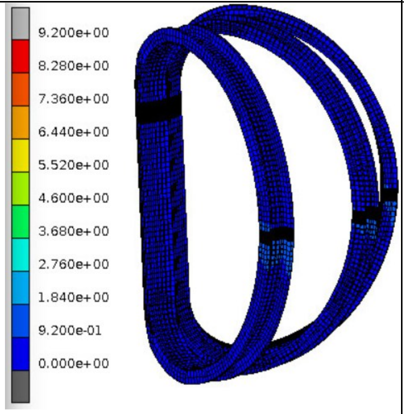	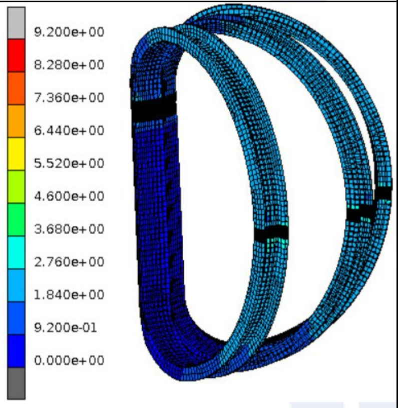	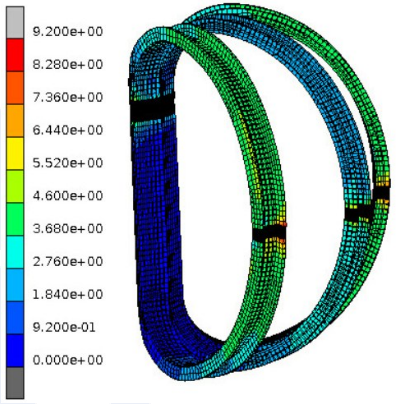

Phase [#]	1	2	3
Deformation [mm]	1.5	4.1	9.1

- At the end of the welding the displacement of the entire segment of the TF structure is almost 9.2 mm.
- For both scenarios the deformations reached at the end of the butt weld are in the order of magnitude some millimeters.
- **These deformation values are high compared to the dimensional tolerance values required by the structure for correct assembly and operation. These aspects need to be analyzed in detail during the conceptual design study.**

Update of the inner case joint

See L. Giannini et al., https://doi.org/10.1016/j.fusengdes.2024.114530

- The **central joint** has been studied in detail due to its complexity. It must withstand part of the **32 MN axial load** transmitted through the coil's **inner leg**.
- The **initial concept**, based only on bolts on the equatorial plane, was **discarded** because it was located at the **point of highest stress** and the **bolts alone could not adequately sustain the loads**.
- Instead, **tie plates were introduced** that pass through the two halves of the straight leg and are **integrated with the case above and below**, effectively **splitting the inner leg**.

  Analyses are ongoing to assess the **efficiency** of this solution.

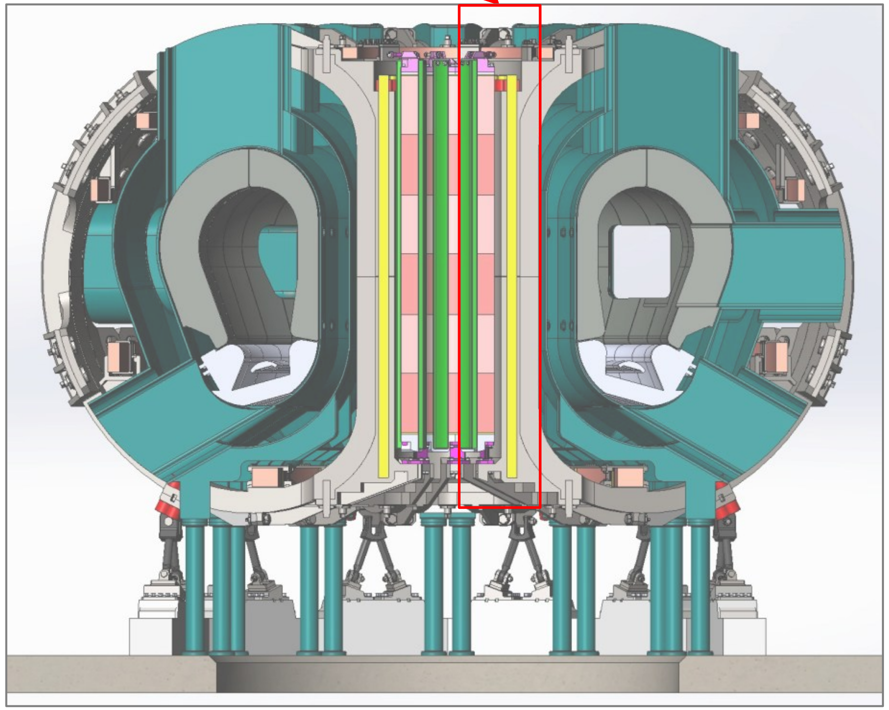

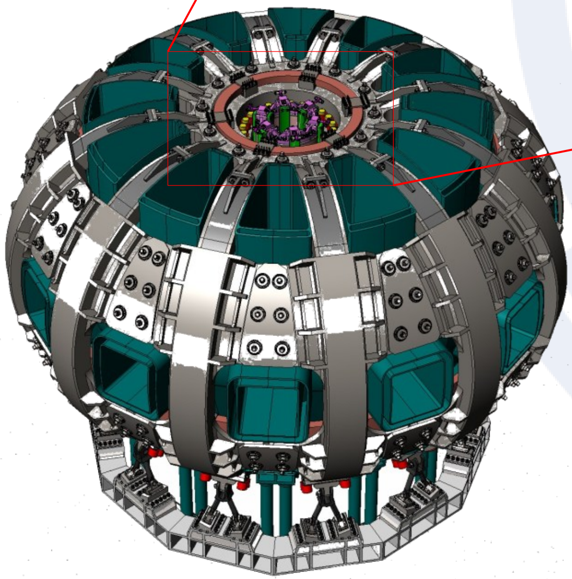

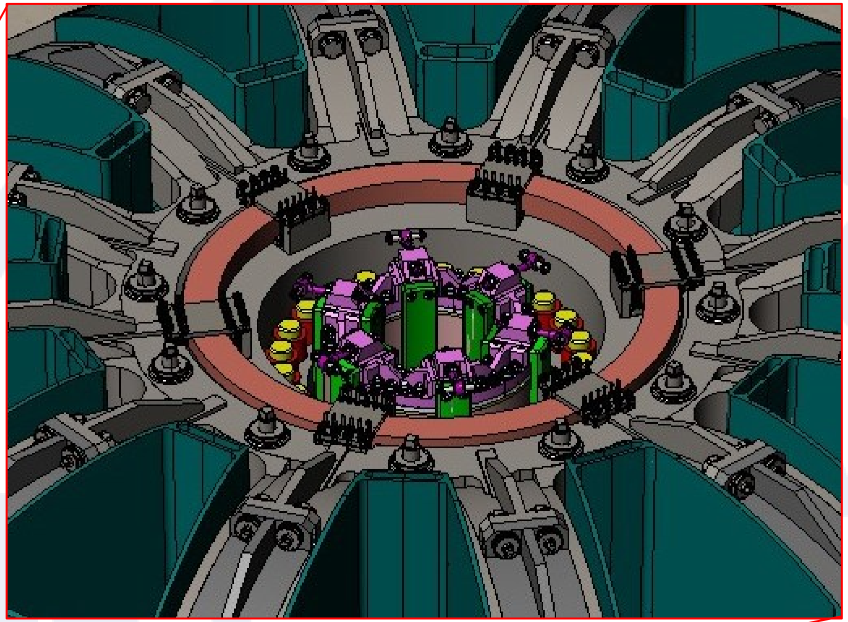

TFC system – structural assessment

Global Model

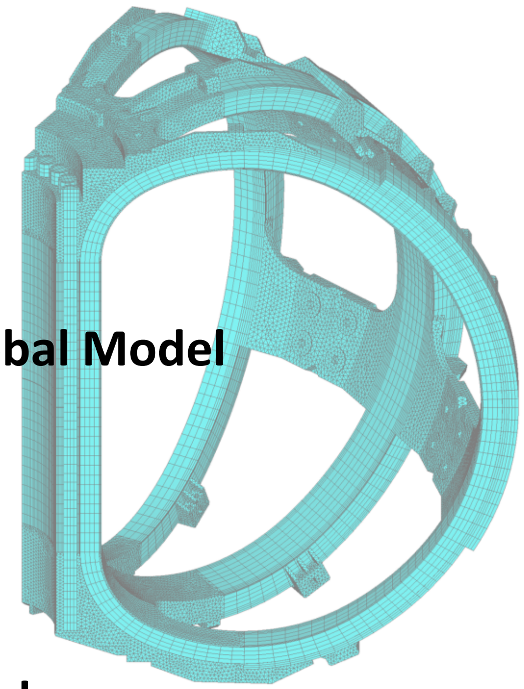

TF only

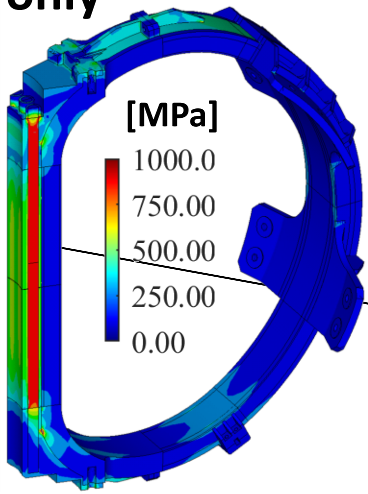

TF only

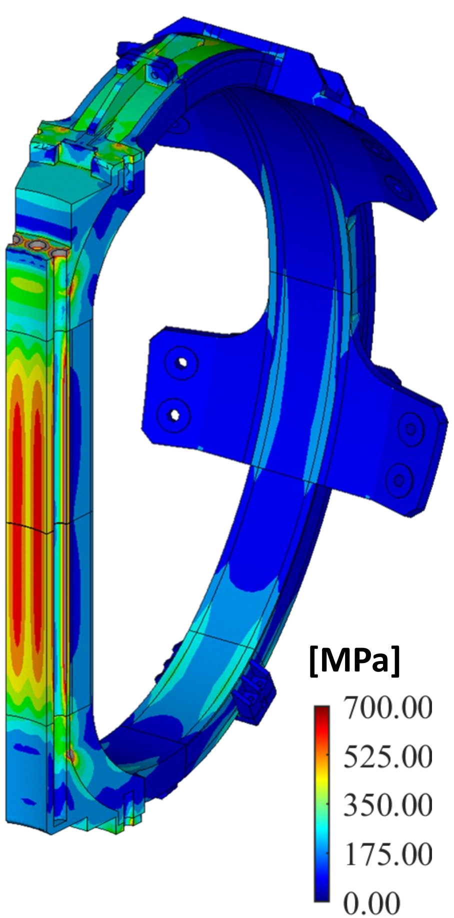

SN – 39 s

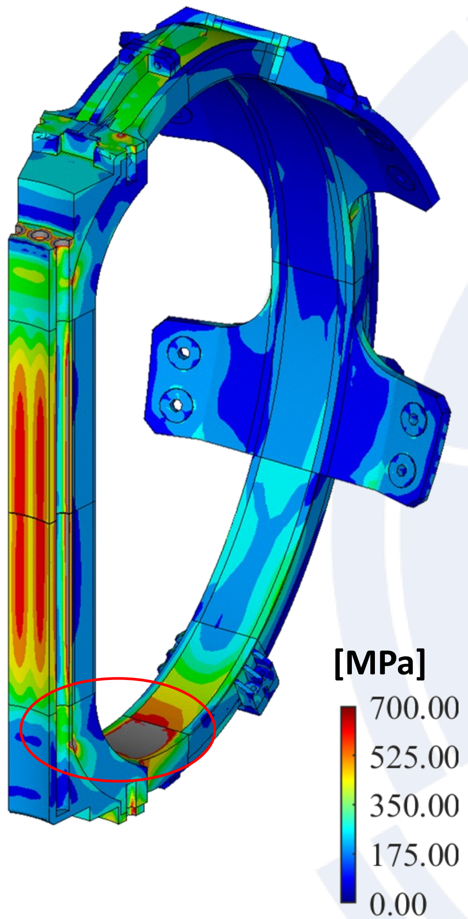

TF only

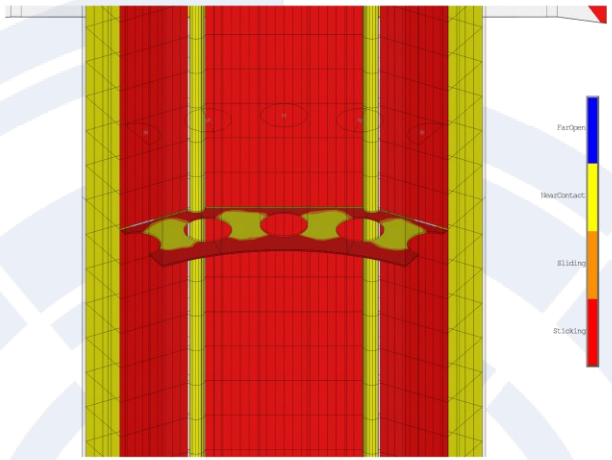

SN – 39 s

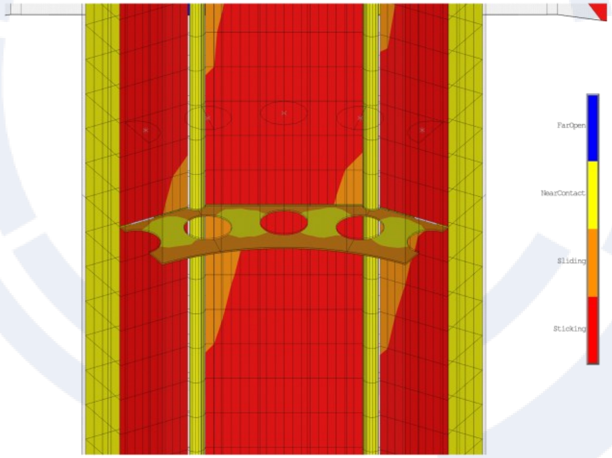

- The stress state of the bar has been pushed to the limit in order to assess the feasibility of the system.
- In this condition, we observe a transition from closed contacts to sliding between the TF-only instant and 39 s of the scenario.
- The situation has improved compared to the previous design, but further modifications are still required.

PFC HTS system – based on LASSO conductor

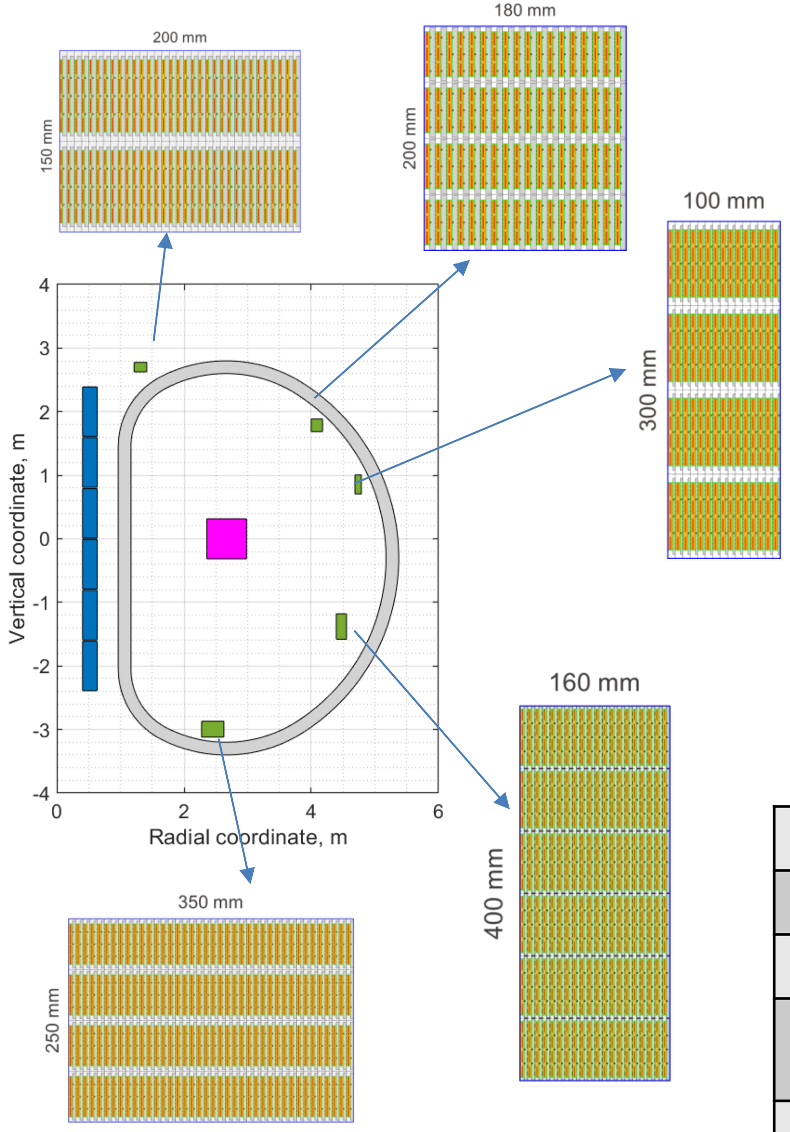

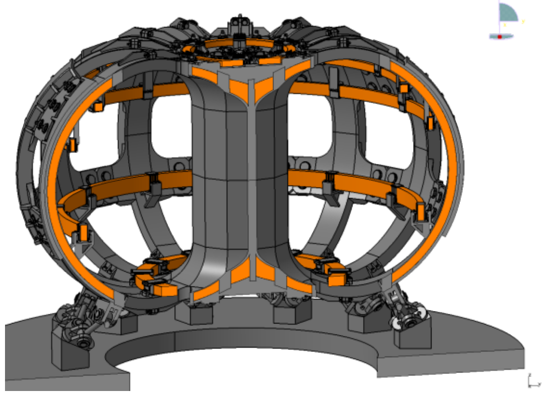

	PF1	PF2	PF3	PF4	PF5
tot. current, MA x t	2.25	2.5	2.1	4	5.4
peak field, T	5.3	6.4	6.3	6.3	8.8
turns	100	72	60	120	160
conductor curren, kA	23	35	35	33	34
number of 12 mm tapes	16	27	28	28	32
conductor width, mm	60	40	60	60	40
Cu, mm2	90	174	159	238	218
stored energy, MJ	12	65	54	164	136
JCu, A/mm2	250	200	220	140	155
conductor length, km	0.9	1.85	1.8	3.6	2.5
tape lenght, km	14	50	50	101	80

- One conductor type could be good enough for PF2–PF5 coils.
- It should contain about 28–30 tapes (12 mm wide).
- Additional copper can be added as co-wound strips.

Any aspect ratio can be used for the PF conductor, because even the thicker one (2 stacks) has only 0.15% peak strain at R=0.5 m.

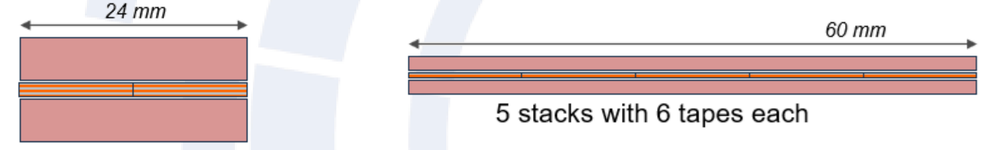

The choice on aspect ratio can be influenced by cooling (more pipes for the low aspect ratio) and AC loss.

PF5 OVER TIME

Time, s	2	3	4	7	9	11	13	20	39
Current, MA.t	1.06	1.36	2.30	3.38	4.07	4.88	5.43	5.25	4.94
Peak field, T	3.98	4.26	5.27	6.42	7.16	8.12	8.80	8.58	8.17
Energy, MJ (self-field)	5.18	8.50	24.4	52.8	76.3	109.9	136.1	127.3	112.7
Energy, MJ (entire PF)	4.86	7.46	21.2	44.2	63.2	91.3	112.6	105.0	92.3

EPFL

Thermal Shields

Design Motivation:

- Reduce length and simplify the cooling pipes (1 poloidal pipe) inside the cryostat (less length, less welds, less insulating breaks --> minimize risk of cryogen leaks in the cryostat)
- Simplify thermal shield installation (moving away from the ITER concept, adopting similar approach to W7X)

Selected Concept:

- Lightweight aluminum panels with MLI thermally anchored to 80K pipes at discrete points (thermal anchoring)
- Mechanical support same as thermal anchors; cooling pipe "cage" acts as support structure (dual function)

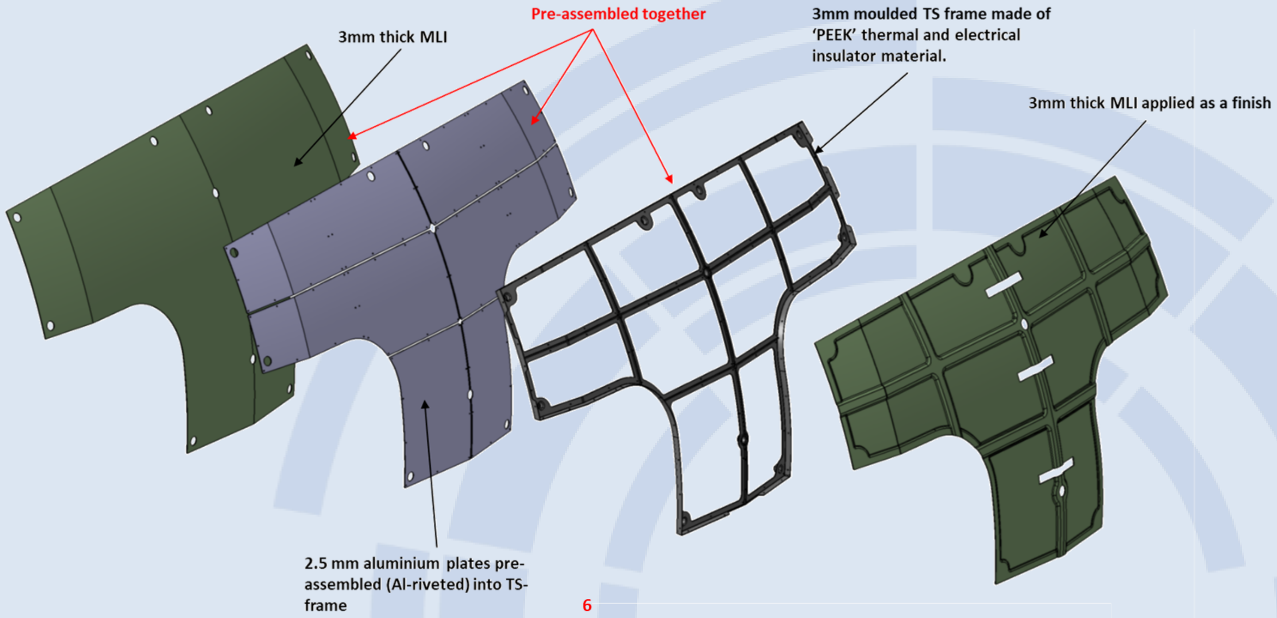

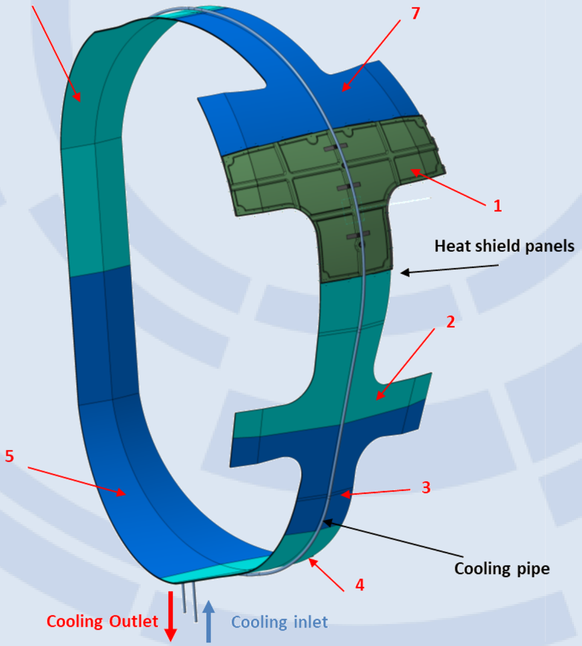

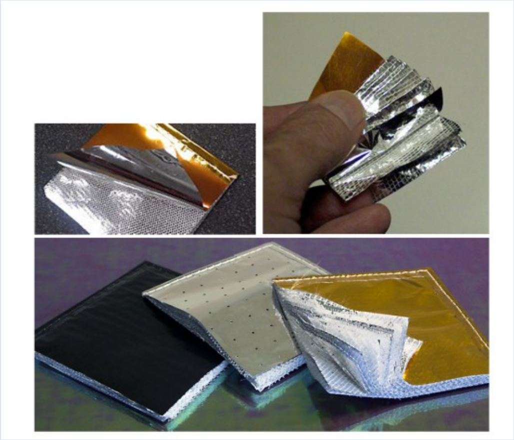

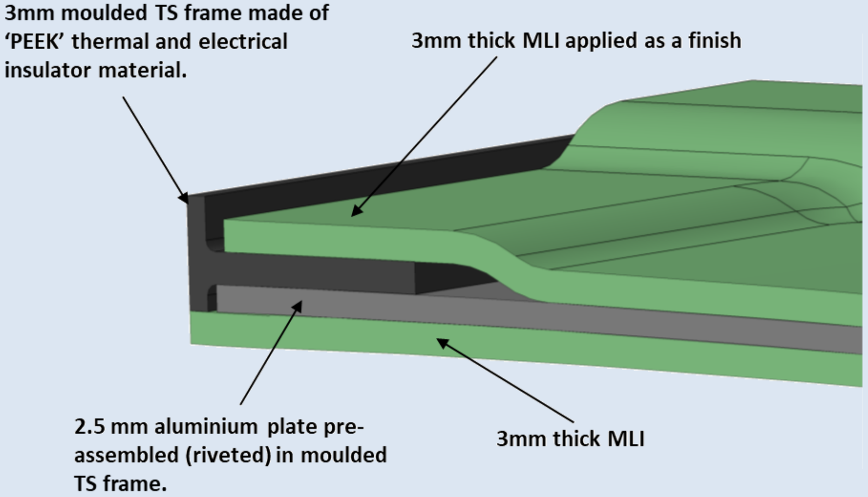

Electrically insulated connection of thermal shield panels to cooling pipes

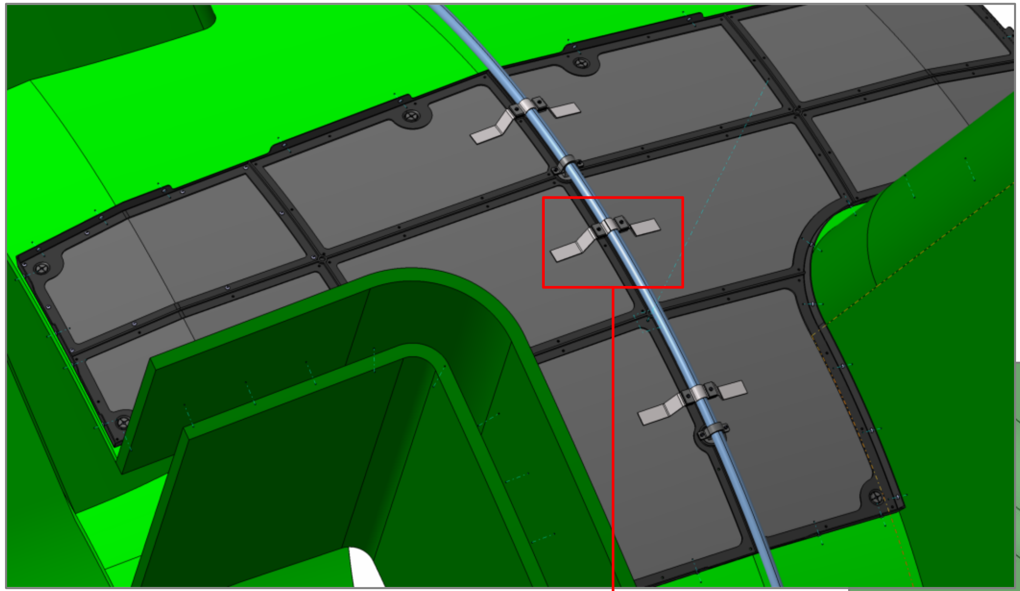

Welded plates with M8 press Studs

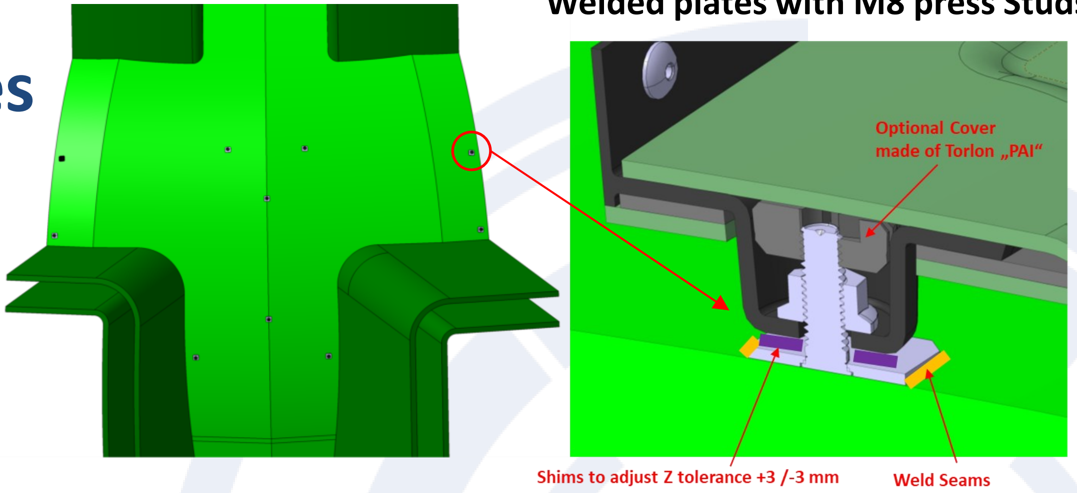

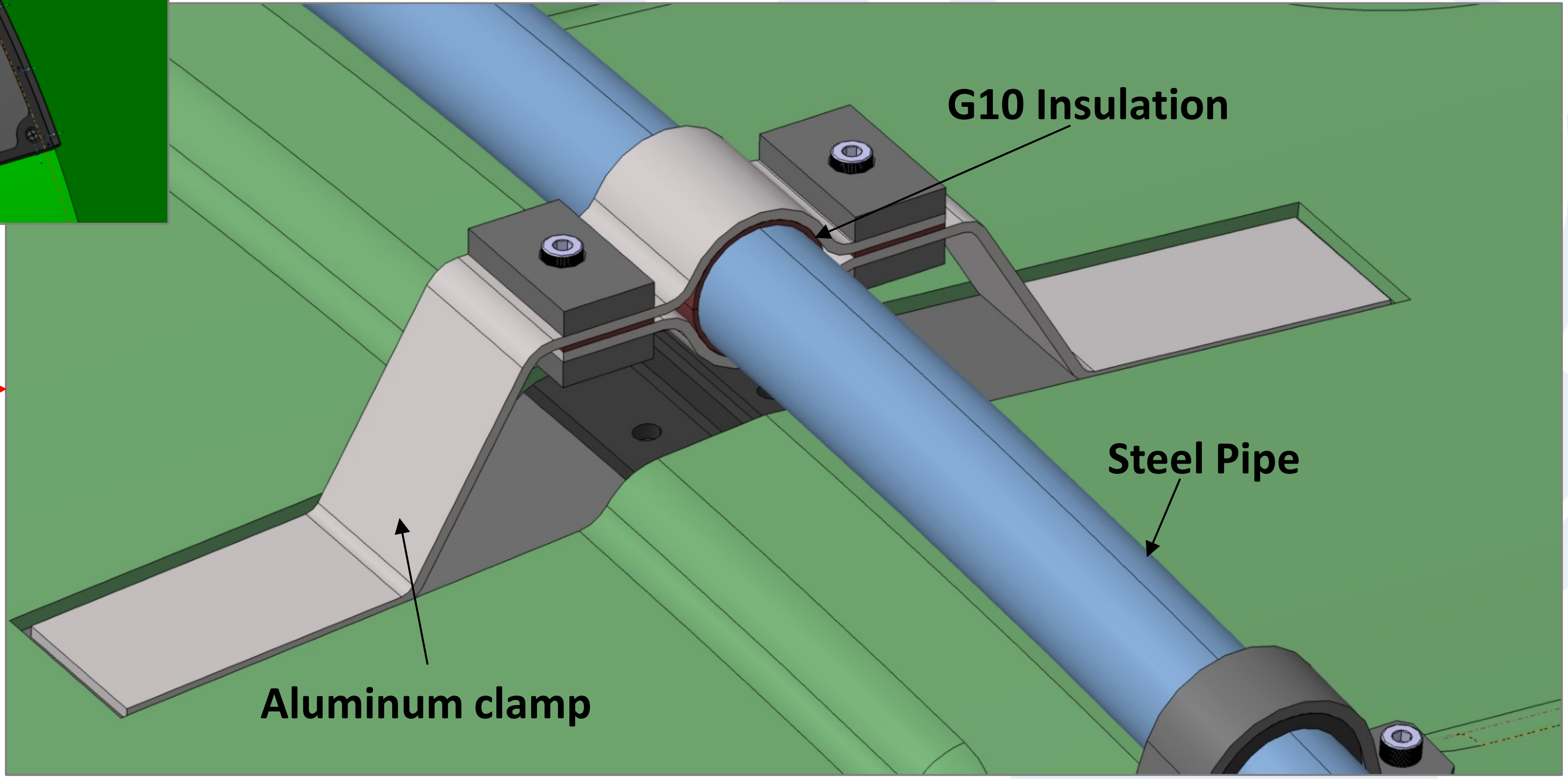

- The thermal shield panels are mounted directly onto the VV
- The panels are screwed to plates welded to the VV

Feeders

- **Concept based on conduction cooling with a “dry” HTS cable**
- Make conductor compact to facilitate feeder routing, multiple feeders share cryostat
- Pipes/conductors wrapped by multi-layered insulation (MLI) to passively limit radiation
- Joints located in two accessible access points within cryostat

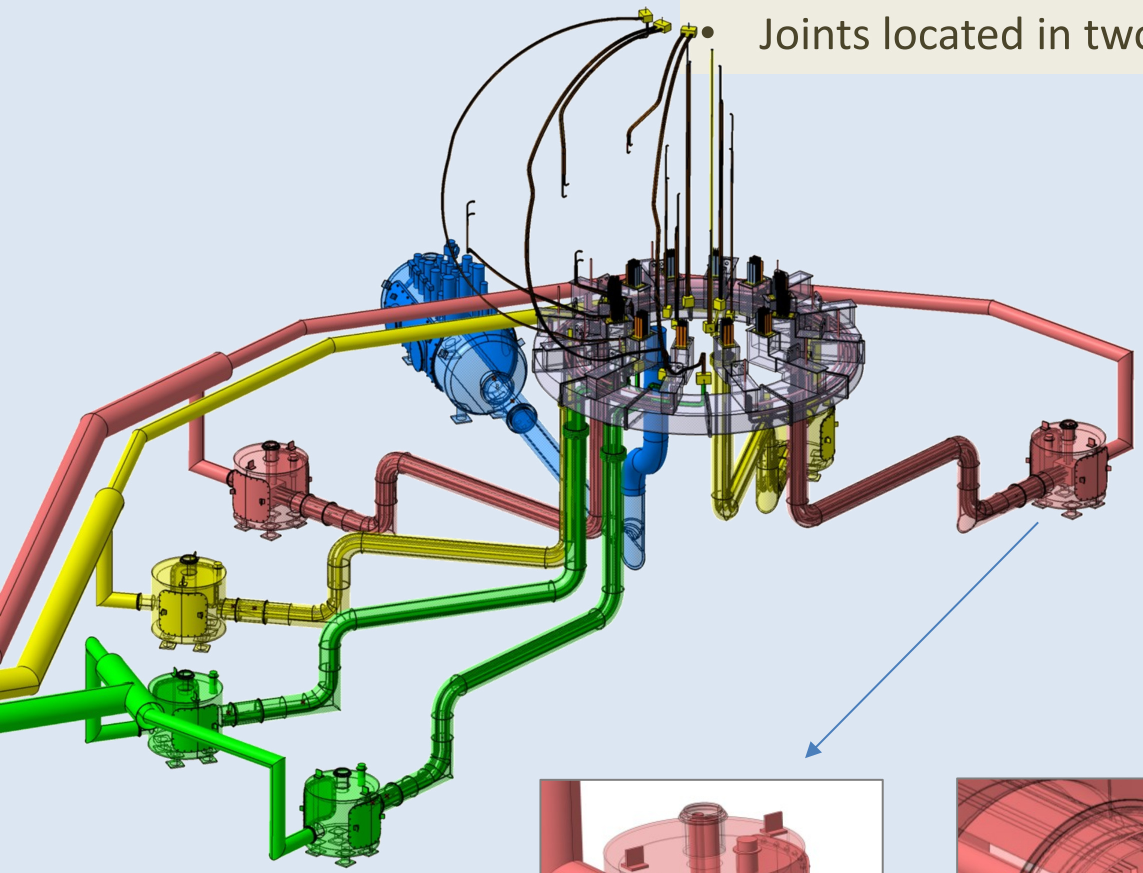

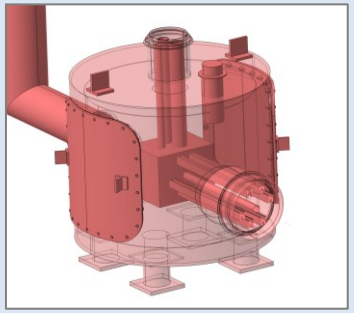

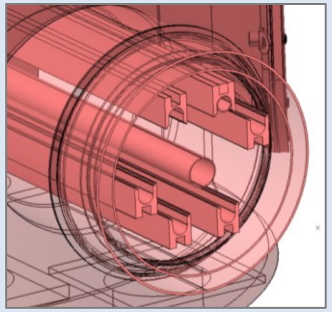

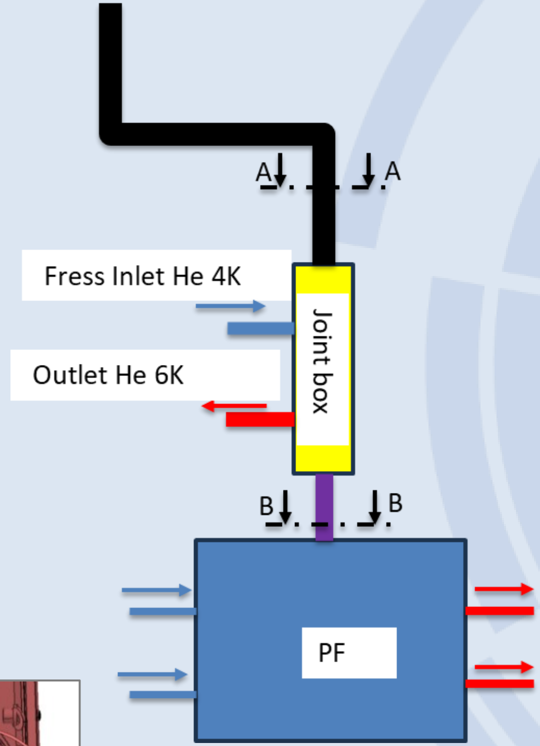

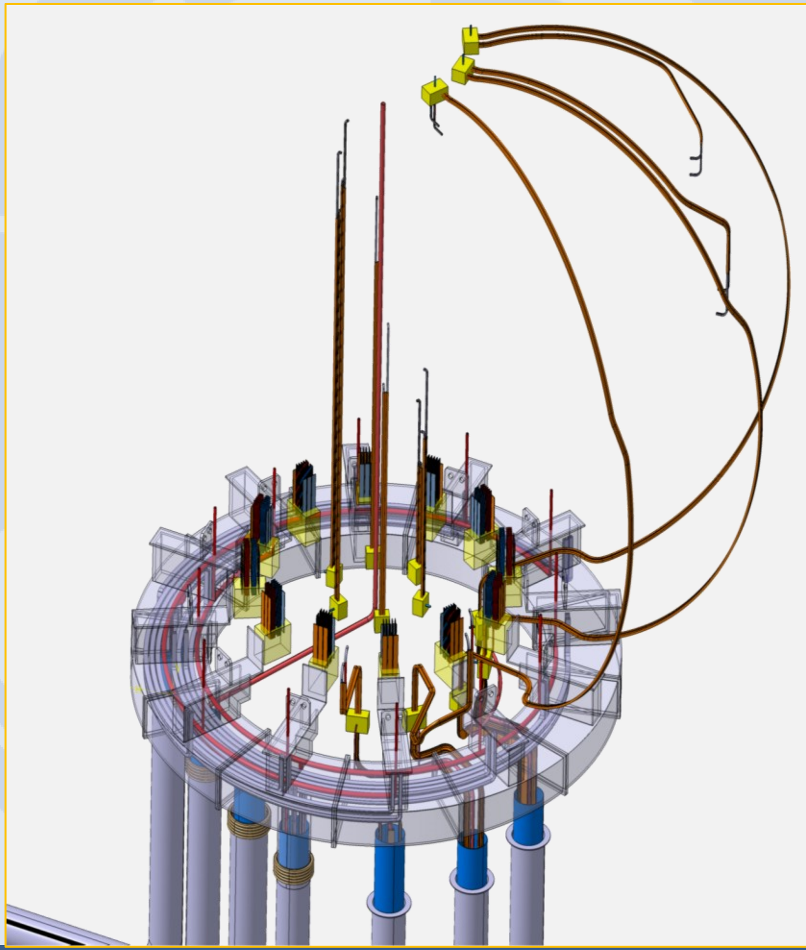

Long Terminations

In both configurations:

- **2 feeder lines for the TFCs**, **2 PFCs**,**2 CS modules and 1 for the structures**
  - **Each line contains three pairs of feeders**
- **18 Fast Discharge Units (FDU)** for coil protection.

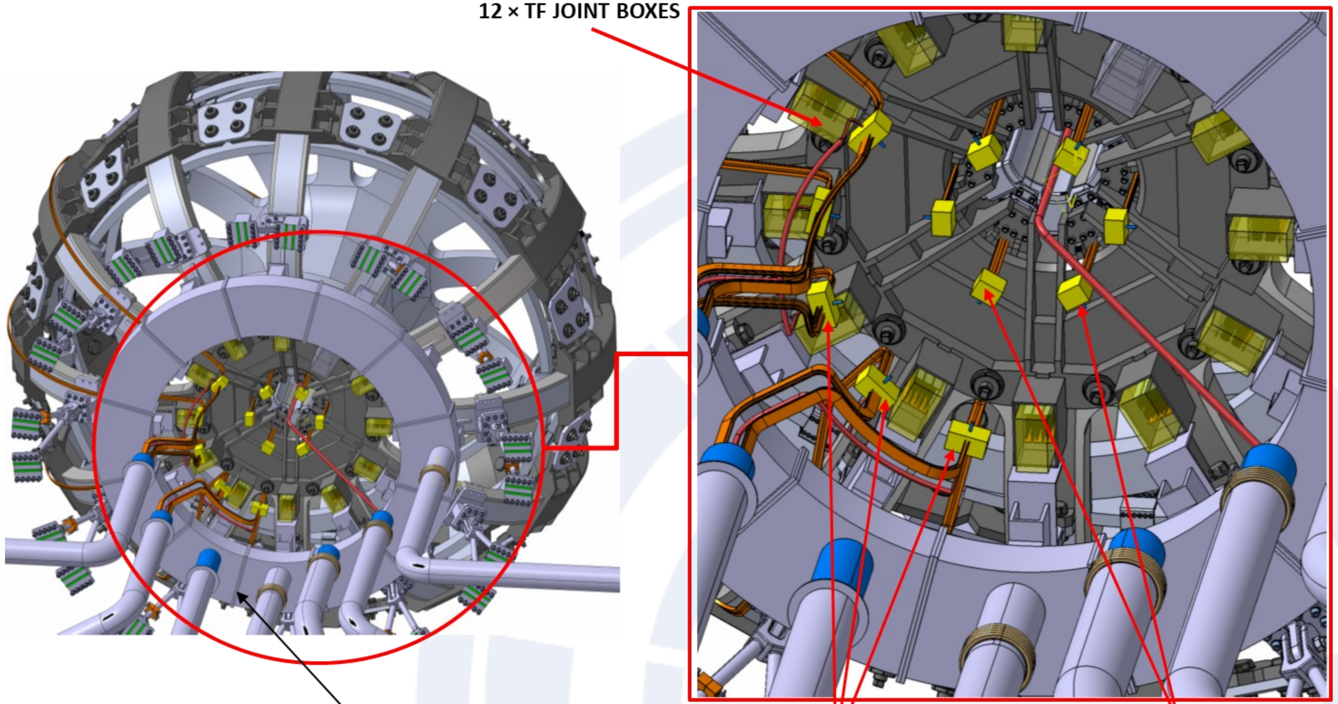

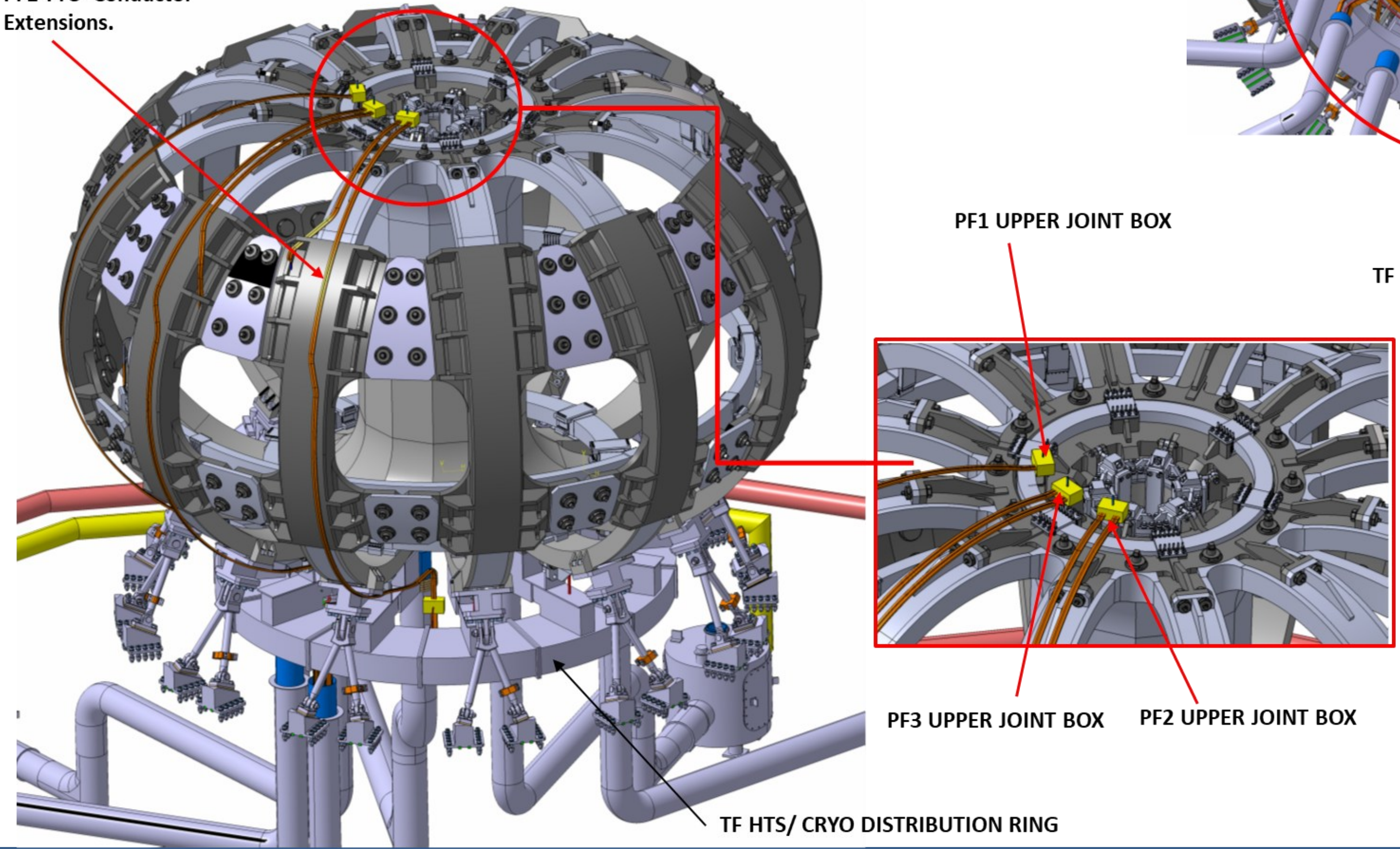

- **All feeders enter from below** the cryostat, optimizing routing and minimizing penetrations.
- The **upper coils are connected using long terminations and extensions**, allowing for easier access and integration, especially for maintenance and assembly operations.

Maintenance Hatches

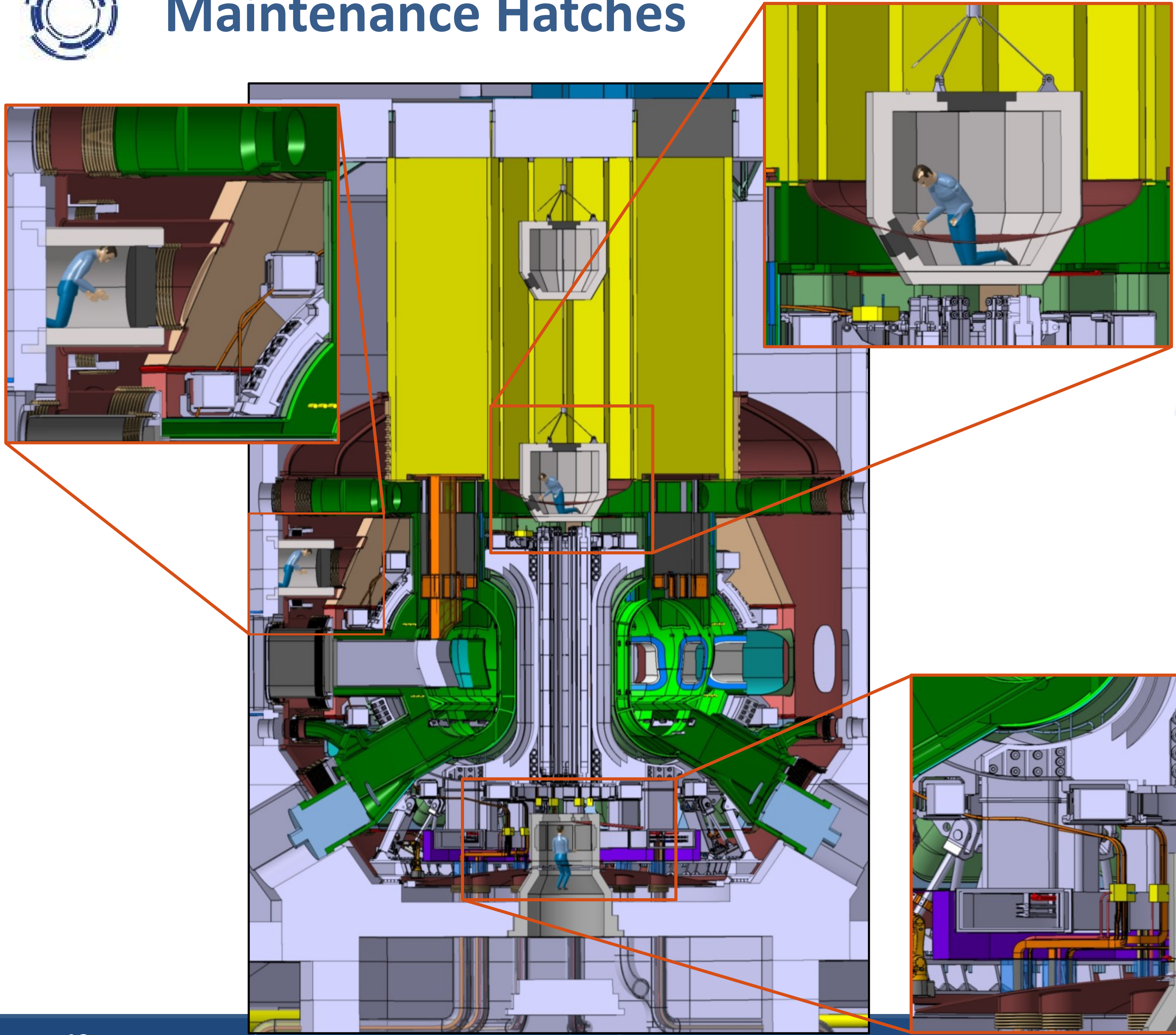

Integration and Access Strategy

- The proposal aims to **create high-protection zones from radiation for operators**, minimizing radiation exposure during operation and maintenance.
- The **locations of feeders, joints, and helium manifolds** have been optimized to **reduce the need for human access** in activated areas.

➢ The proposed layout includes **extended terminations** for both the **NbTi PF coils** and the **Nb_3Sn CS modules**.

  ✓ This solution, **already validated in the DTT design**, ensures reliable performance and does not introduce additional technical challenges.

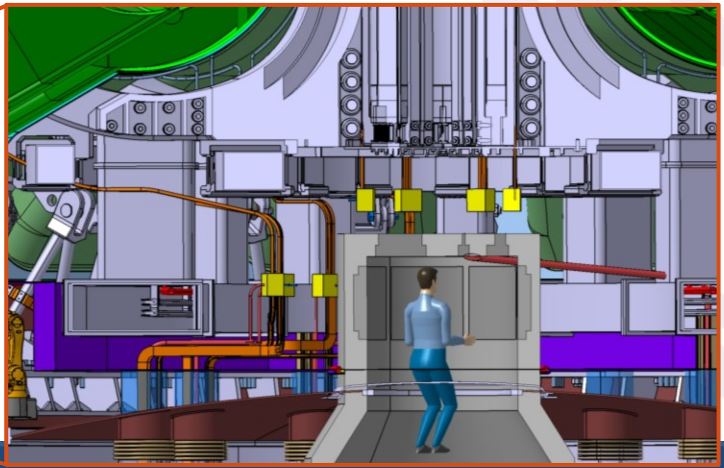

A significant fraction of the cryostat internal volume is assumed to be inaccessible because of excessive radiation.

Conclusions

- Magnet, thermal shield, and feeder concepts have been brought to a level of design detail sufficient to establish feasibility (from multiple points of view) for the reference solution

  - ➢ An alternative solution based on HTS is also available and ready for detailed development

- Design driver for the thermal shields and feeders is simplification to ease manufacturing, assembly and repairability
  - o Thermal shields based on lightweight panels covered by MLI, thermally anchored and supported from cooling pipes that form a "bird cage" (both for VV and Cryostat TS).
  - o Feeders based on HTS conductors, indirectly cooled via contact with helium pipes ("dry conductors").

FAIRNESS

Transparency
Collaboration
Loyalty

OPENNESS

Open doors
Open hearts
Open minds
Open ears

COMMITMENT

Ownership
Critical thinking
Determination
Respect

DIVERSITY

Cooperation
Equal opportunities
Inclusion

Assembly Process- VNS

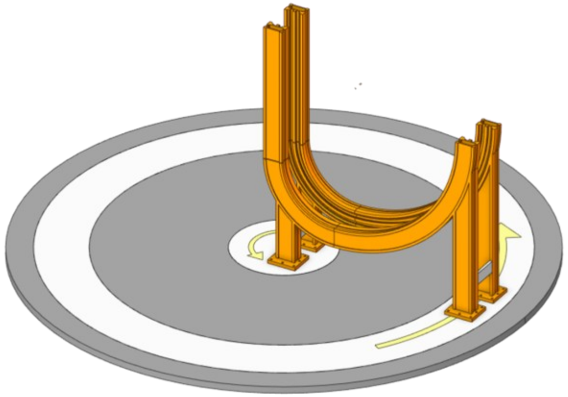

Step 1 - Install lower segment of the winding machine on the

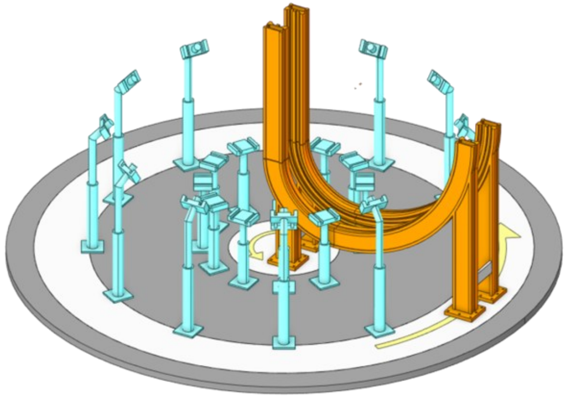

Step 2 – Install TF coils temporary supports

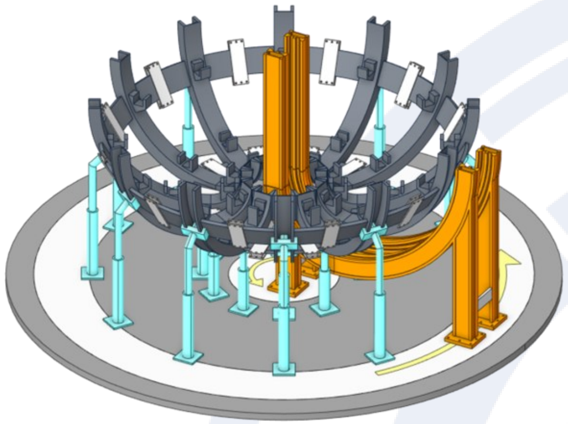

Step 3 - Install lower portion of the TF case outer legs

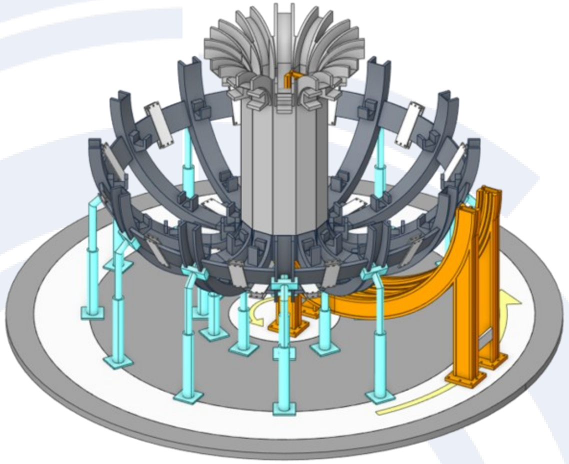

Step 4 – Weld the inner segment of TF case straight legs

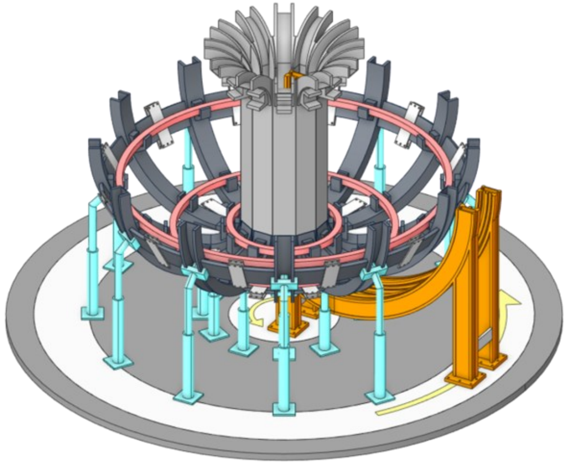

Step 5 - Install PF4-6 coils and connect lower TF inter-coil structures

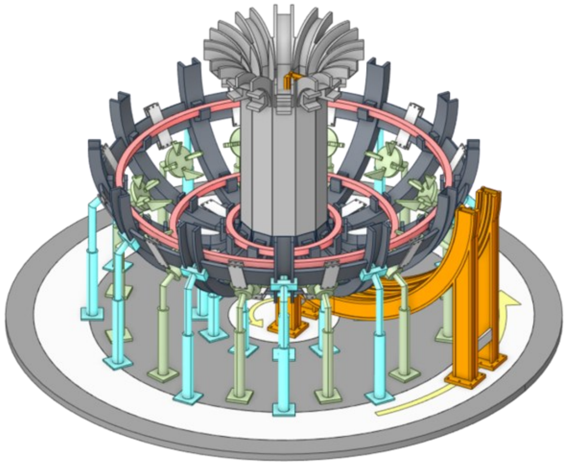

Step 6 - Install temporary supports for the Vacuum Vessel (VV)

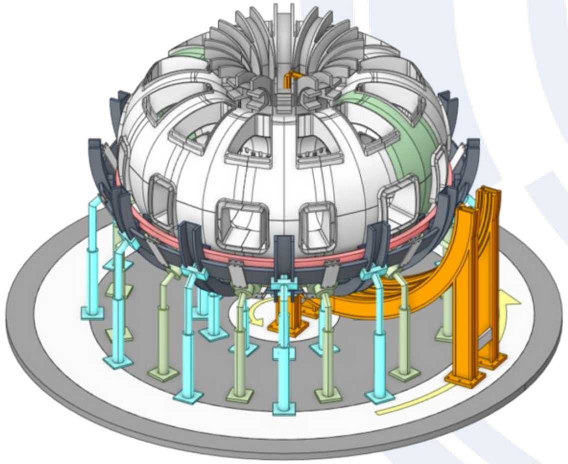

Step 7 - Install the fully assembled VV

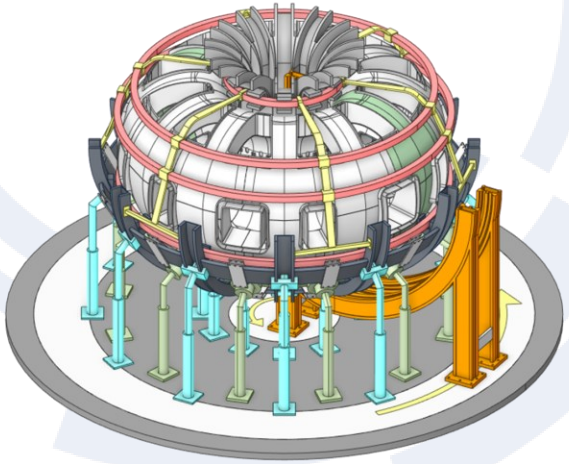

Step 8 - Install the PF1-3 coils on temporary supports

Assembly Process- VNS

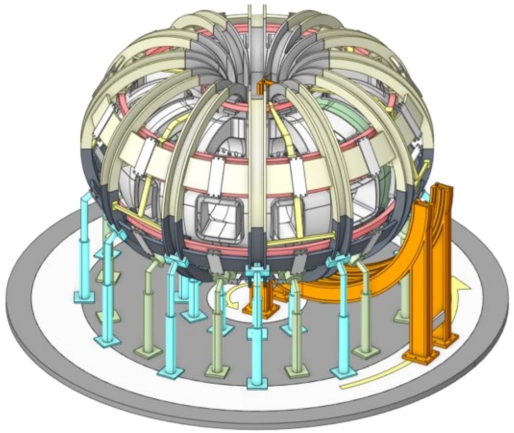

Step 9 - Weld the upper portion of the TF case outer leg and upper inter-coil structures

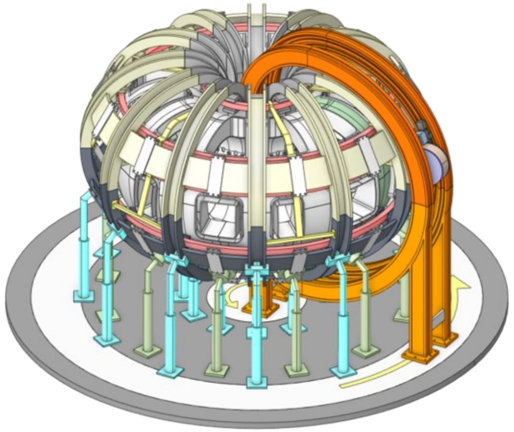

Step 10 - Move the upper PF coils to permanent supports Install the upper portion of the TF winding machine

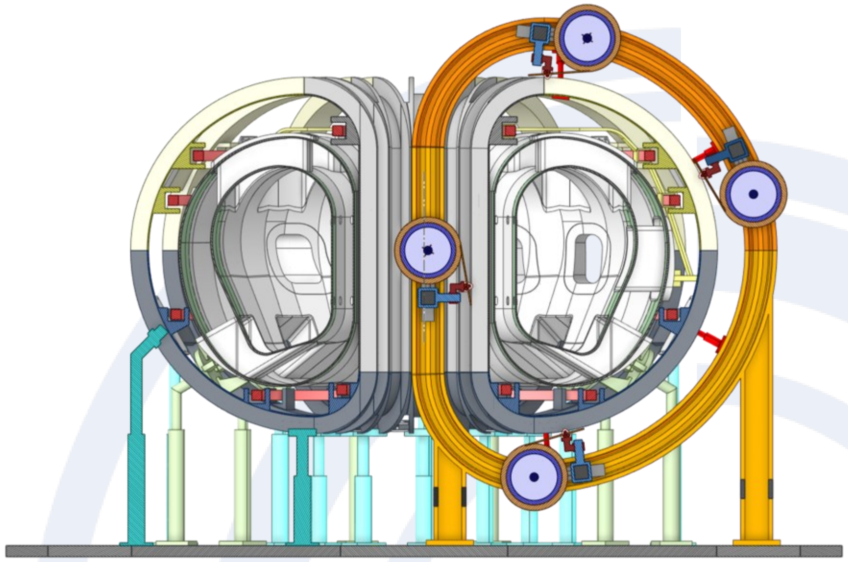

Step 11 - Complete the TF winding by rotating the orbital spool with the conductor

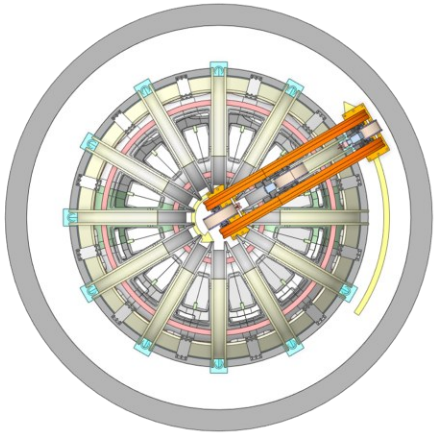

Step 12 - Rotate the winding machine and repeat for each TF coil

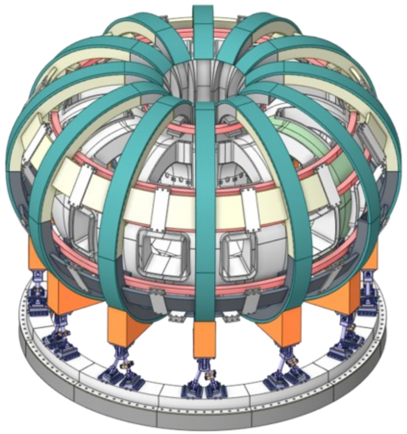

Step 13 - Weld the closure plates of the TF case outer legs

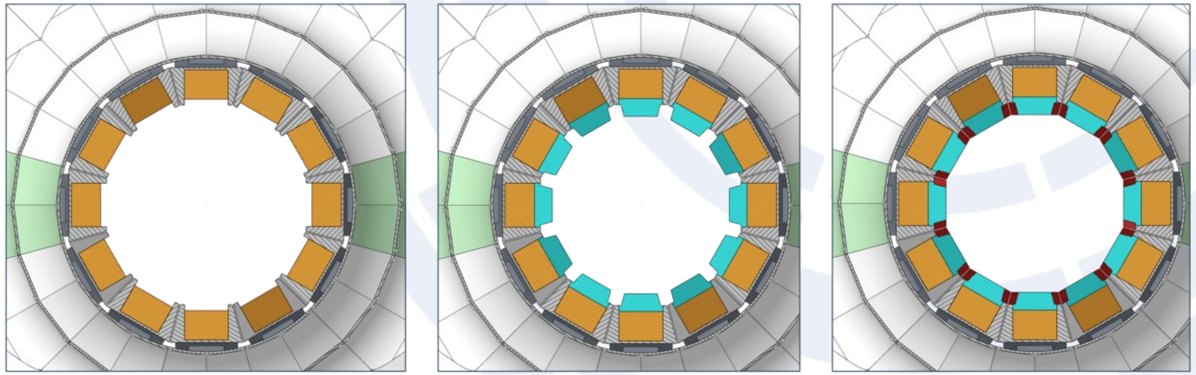

Step 14-16 - Once the windings are completed, the nose of the TF is installed in two steps: a) a T shaped part is inserted and welded to the pre-installed case segments; b) a set of shims are inserted and welded top and bottom to the case closure plates

TFC – 2D structural assessment of casing and jackets

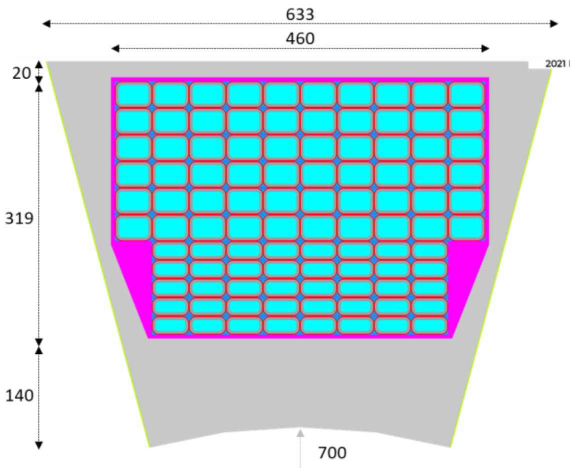

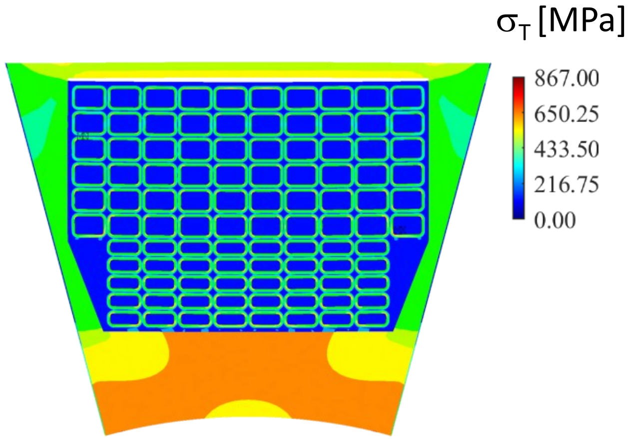

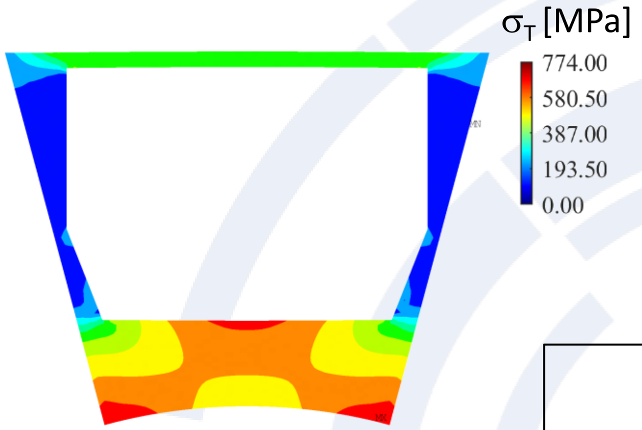

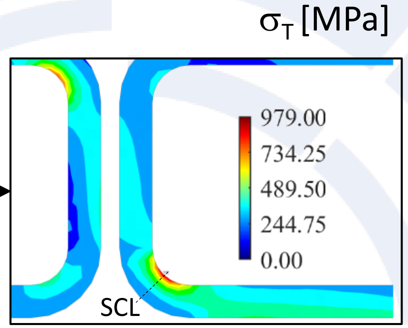

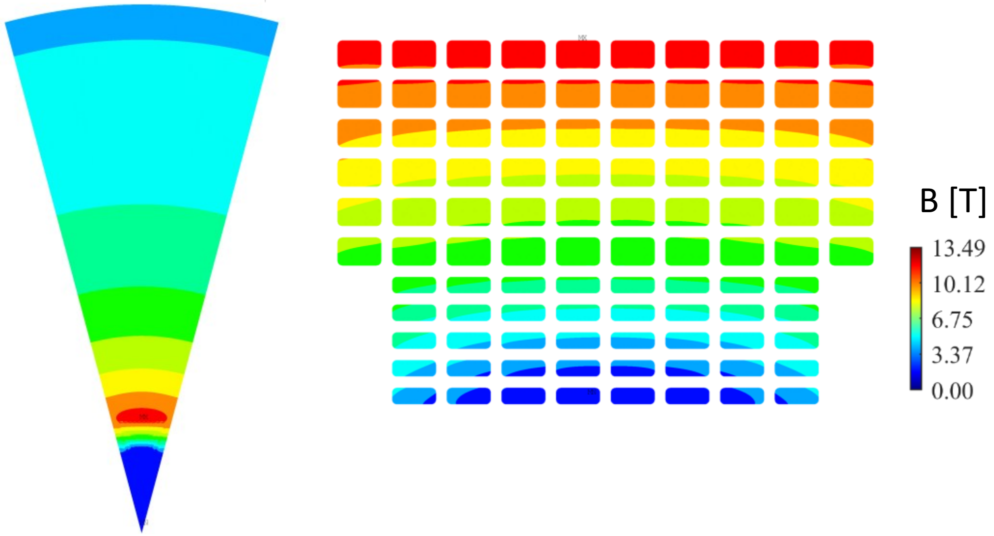

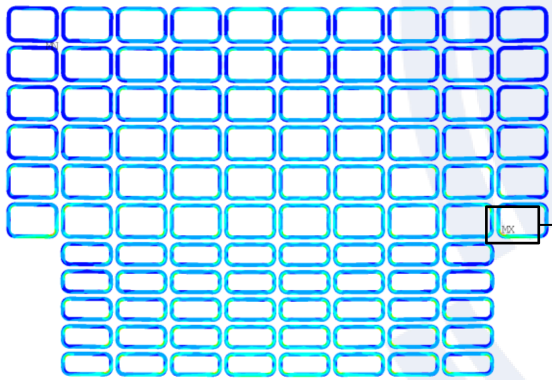

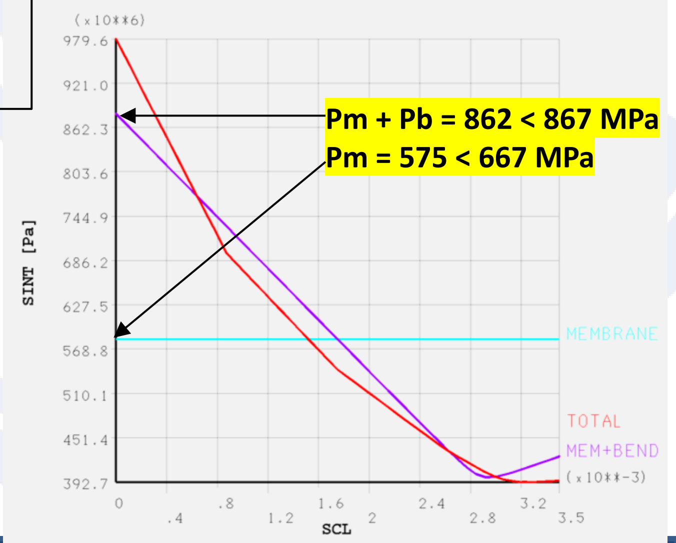

The assessment indicates positive results, with both the membrane and bending stresses remaining within allowable limits

TFC – 2D structural assessment turn insulation

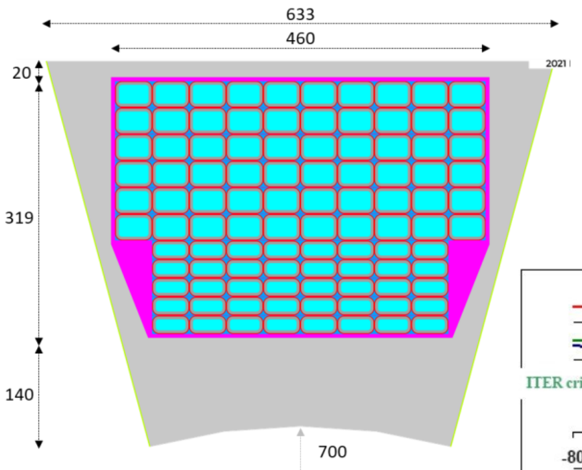

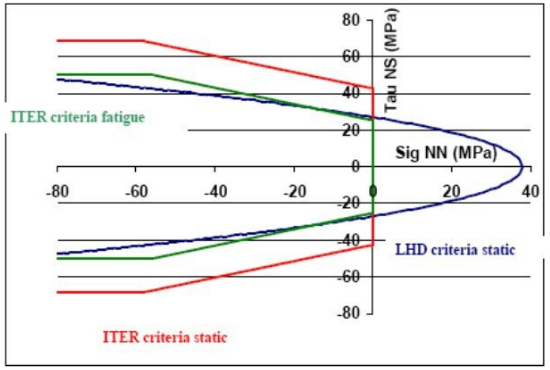

Large Helical Device criterion as a modification of the Mohr-Coulomb criterion

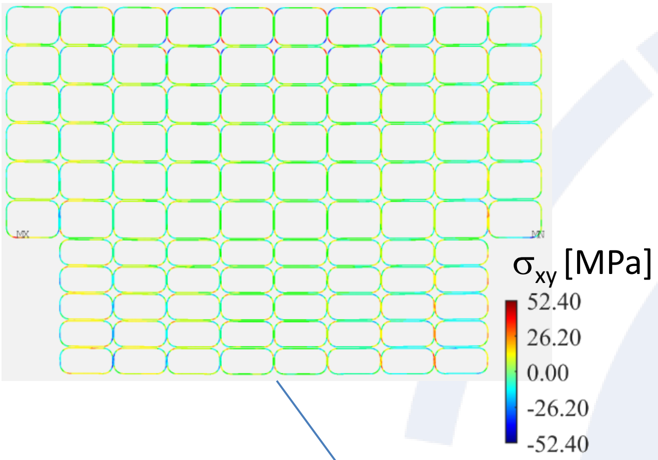

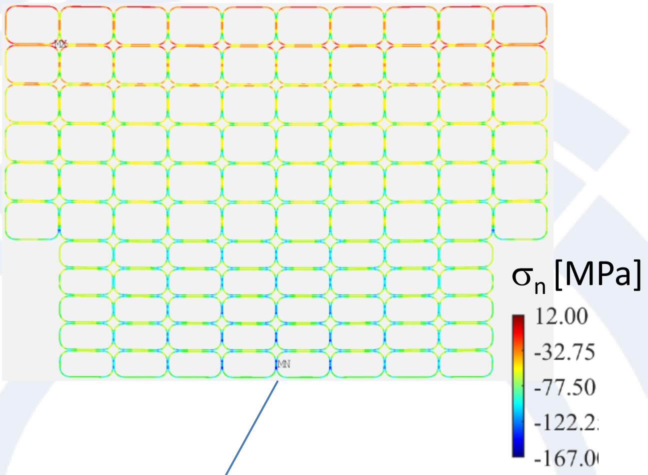

$$\frac{\sigma}{\sigma_n} + \left(\frac{\tau}{\tau_n}\right)^2 < 1$$

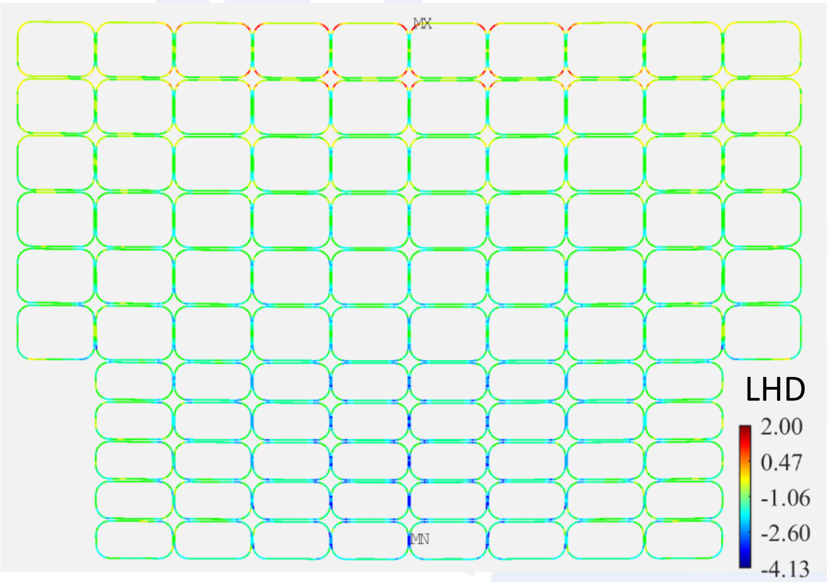

- **Applied LHD criterion** to the model to evaluate the stress state of the turn insulation.
- **Analysis results**: some areas show values above unity → potential delamination zones.
- **Important note**:
  - LHD criterion values refer to **cyclic loads**.
  - Include **safety factors associated with fatigue**.
- **For VNS cases**: these values should be **appropriately relaxed**.

τ = 27 MPa
σ = 38 MPa

CS – 2D structural assessment jackets

- Through detailed design and analysis, we have identified a margin in the CS size.
- Either a larger gap between the CS and TFC can be maintained, or the CS size can be increased to enhance the premagnetization flux it provides.

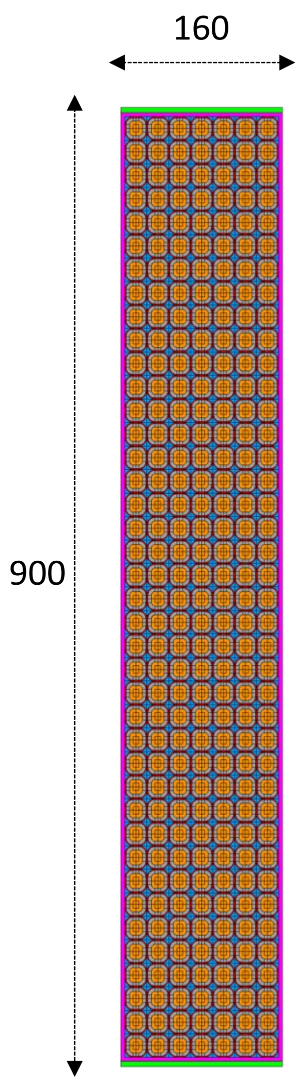

Fz	2 s	3 s	4 s	7 s	9 s	11 s	20 s	39 s
CS3U	-7	-1	-1	-2	-3	-2	-7	-3
CS2U	-6	-4	-4	-7	-7	2	17	11
CS1U	-4	-1	-1	19	26	4	-24	-25
CS1L	0	1	13	-16	-36	-30	-16	-13
CS2L	14	3	-8	5	16	21	7	7
CS3L	2	3	4	6	9	11	32	31

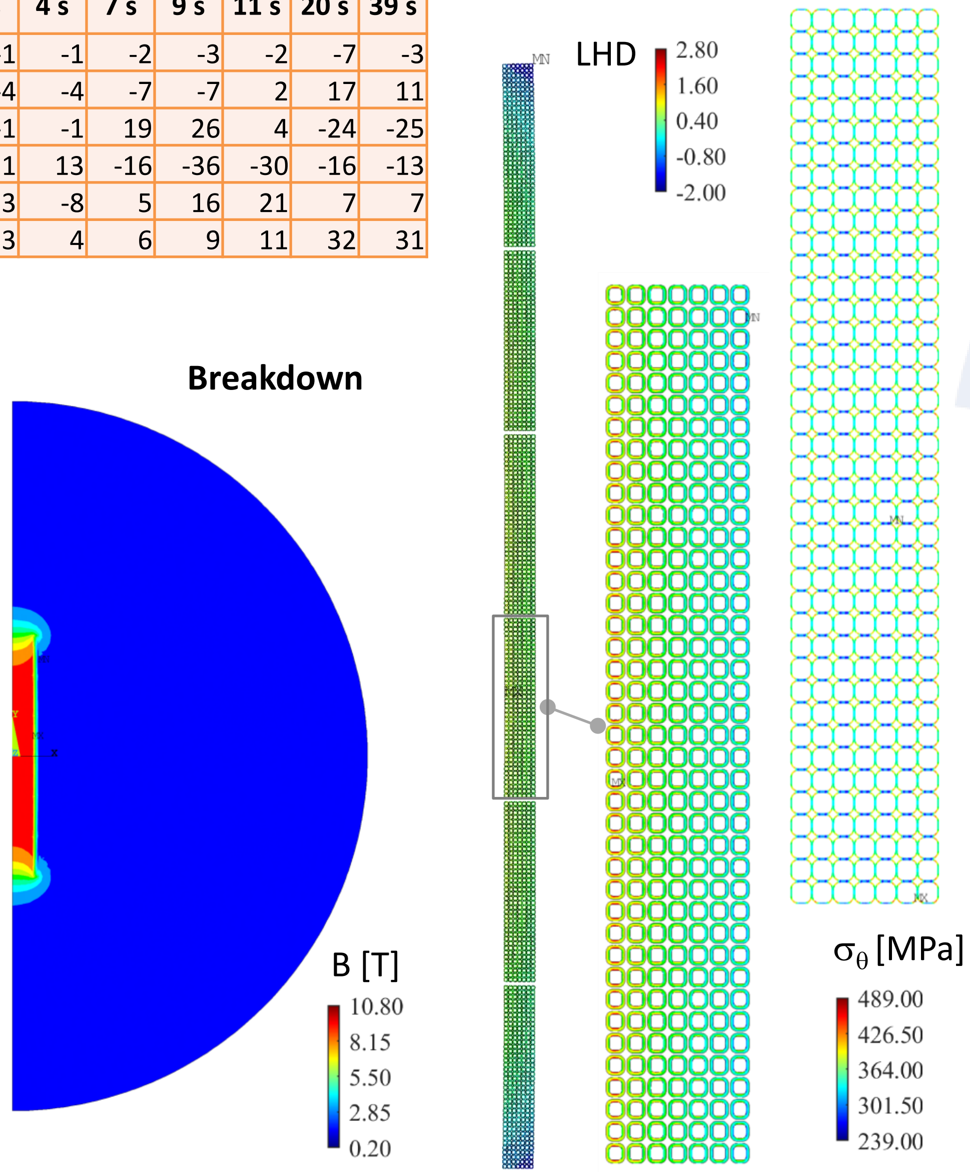

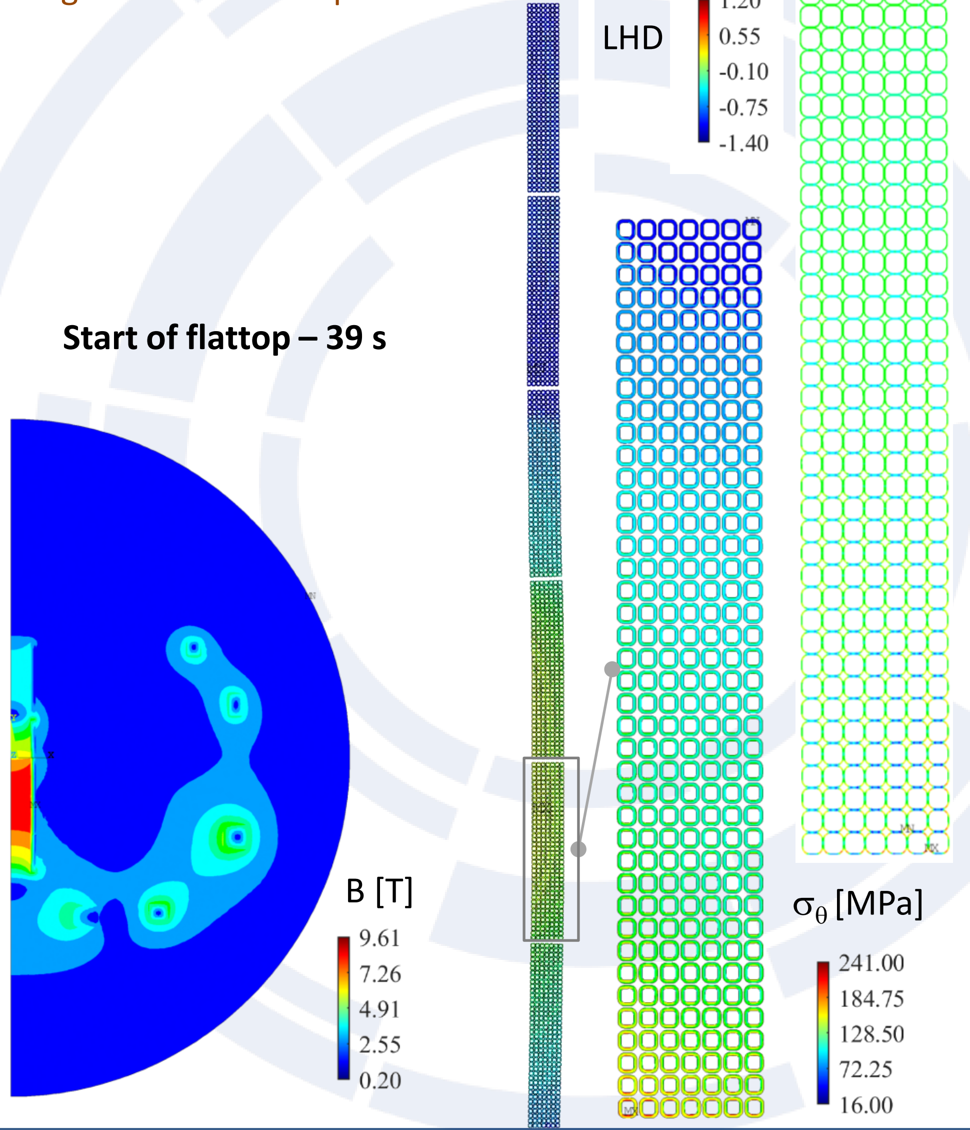

CS – 3D structural assessment

- A simplified model of the CS system is used to obtain the optimal cross-section for the tie plates
- All models are non-linear, with contact interactions modelled in detail
- The coils are represented by an equivalent orthotropic material
- The Tie Plates are represented by means of quadratic beam elements

- **With a 12 MN preload, the stress state in the tie plates remains compliant, and no gaps open during operation. In agreement with lumped model estimate.**

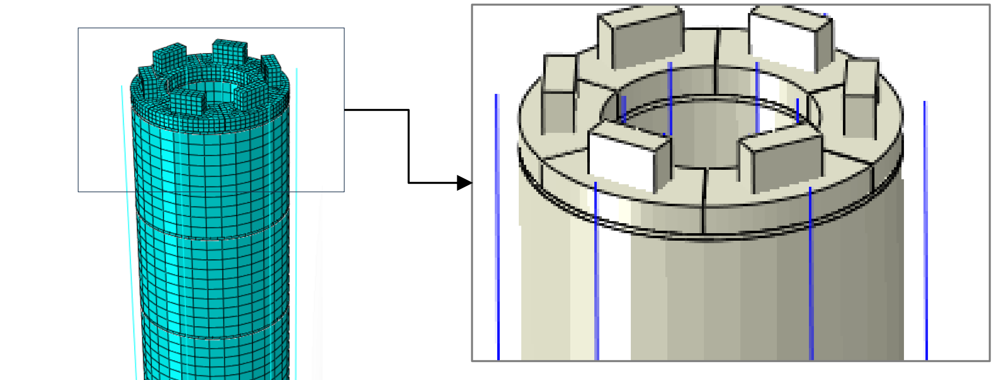

Property	Value	Unit
E1	3.40E+10	Pa
E2	3.40E+10	Pa
E3	9.35E+09	Pa
G12	1.02E+10	Pa
G23	1.87E+10	Pa
G31	1.87E+10	Pa
nu12	3.59E-01	-
nu13	1.04E-01	-
nu23	1.04E-01	-
rho	6.06E+03	kg/m³
aX	1.11E-05	°C⁻¹
aY	1.11E-05	°C⁻¹
aZ	1.01E-05	°C⁻¹

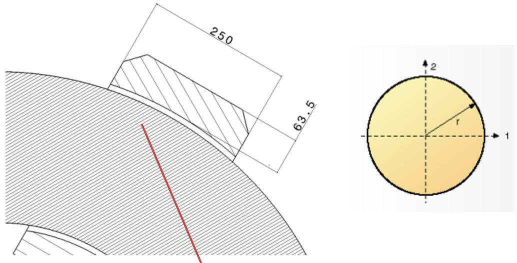

Reduction from the initial space reservation

R eqv	26.1 mm
A	0.002137 m²
Yielding	585 MPa (A453 SS 660 @ RT)
Axial stress (80% fty)	468 MPa
Preload value	1.00 MN per Plate

breakdown

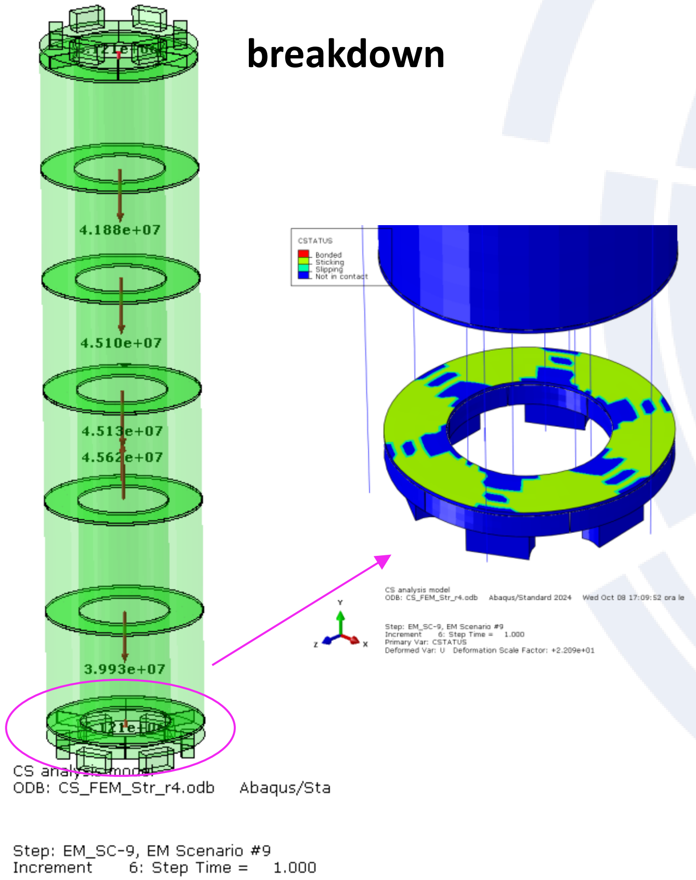

t =20 s

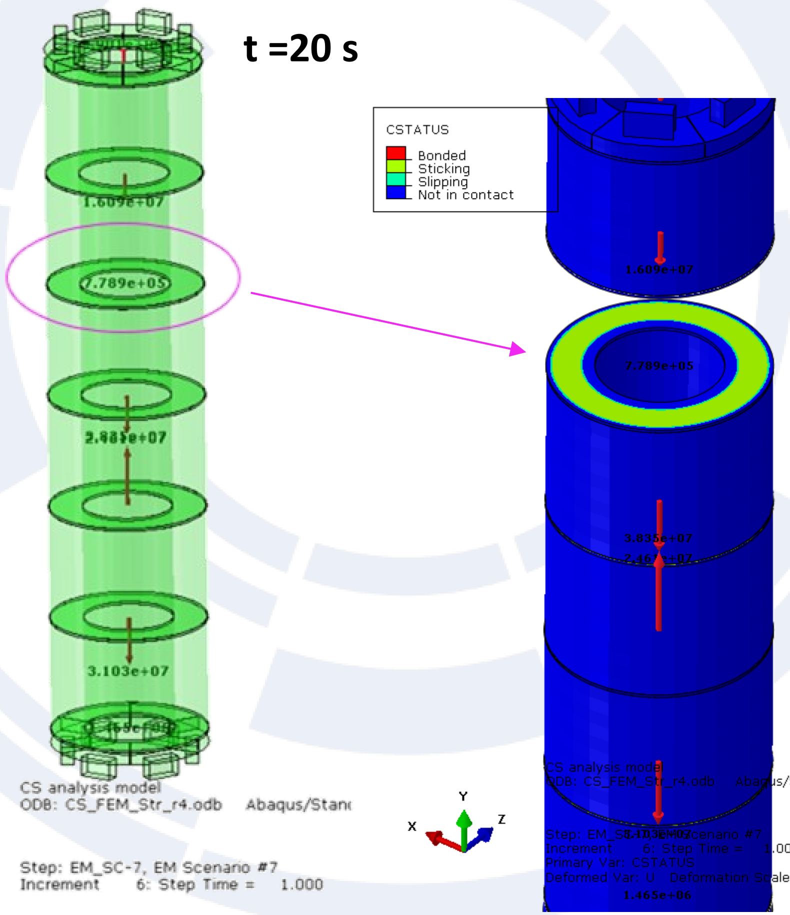

PFC – 2D structural assessment (preliminary axisymmetric)

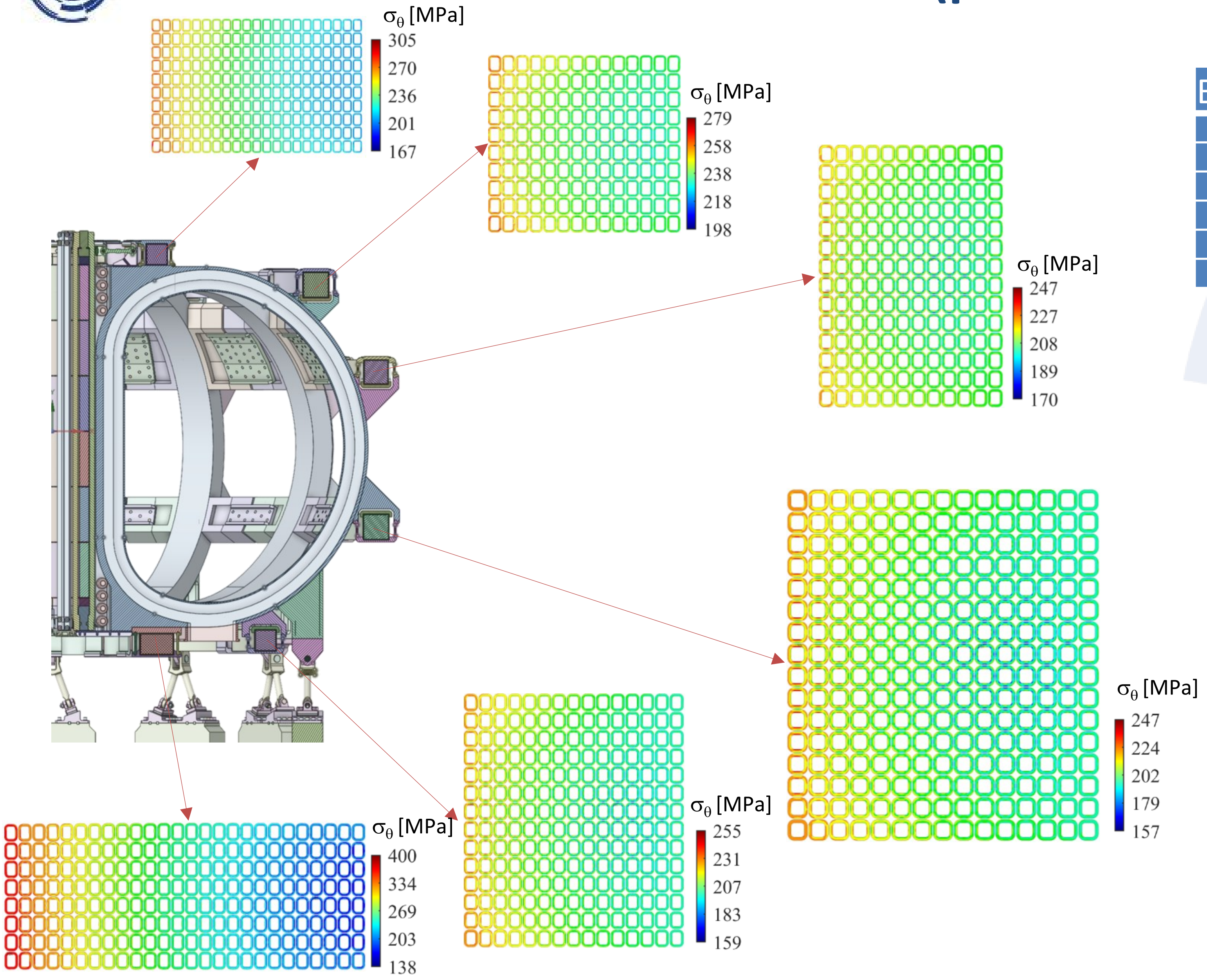

B [T]	2 s	3 s	4 s	7 s	9 s	11 s	20 s	39 s
PF1	2.9	5.8	5.1	2.1	0.8	1.2	1.1	0.3
PF2	0.3	2.7	4.3	4.7	5.6	5.5	3.9	4.4
PF3	0.3	1.7	3.5	4.4	5.7	5.5	4.3	4.4
PF4	0.3	0.7	1.8	3.5	4.9	5.4	5.7	5.7
PF5	0.5	0.1	0.4	2.3	4.4	5.2	5.8	6.0
PF6	5.0	3.8	7.4	7.1	6.2	5.9	6.5	5.8

Fr [MN]	2 s	3 s	4 s	7 s	9 s	11 s	20 s	39 s
PF1	8	23	15	0	-1	-2	5	-1
PF2	0	7	7	5	1	4	2	6
PF3	0	4	19	26	42	37	15	17
PF4	1	3	15	59	116	147	167	167
PF5	3	1	-2	-18	-27	-31	-35	-31
PF6	36	22	80	87	77	75	90	76

Fz [MN]	2 s	3 s	4 s	7 s	9 s	11 s	20 s	39 s
PF1	-3	-4	-3	-2	-1	-1	1	0
PF2	0	7	21	28	41	38	20	23
PF3	0	-5	-10	-1	7	14	24	21
PF4	0	-2	-9	-14	-19	-15	-1	1
PF5	0	0	0	-10	-26	-36	-43	-45
PF6	4	3	-3	-6	-7	-7	-12	-11

The assessment indicates positive results, with the hoop stress remaining within allowable limits

PFC cages – 3D assessment

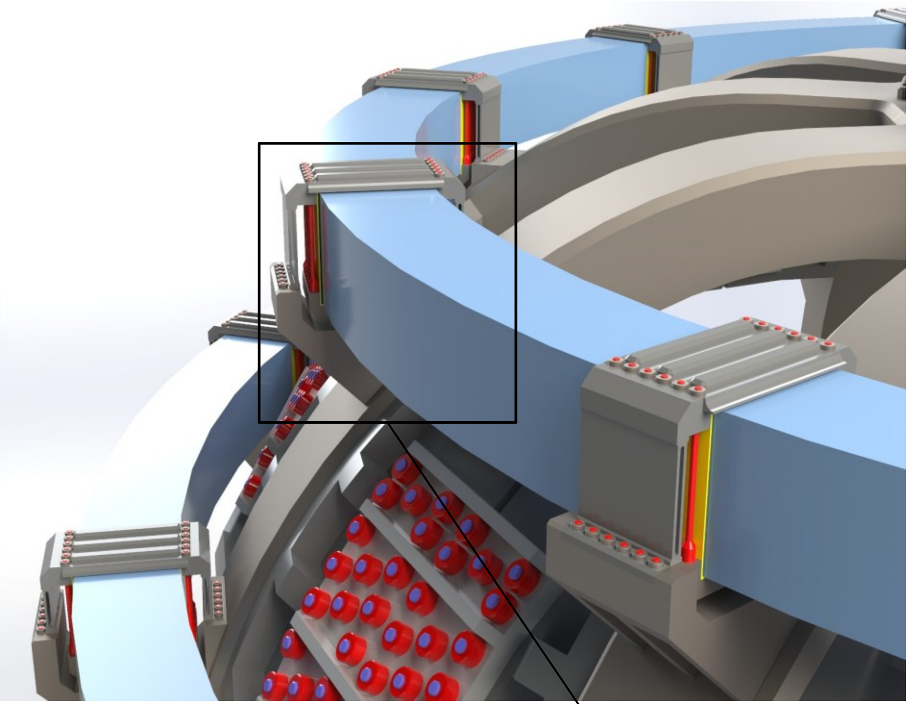

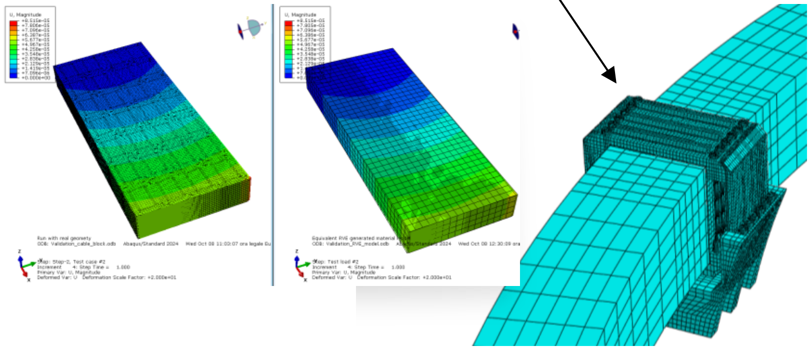

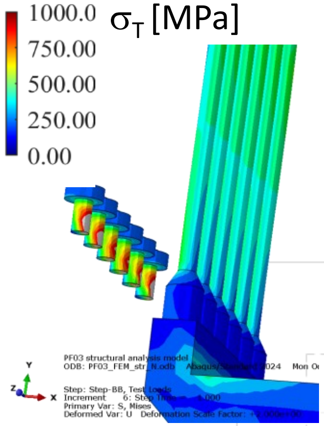

Limitation due to Screw strength

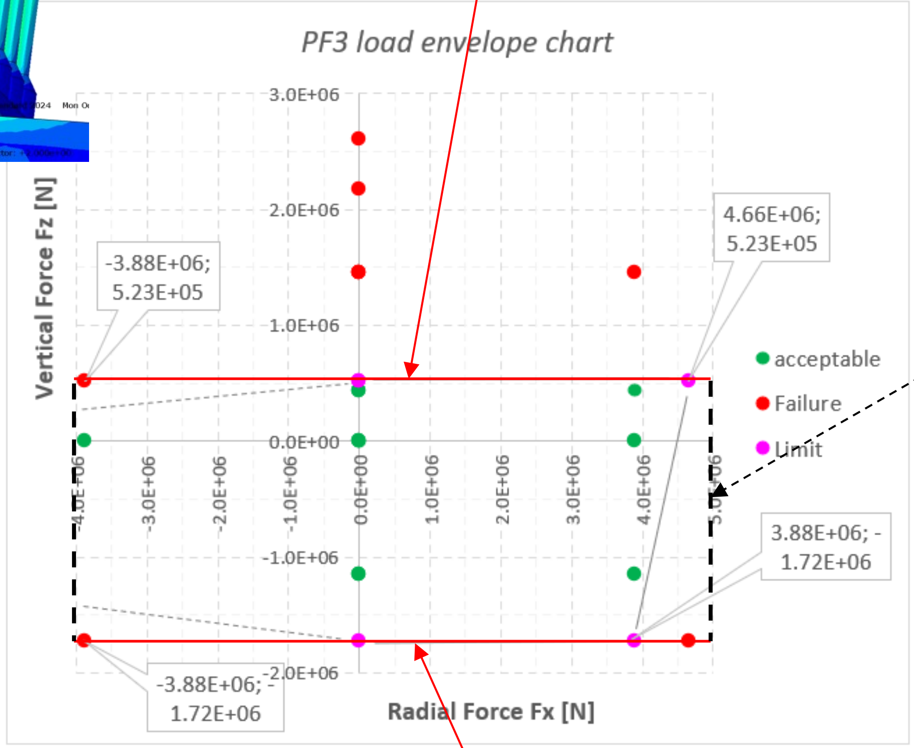

Limitation on Coil strength not yet considered

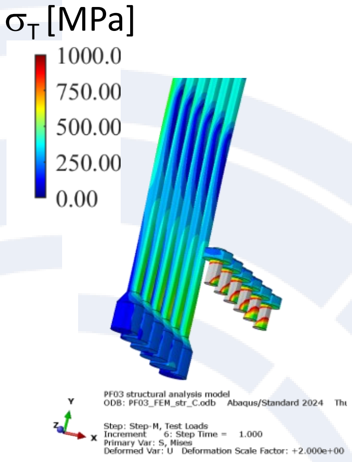

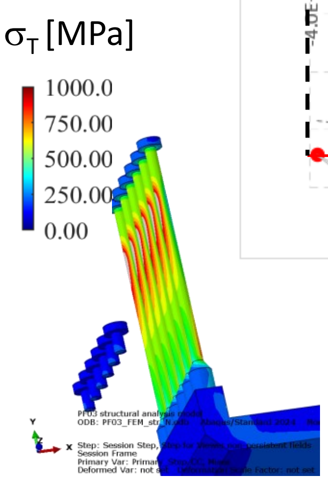

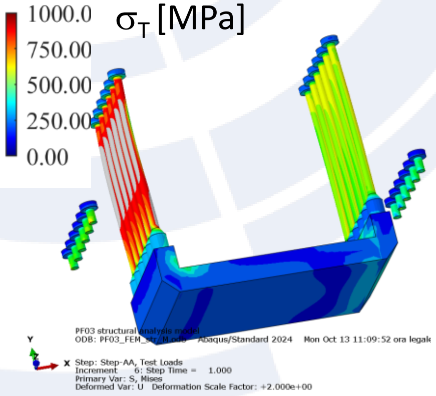

Limitation due to Tie rod/Cage strength

- The coil is modelled using equivalent homogenized materials.
- The cage is represented in full detail.
- Bolts include pretension elements, and contact interactions are defined across the various interfaces.